博士論文番号:1481207
(Doctoral student number)

The metabolic regulation mechanism and physiological role of valine in the yeast *Saccharomyces cerevisiae*

Natthaporn Takpho

Nara Institute of Science and Technology

Graduate School of Biological Sciences

Prof. Hiroshi Takagi

Submitted on 2017/08/30

TABLES OF CONTENTS

TABLES OF CONTENTS

ABSTRACT

Valine is one of the essential branched-chain amino acids (BCAAs), besides leucine and isoleucine, and thus, defects in the biosynthetic pathway can damage human health. Therefore, valine is included in various commercial products, such as animal feeds, human supplementary diets, pharmaceuticals, and cosmetic ingredients. In the past, valine has been commercially produced by bacterial fermentation from glucose using *Escherichia coli* or *Corynebacterium glutamicum*. Instead, this study concerns the biosynthesis of valine in one of lower eukaryotes, the yeast *Saccharomyces cerevisiae*. *S. cerevisiae* holds the generally regarded as safe (GRAS) status for human consumption and is also useful as a model for higher eukaryotes. BCAAs biosynthesis in yeast starts in mitochondria by four major enzymes, threonine deaminase, acetohydroxyacid synthase (AHAS), acetohydroxyacid reductoisomerase, and dihydroxyacid dehydratase. Among them, AHAS, which consists of a catalytic subunit (Ilv2) and a regulatory subunit (Ilv6), plays an important role in the control of valine biosynthesis as a rate-limiting step. The final step of the biosynthetic pathway is conversion of α-keto acids into BCAAs, which occurs in both mitochondria and cytosol via the mitochondrial and cytosolic BCAA aminotransferases (BCATs) Bat1 and Bat2 (Bat1/2), respectively. In this study, I focused on Ilv6 and Bat1/2 for better understanding of the regulation of valine biosynthesis in *S. cerevisiae*.

First, we tested the effects of amino acid substitutions in Ilv6, which may be involved in the feedback inhibition of valine biosynthesis. Based on the previous study of the *E. coli* AHAS regulatory subunit (ilvH) (Kaplun *et. al*., 2006), I introduced several amino acid substitutions into the yeast Ilv6. To screen for high valine-producing candidates, in which the feedback inhibition by valine might be removed, DL-norvaline, a toxic structural analog of valine, was used. As a result, the Asn86Ala, Gly89Asp, and Asn104His variants of Ilv6 displayed the DL-norvaline-resistant phenotype, suggesting that these Ilv6 variants cause valine accumulation in yeast cells. The quantification of intracellular amino acids indicated that cells expressing the Asn86Ala, Gly89Asp, and Asn104His variants contained about 4-fold higher levels of valine than that of wild-type cells. The computational analysis of Ilv6 using PSI-blast (http://blast.ncbi.nlm.gov) and Phyre2 predicted that these residues of Asn86, Gly89, and Asn104 are located in the vicinity of a valine-binding site, suggesting that the amino acid substitutions at these three positions induce the conformational change of the valine-binding site. To test the effects of the Asn86Ala, Gly89Asp, and Asn104His variants on the AHAS enzymatic activity, both recombinant Ilv2 and Ilv6 were purified and reconstituted in vitro. As the results, the Ilv6 variants showed the weaker feedback inhibition by valine than wild-type Ilv6. Intriguingly, only a part of the mutations that were identified in

E. coli enhanced the valine synthesis, suggesting structural and/or functional differences between the *S. cerevisiae* and *E. coli* AHAS regulatory subunits. It should be also noted that these amino acid substitutions did not affect the intracellular pools of the other BCAAs, leucine and isoleucine. Our laboratory previously revealed that an excess amount of intracellular proline increases the tolerance to various kinds of stresses (Takagi, 2008), but the accumulation of intracellular valine did not contribute to stress tolerance, as far as I examined.

The final step of BCAAs biosynthesis is mediated by the mitochondrial BCAT (Bat1) and cytosolic BCAT (Bat2), which share 77% identity of amino acid sequences, although the difference in the functions of Bat1/2 is still unknown. I found that the single disruption of the *BAT1* gene led to a slow-growth phenotype on minimal media and a considerably decreased intracellular valine content. However, the deletion of the *BAT2* gene did not affect the cell growth and valine accumulation. This result suggests that Bat1 predominantly accounts for the BCAT activity to maintain normal cell growth under amino acid-deficient conditions. To address this difference between the Bat1/2 activities in vivo, I further focused on the subcellular localization of these proteins. The putative mitochondrial targeting signal (MTS) at the amino terminus of Bat1 was deleted (Bat1-MTS), while amino-terminal 24 amino acids of Bat1 were fused with Bat2 at the amino terminus (Bat2+MTS). Fluorescent microscopic observations of the GFP-fused Bat1/2 proteins verified that these modifications altered the localization of Bat1 from mitochondria to cytosol and the localization of Bat2 from cytosol to mitochondria. Consequently, Bat2+MTS fully compensated the growth defect in Δ*bat1*Δ*bat2* mutant cells, whereas Δ*bat1*Δ*bat2* mutant cells harboring Bat1-MTS showed the slow-growth phenotype on minimal media. Moreover, the intracellular valine content was restored in Δ*bat1*Δ*bat2* cells harboring Bat2+MTS. According to these results, I concluded that the mitochondrial localization of BCAT, rather than the Bat1-specific enzymatic actions, is essential for the efficient valine production. Recently, it was reported that Bat1/2 contributes to the cell growth not only via the BCAT enzymatic activity but also via the activation of the TCA cycle through the direct interaction with mitochondrial aconitase (Kingsbury *et. al*., 2015). Therefore, loss of mitochondrial BCATs might negatively affect the cell growth also through the decreased mitochondria activity.

In summary, this study revealed the amino acid residues on the AHAS regulatory subunit Ilv6, which are involved in the negative feedback control of valine biosynthesis, and the importance of mitochondrial BCATs on valine synthesis and cell growth. These findings in a eukaryotic model organism will provide a better understanding of how BCAAs synthesis is regulated in higher eukaryotes and related in human diseases, as well as how to develop superior yeast strains for the more effective and safe industrial production of BCAAs.

CHAPTER I
INTRODUCTION

1.1. Metabolism and physiological roles of valine and other branched-chain amino acids

Branched chain amino acids, or BCAAs, are amino acids that contain a branch at the aliphatic side chain, such as three proteinogenic amino acids, valine ($C_5H_{11}NO_2$; Val or V), leucine ($C_6H_{13}NO_2$; Leu or L) and isoleucine ($C_5H_{11}NO_2$; Ile or I) (Figure 1-1), as well as non-proteinogenic α-aminoisobutyric acid ($C_4H_9NO_2$). Among them, valine is an essential aliphatic and nonpolar amino acid with an extremely hydrophobic property. The side chain of valine contains a non-polar branched-chain alkyl group, known as the isopropyl group, and thus, valine is similar to threonine in their shape and volume. Since valine is a hydrophobic amino acid, it is often found in interior proteins to form helical structures. Valine is applied to various commercial products, such as animal feed, human supplementary diet, pharmaceuticals and cosmetics. In addition, derivatives of valine from chemical synthon can be used as antibiotics, antivirals, as well as herbicides. In 2001, valine in the global market was approximately 500 tons/year (Eggeling *et. al.*, 2001) and its value was recently reached 45 million US$ in 2014 only for feed-grade valine (CheilJedang, 2013), indicating the progression of valine production in the amino acids market. Therefore, the intensive study of BCAAs metabolism is essential to provide a better understanding of the valine metabolic regulation mechanism, which may be applicable for industrial applications and medical research fields.

In particular, valine and other BCAAs not only provide building blocks for protein synthesis, but also play a role in cellular metabolism by connecting pyruvate metabolism, TCA-cycle and fatty acid oxidation together. The utilization of valine exclusively participates in carbohydrates metabolism, whereas leucine is solely involved in fats metabolism, and isoleucine contributes to both. BCAAs participate in the regulation of nutrient sensing pathway (target-of-rapamycin (TOR) signaling), cellular energy production (ATP production) and mammalian diseases. In human, valine deficiency leads to several diseases, including brain diseases caused by neurological defection and maple syrup urine disease. In addition, valine has been particularly used in supplemental therapy for unhealthy

liver conditions (Wishart *et. al.,* The Human Metabolome Database), metabolic disorders, trauma, sepsis, and cancer (Manelli *et. al*., 1984; Skeie *et. al*., 1990; De Bandt and Cynober, 2006). Therefore, the unique metabolic and physiological roles of valine and other BCAAs including their catabolic products are highlighted in this section.

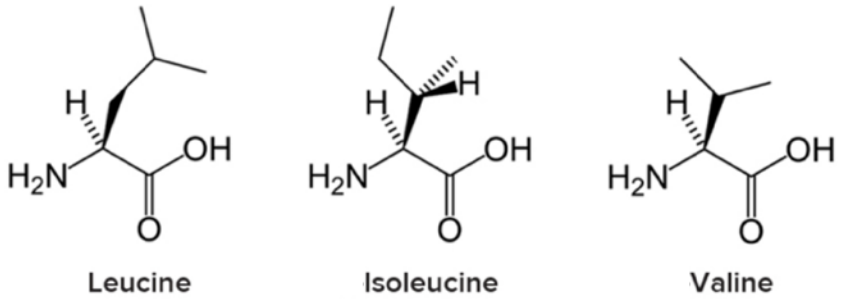

Figure 1-1 Structures of BCAAs.

1.1.1. Metabolism of valine and other BCAAs

BCAAs metabolism has been intensively studied in mammals as its deficiency is linked to several human diseases. BCAAs metabolism is also associated with protein synthesis and turnover, glucose metabolism as well as energy metabolism (Monirujjaman and Ferdouse, 2014). In mammals, BCAAs cannot be synthesized, while the BCAAs catabolic pathway is well characterized. Catabolism of BCAAs in mammals is mostly carried out in mitochondria and produces acetyl-CoA and succinyl-CoA as the endoproducts (Figure 1-2). BCAAs aminotransferase (BCATs) catalyze the first step of BCAAs catabolism in which the transamination of valine, leucine, and isoleucine to α-ketoisovalerate (KIV), α-ketoisocaproate (KIC), and α-keto-β-methylvalerate (KMV), respectively, occurs. BCATs consist of two isoforms, mitochondrial BCAT (mBCAT) and cytosolic BCAT (cBCAT). The distribution of theses isoforms depends on the requirement of nitrogen metabolism of each cellular part (Goichon *et. al.,* 2013). The second step of BCAAs catabolism, which is driven by a mitochondrial enzyme, branched-chain α-ketoacid dehydrogenase (BCKD), is an irreversible reaction and regulates the BCAAs catabolism rate (Cole, 2015).

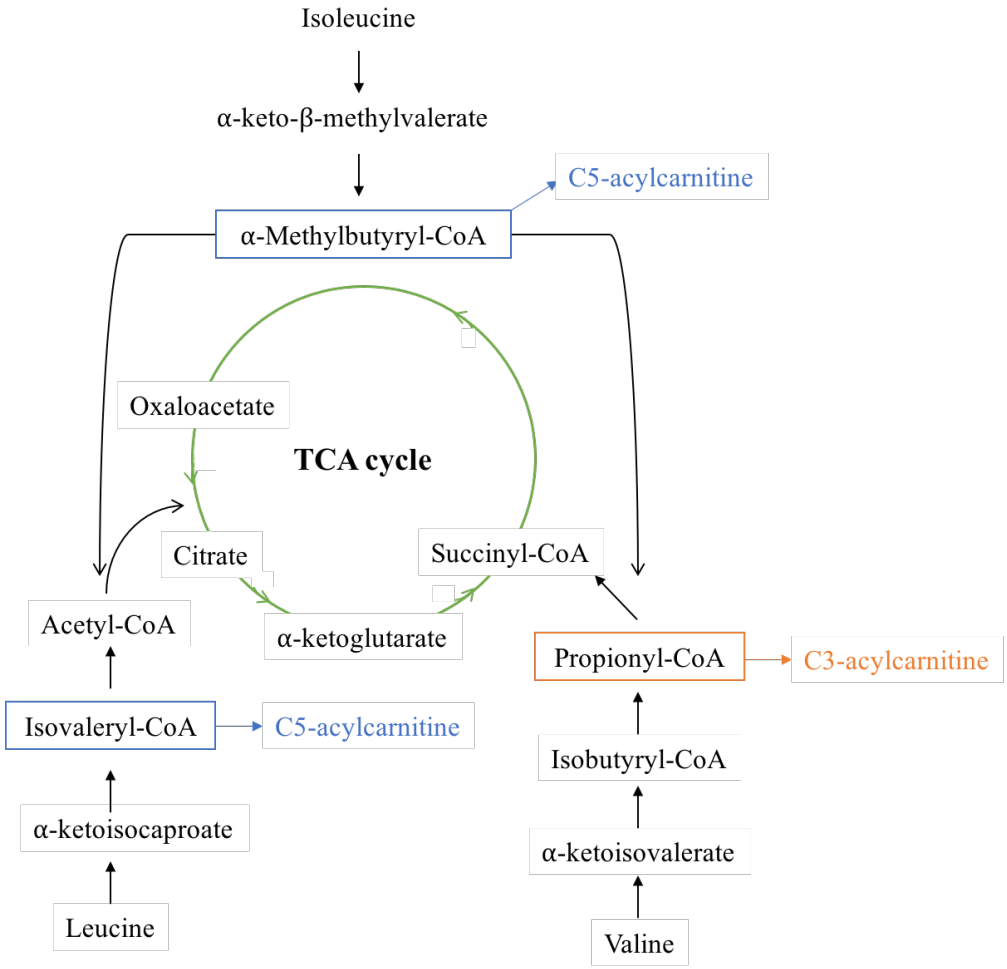

Figure 1-2 BCAAs catabolic pathway to produce acetyl-CoA and succinyl-CoA for TCA-cycle. (modified from Zhang *et. al.,* 2017)

1.1.2. Physiological functions of BCAAs

Preclinical studies propose that BCAAs provide benefits in various physiological aspects. For instance, supplementation of BCAAs improves the immune system and lymphocytes growth and proliferation, including cytotoxic T lymphocytes and natural killer (NK) cells (Calder, 2006). BCAAs-deficient diet leads to a higher mortality rate and severer susceptibility to pathogen infection, suggesting that BCAAs are implicated in the host defense system (Petro and Bhattacharjee, 1981). Table 1-1 summarizes the effect of BCAAs on immune functions. Supplementation with BCAAs increases CD4+, CD4+/CD8+, interleukin-2R, IgA, sIgA and accelerates neutrophil cycling (Ren *et. al.,* 2015; Kephart *et. al.,* 2016 and Zhang *et. al.,* 2017). It also enhances phagocytes function of neutrophils and NK activity of lymphocytes (Nakamura, 2014).

Furthermore, each BCAA is beneficial to immunity. Isoleucine up-regulates the RNA and protein expression of β-defensins 1, 2 and 3 in piglets and β-defensins 3 and 4 in tuberculosis patients (Mao *et. al.,* 2013; Rivas-Santiago *et. al.,* 2011). Leucine and valine increase cytokines production (Calder, 2006), although the detailed mechanisms are not well understood. In addition, leucine and valine deficiency impairs the immune system by up-regulating pro-inflammatory cytokines, on the other hand, anti-inflammatory cytokines are down-regulated (Luo *et. al*., 2014; Jiang *et. al*., 2015). This phenomenon is the result from changes in the nuclear factor (NH)-*κ*B and mammalian TOR (mTOR) signaling pathways.

Table 1-1 BCAAs and immune functions (modified from Zhang *et. al.,* 2017).

Amino acid	Regulation of immune function
BCAA mix	↑ fuel sources for immune cells ↑ immune function of neutrophils and lymphocytes ↑ CD4+, CD4+/CD8+ ↑ intestinal immunoglobulins
Isoleucine	↑ excrete β-defensin
Leucine	↑ regulation of innate and adaptive immune response ↑ pro-inflammatory cytokines ↓ anti-inflammatory cytokines
Valine	↑ pro-imflammatory cytokines ↓ anti-inflammatory cytokines

Besides the immune functions, BCAAs are also involved in multiple cellular events. BCAAs induce the expression of mitochondrial enzyme genes, such as PCG-1α for oxidative phosphorylation, in mice (D' Antona *et. al.,* 2010). BCAAs also upregulate the genes related to the reactive oxygen species (ROS) defense system (e.g. the superoxide dismutase genes SOD1 and SOD2) (D' Antona *et. al.,* 2010). Among BCAAs, leucine is well-analyzed as the key activator of mTOR signaling, which governs the cellular proliferation, metabolism and other activities (Avruch *et. al*., 2009).

1.2. Valine biosynthesis and catabolism in microorganisms

BCAAs biosynthesis is an essential pathway in plants, algae, fungi, bacteria, and archaea, but not in animals. To fulfill the consumer needs, biotechnology processes were applied to industrial BCAAs production for decades. Microorganisms are the promising hosts for large-scale production according to high productivity, rapid growth rates, ability to utilize several substrates and climate-independent culture process. Here, the valine biosynthetic pathways in industrial microorganisms *Escherichia coli*, *Corynebacterium glutamicum* and *Saccharomyces cerevisiae* are emphasized.

1.2.1. Valine biosynthesis in bacteria

The valine biosynthesis in *E. coli* and *C. glutamicum* are similar: valine is produced from two pyruvate molecules by the activation of four enzymes, acetohydroxyacid synthase (AHAS), acetohydroxyacid isomeroreductase (AHAIR), dihydroxyacid dehydratase (DHAD), and transaminase B (TA) (Oldiges *et. al*., 2014). The key regulator of valine biosynthesis is AHAS, which is subjected to the feedback inhibition by valine (Pang and Duggleby, 1999). The only one type of AHAS is found in *C. glutamicum*, whereas three isozymes are reported in *E. coli* as AHAS I, II and III. It is noted that AHAS III in *E. coli* showed the highest similarity to the AHAS of *C. glutamicum* and its regulatory subunit (IlvH) contains an ACT domain at the N-terminal which is responsible for the binding of valine (Pátek, 2007). Meanwhile, the activity of AHAS I (IlvBN) is also inhibited in the presence of valine, on the other hand, AHAS II (IlvGM) activity is not affected by valine. In general, the feedback inhibition of AHAS by valine in *C. glutamicum* is weaker than in *E. coli*: 50% of the maximum AHAS specific activity in *C. glutamicum* remains even in the presence of 10 mM valine (Elišáková *et. al*., 2005), whereas 80% of the maximum AHAS specific activity in *E. coli* is inhibited by 4.8 μM valine (Mendel *et. al*., 2001). Therefore, *E. coli* AHAS is a suitable model for the study of feedback inhibition by valine.

E. coli is widely used for the industrial applications due to the rapid growth, high glucose uptake rates and availability of genetic databases, as well as the well-analyzed metabolic regulation. Valine biosynthetic pathway of *E. coli* is

illustrated in Figure 1-3. Valine biosynthesis in *E. coli* is regulated by feedback inhibition of AHAS (Umbarger, 1996). Among three AHAS isozymes (AHAS I IlvBN, AHAS II IlvGM and AHAS III IlvIH), AHAS I and III are subjected to feedback inhibition caused by valine. It is known that the *E. coli* AHAS consists of a catalytic subunit and a regulatory subunit. The catalytic subunit is responsible for catalytic activity, while the regulatory subunit is the target of feedback inhibition by valine (Hill *et. al*., 1997). AHAS III, which shows the highest similarity to the AHAS of *C. glutamicum*, contains the ACT domain responsible for valine binding at the amino terminal (Kaplun *et. al*., 2006). Besides feedback inhibition, valine biosynthesis in *E. coli* is partially regulated by the attenuation of the *ilvGMEDA* operon by BCAAs via the master regulator Lrp (Pátek, 2007).

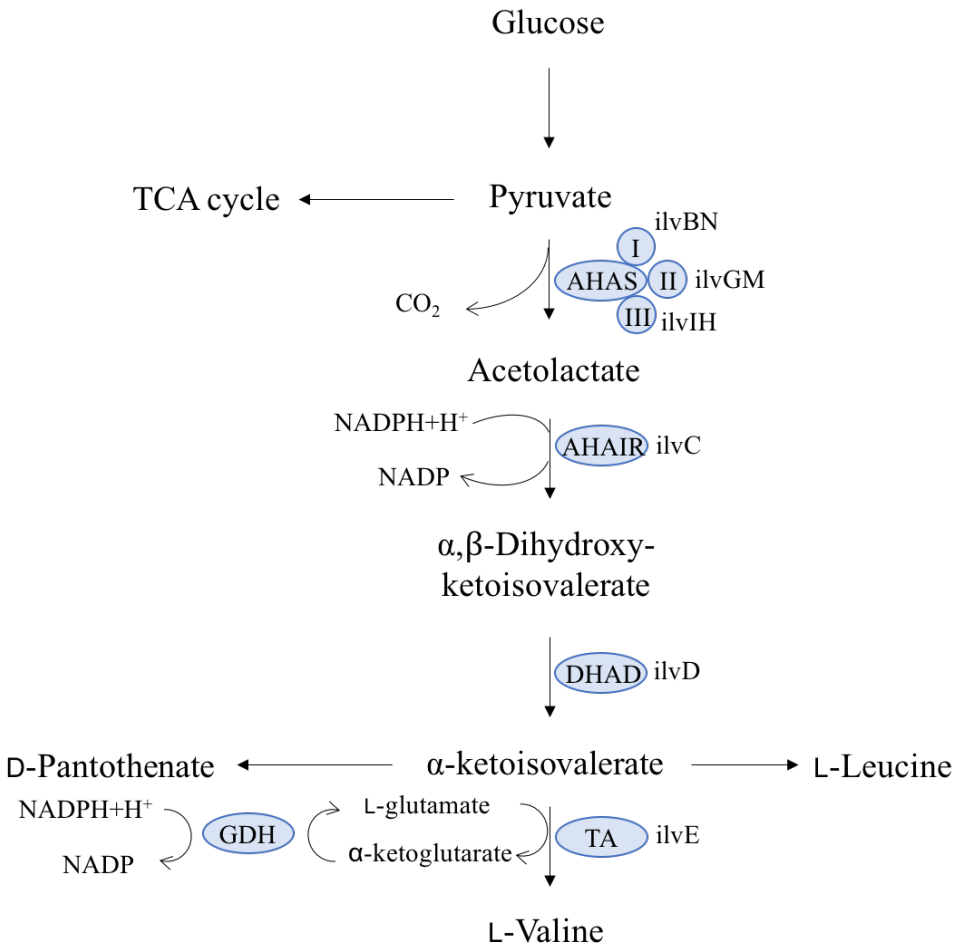

Figure 1-3 The L-valine biosynthetic pathway in a *E. coli*.

AHAS (IlvBN [AHAS I], IlvGM [AHAS II] and IlvIH [AHAS III]): acetohydroxyacid synthase; AHAIR (IlvC): acetohydroxyacid isomeroreductase; DHAD (IlvD): dihydroxyacid dehydratase; GDH: L-glutamate dehydrogenase; TA (IlvE): transaminase B (modified from Oldiges *et. al.*, 2014).

To increase the valine production in *E. coli,* metabolic engineering approach is carried out by several genes knockout (*ilvA*, *panB* and *leuA*, encoding threonine dehydratase, β-methyl-α-oxobutanoate hydroxymethyltransferase and α-isopropylmalate synthase, respectively) to block the competitive pathways for leucine and isoleucine production (Park *et. al.*, 2007). The valine feedback inhibition is overcome by introducing the mutations on IlvH, the regulatory subunit of AHAS III (Kaplun *et. al*., 2006). Finally, the transcriptional attenuation of the *ilvBN* (encoding AHAS I) and the *ilvGMEDA* operons are avoided by replacing the *tac* promoter at the attenuator leader regions (Park *et. al.*, 2007). Considering the phage infection or endotoxins production, however, valine production in bacteria for food and pharmaceutical products still has a limitation due to its safety and customer confidence.

1.2.2. Valine biosynthesis in *S. cerevisiae*

The yeast *S. cerevisiae* is focused as a more suitable host for food- and pharmaceutical-grade valine production due to its safety and the generally recognized as safe (GRAS) status. In *S. cerevisiae*, valine is synthesized in mitochondria by conversion of pyruvate as a substrate (Figure 1-4). The biosynthetic pathway begins with transport of pyruvate from cytosol into mitochondria by mitochondrial pyruvate transporters (Mpc1, Mpc2, Mpc3 and Yia6), where the whole process takes place. Two mitochondrial pyruvate molecules are converted into α-acetolactate by AHAS (Ilv2/Ilv6), which is the key enzyme for the BCAAs biosynthetic pathway, acts in a rate-limiting step and is controlled through the feedback inhibition caused by valine (see details in a) below). Keto-acid reductoisomerase or acetohydroxyacid reductoisomerase (AHIR; Ilv5) catalyzes isomerization of α-acetolactate to α,β-dihydroxyisovalerate in the presence of NADPH and Mg^{2+} (Petersen and Holmberg, 1986). This compound is used as a substrate for $[2Fe\text{-}2S]^{2+}$-dependent DHAD (Ilv3) to produce a key intermediate KIV. By the assistance of unknown keto-acid transporters, KIV is partially transported to cytosol. The final step of valine biosynthesis occurs in both mitochondria and cytosol by BCATs Bat1 and Bat2, respectively (see details in b) below). Unlike other enzymes in the pathway,

BCATs are homologous to the human BCAT, ECA9. However, since no BCAAs biosynthesis occurs in mammals, the only known role of ECA9 is limited to degradation of BCAAs. Interestingly, this enzyme is a target for neurological disorder drug development and involved in several diseases in human, hence elucidating the unrevealed cellular roles of BCATs is important (McCourt and Duggleby, 2005). Catabolism of valine and other BCAAs in *S. cerevisiae*, which is totally different from that in mammals, is argued separately in the section 1.3.

a) Acetohydroxyacid synthese (AHAS): the key enzyme for valine biosynthesis

AHAS (EC 2.2.1.6) is the first common enzyme that catalyzes the first step of BCAAs biosynthesis, which is a thiamin diphosphate (ThDP)-dependent enzyme for non-oxidative decarboxylation of pyruvate (Figure 1-4). The reaction releases CO_2 and reactive resonating hydroxyl-ethyl-ThDP as an intermediate (Umbarger and Brown, 1958; Holzer *et. al.,* 1960; Tittmann *et. al.,* 2003). In *S. cerevisiae*, AHAS consists of the catalytic (Ilv2) and the regulatory (Ilv6) subunits, and does not contain any isozymes. Expression of AHAS is controlled by transcription factor Gcn4 and BCAAs feedback inhibition (Magee and Hereford, 1968; Xioa and Rank, 1988). Gcn4 induces the transcription of the genes related to amino acids biosynthesis, as well as *ILV2*, in response to amino acids starvation by binding to the *cis*-acting TGACTC element, leading to an increase in the AHAS activity. In addition, transcriptional regulation of the regulatory subunit, *ILV6*, has not been described, although it is probably regulated in the same manner as *ILV2* since *ILV6* also contains the Gcn4-binding consensus sequences (Pang and Duggleby, 1999)

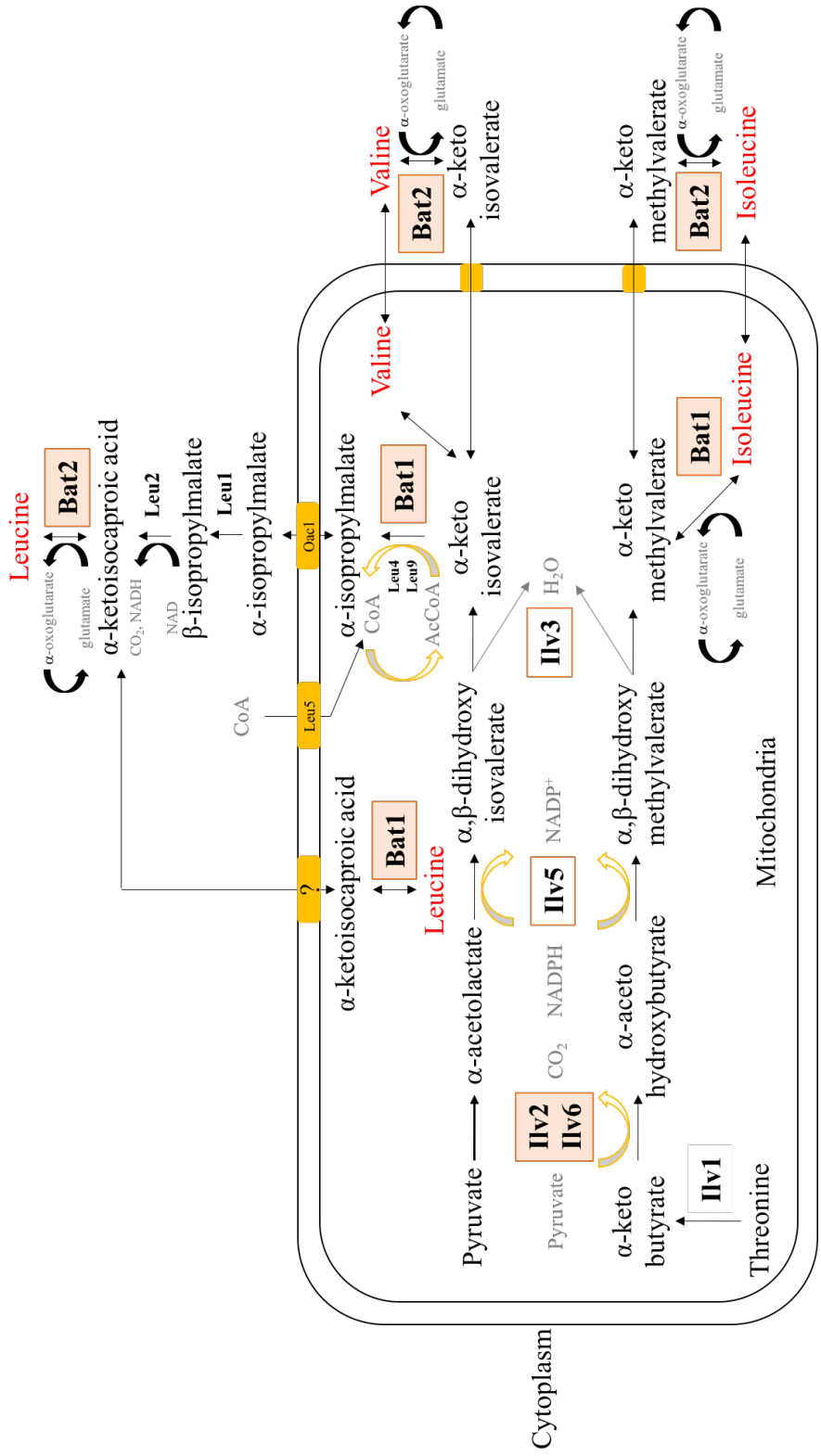

Figure 1-4 BCAAs biosynthetic pathway in *S. cerevisiae.*

Modified from the KEGG pathway (Kanehisa and Goto, 2000) and SGD (Cherry *et. al.,* 2012)

As the complete structure of yeast AHAS has not been fully determined, the studies of yeast AHAS are based on the *E. coli* AHAS structures from PDB: Protein Data Bank (Berman *et. al.,* 2000). Crystal structure of the *S. cerevisiae* AHAS, as well as that of other ThDP-dependent enzymes, reveals a dimer arrangement (Pang *et. al.,* 2002; 2003) of catalytic (Ilv2) and regulatory (Ilv6) subunits, and the active site is located at the interface of two Ilv2 monomers. As shown in Figure 1-5, the yeast AHAS catalytic subunit is a dimer (Figure 1-5B) in which its monomer is folded into three domains, α, β and γ (Figure 1-5A). The dimer structure is mainly formed by α and γ domains, with the β domains on either side of the protein. The active site is a flexible tunnel that can bind to other compounds, for examples, ThDP, Mg^{2+} and FAD. Upon the binding of an herbicide to the catalytic subunit of *Arabidopsis thaliana*, the binding pocket displays a closed structure. Therefore, it is suggested that the yeast AHAS can form "open" and "closed" conformations, and the closed conformation is referred to as the active form of this enzyme (Pang *et. al.,* 2003). In general, AHAS contains two substrate-binding sites which specific to pyruvate and α-ketobutyrate and the AHAS reaction involved in two stages. The first reaction is the decarboxylation of pyruvate to binds with ThDP in order to form the catalytic intermediate, HE-ThDP (hydroxymethyl-thiamine diphosphate), follow by the the carboligation of a second substrate, pyruvate or 2-ketobutyrate, to HE-ThDP which gives α-acetolactate or α-acetohydroxybutyrate, respectively (Lonhienne *et. al*., 2017). In addition, there has been reported that AHAS can also convert pyruvate into other chiral pharmaceutical precursors, such as R-phenylacetylcabinol (PAC) for ephedrine and pseudoephedrine synthesis and other chiral hydroxyketones (Engel *et. al.,* 2003; Engel *et. al.,* 2004).

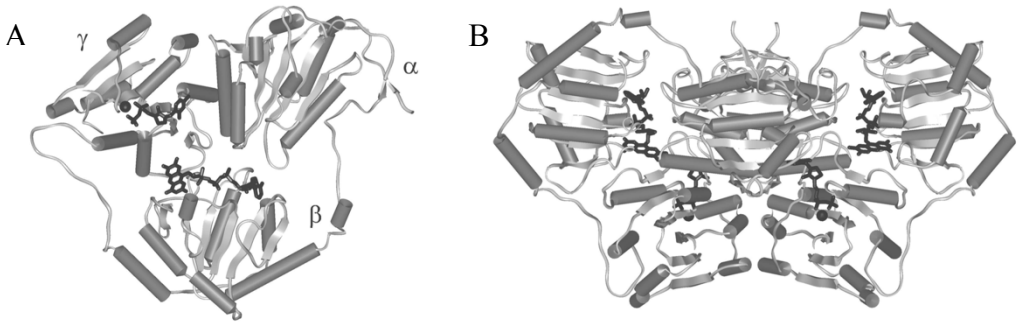

Figure 1-5 The three-dimensional structures of the yeast AHAS catalytic subunit.

(A) The AHAS monomer is folded into three domains designated α, β and γ. (B) In the AHAS dimer, the α and γ domains of each subunit associate with each other to form the central core of the enzyme with the β domains on either side. Cofactors $^{2+}$ ThDP and FAD are depicted as stick model and Mg as CPK sphere (originally from Pang *et. al.,* 2002).

The activity of AHAS is negatively regulated by valine, one of the final products of BCAAs biosynthesis, via the process known as feedback inhibition. First, the *E. coli* AHAS subunits were purified for biochemical studies of the enzymatic activities of individual subunits. The AHAS activity of the catalytic subunit alone is unaffected by high BCAAs concentrations, indicating a significant role of the regulatory subunit in feedback regulation (Hill *et. al*., 1997). In the yeast AHAS, 0.1 M valine inhibits the AHAS activity to 10 - 15% (similar to the activity of the catalytic subunit alone) only when the catalytic and regulatory subunits are reconstituted. Valine derivatives, such as *N*-acetylvaline, *N*-methylvaline, and valinamide, has no effect on the AHAS activity, suggesting that valine binds to the regulatory subunit in a specific manner. Taken together, the AHAS regulatory subunit Ilv6 is essential for the feedback inhibition by valine and for the full enzymatic activity (Pang and Duggleby, 2001).

b) BCAAs aminotransferase (BCAT)

BCAT (EC 2.6.1.42) catalyzes transfer of an α-amino group to α-keto acids KIV, KIC and KMV to produce valine, leucine and isoleucine, respectively. Thus, BCAT acts as a hub that links energy metabolism and amino acids metabolism. In eukaryotic organisms, there are two isoforms of BCATs: mitochondrial BCAT (mBCAT) and cytosolic BCAT (cBCAT),

which correspond to Bat1 and Bat2 in *S. cerevisiae*, respectively (Figure 1-6). Bat1 and Bat2 are homologous proteins with 77% identity, although Bat1 contains a mitochondrial target signal (MTS) at the N-terminus, which may be responsible for mitochondrial localization (Kispal *et. al*., 1996). Figure 1-6 shows Bat1 is localized into mitochondria either under amino acid starvation or in the presence of BCAAs, while Bat2 is resided in cytosol. Although it has been reported that the human BCATs function as heterodimers and homodimers (Woontner and Jaehning, 1990), only the homodimer structure is an active form in *S. cerevisiae* (Prohl *et. al.,* 2000). The transcription factor Gcn4 for general amino acid control also regulates both Bat1 and Bat2 at the transcriptional level in response to cellular utilization of nitrogen (Ben-Yosef *et. al.,* 1996).

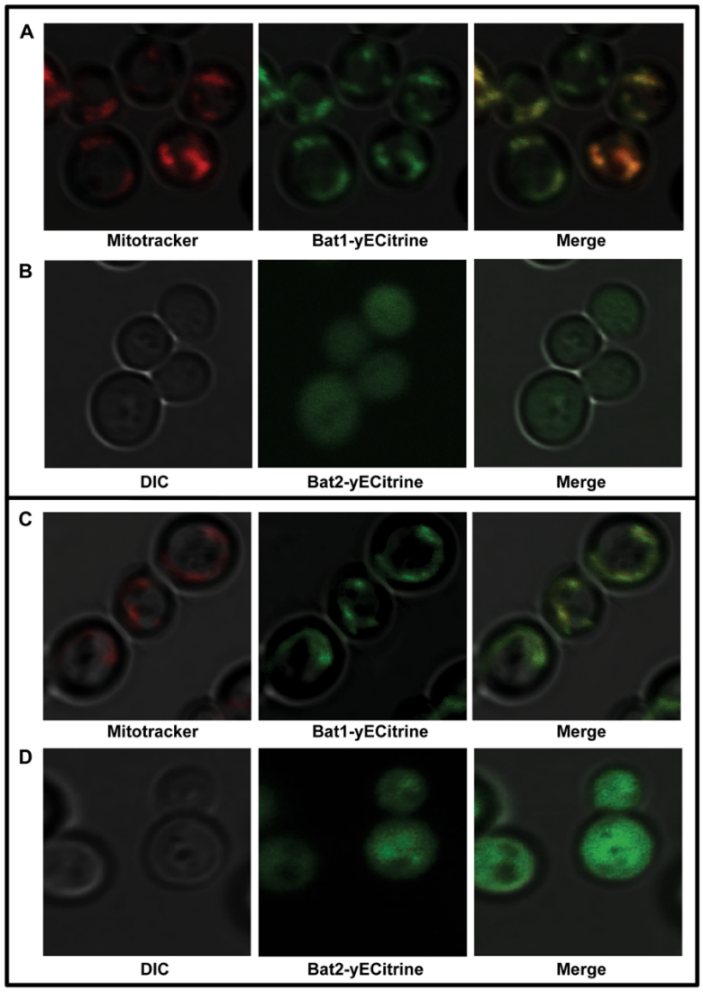

Figure 1-6 mBCAT Bat1 and cBCAT Bat2.

Fluorescent images show the subcellular localization of the paralogous Bat1 and Bat2 under glucose+ammonium (A, B) or glucose+BCAAs (C, D) conditions (originally from Colón *et. al,* 2011).

1.2.3 Valine catabolism in *S. cerevisiae*

The metabolic disorders, such as diabetes mellitus, are common diseases that caused by unusual BCAAs catabolism. Several clinical studies suggest that BCAAs supplementation enhances glycogen synthesis via energy metabolism. BCAAs also facilitate glucose uptake in liver and skeletal muscle by enhancing the expression of glucose transporters GLUT1 and GLUT4 in an insulin-dependent manner through phosphatidylinositol 3 kinase (PI3K) and protein kinase C (PKC) (Nishitani *et. al*., 2002; Doi *et. al*., 2003; Nishitani *et. al*, 2005). In addition, isoleucine and valine deprivation reduces fatty acid synthesis and enhances fatty acid oxidation by transcriptional control of key enzymes for fatty acid metabolism via the AMPK-mTORC1-FoxO1 pathway in mice (Bai *et. al*., 2015). These examples illustrate how BCAAs catabolism contributes to essential cellular signaling in mammal.

Valine and other BCAAs catabolism in *S. cerevisiae* is different from mammal in which it is related to the production of fusel acid or fusel alcohol via the Ehrlich pathway (Figure 1-7). The initial step of the fusel alcohol biosynthetic pathway is transamination by aminotransferases including BCATs. An α-keto acid is first decarboxylated to aldehyde by Aro10, Pdc1, Pdc5 and Pdc6. This fusel aldehyde is subsequently reduced into fusel alcohol. Valine is converted into isobutyrate or isobuthanol, important compounds in fermentation industries.

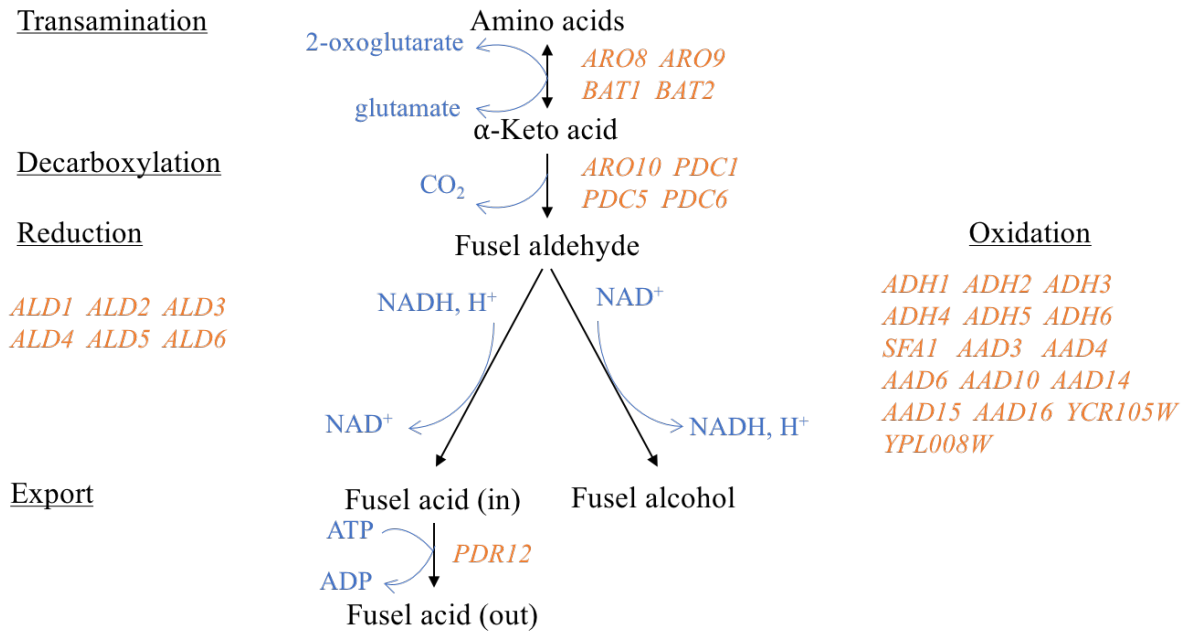

Figure 1-7 The Ehrlich pathway.

Catabolism of BCAAs (valine, leucine and isoleucine), aromatic amino acids (phenylalanine, tyrosine and tryptophan) and sulfur-containing amino acid (methionine) leads to the formation of fusel acids and fusel alcohols. The genes encoding the enzymes for individual steps are indicated (modified from Hazelwood *et. al.,* 2008).

Based on the previous information, the regulation mechanism of valine biosynthesis between *S. cerevisiae* and *E. coli* is very similar in which the process is regulated by the acetohydroxyacid synthase (AHAS) via valine feedback inhibition. There are three AHAS isozymes are found in *E. coli* (AHAS I, II and III), whereas, only one isozyme exists in *S. cerevisiae*. In case of *E. coli*, the regulation of valine biosynthesis is tended to be more complicated as compared to yeast since these three AHAS isozymes have a differ biochemical properties and regulatory mechanism (Umbarger, 1996). The enzymatic activity of *E. coli* AHAS I and AHAS III are inhibited in the presence of valine via the regulatory subunit, IlvN and IlvH, which are responsible for valine feedback inhibition. Nevertheless, the protein alignment of *E. coli* IlvN is very unique and rather different from the yeast Ilv6 in comparable to the *E. coli* IlvH (PSI-Blast: Altschul *et. al.,* 1997), therefore, the *E. coli* AHAS III is applied for study the valine feedback inhibition in yeast. In general, the primary substrate for AHAS is pyruvate, although, the *E. coli* AHAS III prefers α-ketobutyrate as the first substrate (Gallop *et. al*., 1990). Hence, in the presence of α-ketobutyrate, AHASIII prefers to synthesize isoleucine rather than valine (Pátek, 2007). Unlike bacteria, the AHAS enzymatic activity in yeast is partially inhibited by valine in which at the saturation point, increasing of

valine concentration does not further inhibit the AHAS activity (Pang and Duggleby, 1999). This result proposes the difference of AHAS regulatory subunit in eukaryote cells. However, since the crystal structure of the yeast Ilv6 has not been determined, therefore, the report on regulation of valine biosynthesis via the AHAS regulatory subunit in *S. cerevisiae* is not plentifully demonstrated.

1.3 Industrial application of valine biosynthesis and catabolism

Valine is used for industrial applications, such as animal feed, human supplementary diet, pharmaceuticals and cosmetics. Therefore, previous researches have focused on improvement of bacterial valine production in *E. coli* and *C. glutamicum*. For instance, overexpression of the genes on the valine biosynthetic pathway and blocking the competitive pathways have been performed to abolish the feedback inhibition by valine and to increase valine yields (Park *et. al.,* 2007; Park and Lee, 2010). In comparison, valine production in *S. cerevisiae* is not widely practiced for the commercial scale mainly because of low valine yields compared to *C. glutamicum*. However, the fermentative products from *S. cerevisiae* are very safe for human consumption since the cell itself as well as its products are approved by FDA, given its GRAS status (Generally Recognized As Safe). Based on its reliability and safety in food production, the development of a novel valine overproduce yeast strain may promisingly contribute to bioindustries such as high-value functional foods, drinks and feed additives.

Another applicable aspect of valine biosynthesis in *S. cerevisiae* is isobutanol production (Hazelwood *et. al.,* 2008). Isobutanol is a second-generation biofuel, which provides benefits if used instead of gasoline. At the present, the large-scale production of isobutanol is based on the chemical reaction which is the cabonylation of carbon monoxide, however, it can be produced from glucose fermentation in microorganisms. In the screening of butanol tolerance microorganisms, *S. cerevisiae* was categorized as a good candidate for industrial butanol production due to its ability to grow in the presence of 2 % butanol as well as able to ferment alcohol at high temperature (up to 43 ºC) including its ethanol tolerance phenotype (up to 14 %) as compared to *E. coli* (Knoshaug and Zhang, 2009). *S. cerevisiae* is known as a beneficial fermentative microorganism because of the ability to grow at low pH and under high substrate concentrations, both of which prevent contamination during fermentation (Peralta-Yayah *et. al.,* 2012). In the large-scale production, the saccharification

fermentation (SSF) can be performed by using dry yeast which allow the convenient fermentation and efficient productivity (Dahnum *et. al.,* 2015). In general, isobutanol is produced from the valine degradation in cytosol, therefore, the enzymes associated with valine biosynthesis has been engineered to be relocalized from mitochondria to cytosol (Brat *et. al*., 2012) (Figure 1-8). Together with the overexpression of the cytosolic enzymes, the α-keto acid decarboxylase Aro10 and the alcohol dehydrogenase Adh2, isopropanol production can be further increased (Brat *et. al.,* 2012). Alternately, compartmentalization of the Ehrlich pathway to mitochondria greatly increases the isobutanol production (Avalos *et. al.,* 2013). Concerns about the current energy crisis and global warming issues have increased interest in the production of more sustainable energy, such as biofuels. Consequently, metabolic engineering of isobutanol production from valine biosynthesis pathway is drawing more attention instead of bioethanol. In the light of this, researching on a cutting-edge technology and better understanding in valine biosynthesis regulation can be beneficial for the development of superior yeast strains tailored to needs of industrial application.

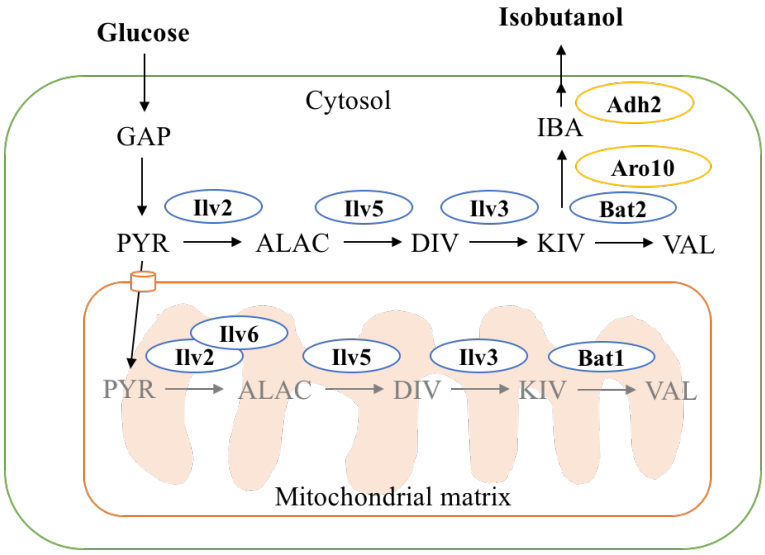

Figure 1-8 Schematic illustration of the synthetic isobutanol biosynthesis pathway

Glucose is converted to pyruvate via glycolysis. Pyruvate can be further converted into α-ketoisovalerate (KIV) in the cytosol by the relocalized Ilv2, Ilv5 and Ilv3 enzymes. KIV is metabolized into isobutanol via the Ehrlich pathway reactions catalyzed by Aro10 and Adh2. This pathway is spatially distinguished from the mitochondrial valine synthetic pathway. GAP = glyceraldehyde-β-phosphate; PYR = pyruvate; ALAC = α-acetolactate; DIV = α,β-dihydroxyisovalerate; IBA = isobutyraldehyde (modified from Brat *et. al.,* 2012).

Research objectives

In this study, the regulatory subunit of AHAS (Ilv6) and BCATs (Bat1/2) are mainly focused in order to fulfill better understanding of the regulation of valine biosynthesis in *S. cerevisiae*:

(1) Identification of amino acid residues in Ilv6 responsible for the feedback inhibition of AHAS by valine.

(2) Analysis of cellular localization of Bat1 and Bat2 to understand its significance in valine biosynthesis.

CHAPTER II
MATERIALS AND METHODS

2.1 Materials

2.1.1 Microorganisms

Saccharomyces cerevisiae and *Escherichia coli* strains used in this study are shown in Table 2-1.

Table 2-1 Strains used in this study

Strains	Description	Sources
***Saccharomyces cerevisiae* BY4741 (wild-type)**	*MATa his3Δ1 leu2Δ0 met15Δ0 ura3Δ0*	
***Escherichia coli* DH5α**	*F⁻, φ80dlacZΔM15, Δ(lacZYA-argF) U169, deoR, recA1, endA1, hdR17 (r_k^-, m_k^+), phoA, supE44, λ⁻, thi-1, gyrA96, relA1*	
Rosetta™ (DE3) pLysS	*F⁻ ompT hdS*$_B$(r_B^- m_B^-) *gal dcm* (DE3) pLysSRARE (Cam^R)	
BY4741 Δ*bat1*	BY4741 Δ*bat1::kanMX6*	This work
BY4741 Δ*bat2*	BY4741 Δ*bat2::kanMX6*	This work
BY4741 Δ*bat1* Δ*bat2*	BY4741 Δ*bat1::hphNT1* Δ*bat2::kanMX6*	This work
BY4741 Δ*aro10*	BY4741 Δ*aro10::hphNT1*	This work
BY4741 Δ*bat2* Δ*aro10*	BY4741 Δ*bat2::kanMX6* Δ*aro10::hphNT1*	This work
BY4741 [pRS416/pRS415-Cg*HIS3MET15*]	BY4741 harboring pRS416 and pRS415-Cg*HIS3MET15*	This work
BY4741 [pRS416/pRS415]	BY4741 harboring pRS416 and pRS415	This work
BY4741 [pRS416-N86A/pRS415-Cg*HIS3MET15*]	BY4741 harboring pRS416 with Ilv6 (Asn86Ala) and pRS415-Cg*HIS3MET15*	This work
BY4741 [pRS416-G89D/pRS415-Cg*HIS3MET15*]	BY4741 harboring pRS416 with Ilv6 (Gly89Asp) and pRS415-Cg*HIS3MET15*	This work

Table 2-1 Strains used in this study (continued)

Strains	Description	Sources
BY4741 [pRS416-N104H/pRS415-Cg*HIS3MET15*]	BY4741 harboring pRS416 with Ilv6 (Asn104His) and pRS415-Cg*HIS3MET15*	This work
BY4741 [pRS416-V132I/pRS415-Cg*HIS3MET15*]	BY4741 harboring pRS416 with Ilv6 (Va132Ile) and pRS415-Cg*HIS3MET15*	This work
BY4741 [pRS416-I255A/pRS415-Cg*HIS3MET15*]	BY4741 harboring pRS416 with Ilv6 (Ile255Ala) and pRS415-Cg*HIS3MET15*	This work
BY4741 [pRS416-I255R/pRS415-Cg*HIS3MET15*]	BY4741 harboring pRS416 with Ilv6 (Ile255Arg) and pRS415-Cg*HIS3MET15*	This work
BY4741 [pRS416-M276A/pRS415-Cg*HIS3MET15*]	BY4741 harboring pRS416 with Ilv6 (Met276Ala) and pRS415-Cg*HIS3MET15*	This work
BY4741 [pRS416-M276D/pRS415-Cg*HIS3MET15*]	BY4741 harboring pRS416 with Ilv6 (Met276Asp) and pRS415-Cg*HIS3MET15*	This work
BY4741 [pRS416-*BAT1-GFP*/pRS415]	BY4741 harboring pRS416 with Bat1-GFP tagged and pRS415	This work
BY4741 [pRS416-*bat1*^{K219A}/pRS415]	BY4741 harboring pRS416 with Bat1^{K219A} and pRS415	This work
BY4741 [pRS416 *BAT1*Δ*N18-GFP*/ pRS415]	BY4741 harboring pRS416 with Bat1ΔN18-GFP tagged and pRS415	This work
BY4741 [pRS416 *BAT1*Δ*N24-GFP*/ pRS415]	BY4741 harboring pRS416 with Bat1ΔN24-GFP tagged and pRS415	This work
BY4741 [pRS415 *BAT1*Δ*N30-GFP*/ pRS415]	BY4741 harboring pRS416 with Bat1ΔN30-GFP tagged and pRS415	This work
BY4741 [pRS415 *BAT2*+MTS-*GFP*/ pRS416]	BY4741 harboring pRS415 with Bat2+MTS-GFP tagged and pRS416	This work
BY4741 [pRS415-*bat2*^{K202}/pRS416]	BY4741 harboring pRS415 with Bat2^{K202A} and pRS416	This work
BY4741 Δ*bat1* Δ*bat2* [pRS416-*bat1*^{K219A}/ pRS415]	Δ*bat1*Δ*bat2* harboring pRS416 with Bat1^{K219A} and pRS415	This work
BY4741 Δ*bat1* Δ*bat2* [pRS416 *BAT1*Δ*N18-GFP*/pRS415]	Δ*bat1*Δ*bat2* harboring pRS416 with Bat1ΔN18-GFP tagged and pRS415	This work
BY4741 Δ*bat1* Δ*bat2* [pRS416 *BAT1*Δ*N24-GFP*/pRS415]	Δ*bat1*Δ*bat2* harboring pRS416 with Bat1ΔN24-GFP tagged and pRS415	This work
BY4741 Δ*bat1* Δ*bat2* [pRS416 *BAT1*Δ*N30-GFP*/pRS415]	Δ*bat1* Δ*bat2* harboring pRS416 with Bat1ΔN30-GFP tagged and pRS415	This work
BY4741 Δ*bat1* Δ*bat2* [pRS415-*bat2*^{K202}/ pRS416]	Δ*bat1* Δ*bat2* harboring pRS415 Bat2^{K202A} and pRS416	This work

Table 2-1 Strains used in this study (continued)

Strains or plasmids	Description	Sources
BY4741 Δ*bat1* Δ*bat2* [pRS415 *BAT2*+MTS-*GFP*/pRS416]	Δ*bat1* Δ*bat2* harboring pRS415 with Bat2+MTS-GFP tagged and pRS416	This work
***Escherichia coli* DH5α for plasmid multimerization**	*E. coli* DH5α harboring all constructed pRS416 and pRS415 plasmids	This work
Rosetta™ (DE3) pLysS for protein expression	Rosetta™ (DE3) pLysS harboring all constructed pET-53-DEST plasmids	This work

2.1.2 Primers

Primers used in this study are shown in Table 2-2.

Table 2-2 Primers used in this study. Restriction sites are underlined

Primers	Sequences (5′– 3′)	Restriction sites
F-*ILV2*-500bp-SmaI	5’-TTTCCCGGGTTGCCACTAATACCATAATT-3’	*Sma*I
R-*ILV2*-500bp-NotI	5’-TTTGCGGCCGCATCAAAAGTAGCTTTCTTGA-3’	*Not*I
F-*ILV6*-500bp-SmaI	5’-TTTCCCGGGAGAACCATTTACGAGCCGTT-3’	*Sma*I
R-*ILV6*-500bp-NotI	5’-TTTGCGGCCGCTGACTGATTCAACATCAACGAC-3’	*Not*I
F-*ILV2*-attB1-2	5’-GGGGCAACTTTGTACAAAAAAGTTGTAATGCCA GAGCCTGCTCCAAGTTT-3’	
F-*ILV2*-attB1-2 w/o transit peptides	5’-GGGGCAACTTTGTACAAAAAAGTTGTAATGCCA GAGCCTGCTCCAAGTTT-3’	
R-*ILV2*-attB1	5’-GGGGACCACTTTGTACAAGAAAGCTGGGTCTCAG TGCTTACCGCCTGT-3’	
F-*ILV6*-attB1-2	5’-GGGGCAACTTTGTACAAAAAAGTTGTAATGG CAA CAAGACCTCCCTTGCC-3’	
F-*ILV6*-attB1-2 w/o transit peptides	5’- GGGGCAACTTTGTACAAAAAAGTTGTAATGG CAACAAGACCTCCCTTGCC-3’	
R-*ILV6*-attB1	5’- GGGGCAACTTTGTACAACAAAGTTGCCTAAC CAGGTGGTAGTTGGG-3’	
F-*ILV2*-si1	5’- GTAATTTGTATTGTTTTTTTCCTTC-3’	
R-*ILV2*-si1	5’- CTTAATTTTAGCCGTCATTAGTTT-3’	
F-*ILV2*-si3	5’- ACCAATTAACCAGTCGCG-3’	
R-*ILV2*-si3	5’- TAATACCACCTCTACCCTCG-3’	
F-*ILV6*-Si1	5’- CCATAAAAAATATTTTTTTAACCTT-3’	
R-*ILV6*-Si1	5’- TCACCTCGTACAAACGTACA-3’	

Table 2-2 Primers used in this study. Restriction sites are underlined (continued)

Primers	Sequences (5′– 3′)	Restriction sites
***ILV6*-N(86)A-F** ***ILV6*-N(86)A-R**	5'- CTGTTTGGTGCAAGCCGAACCCGGTGTC-3' 5'- GACACCGGGTTCGGCTTGCACCAAACAG-3'	
***ILV6*-G(89)D-F** ***ILV6*-G(89)D-R**	5'- CAAAACGAACCCGATGTCTTGTCCAGAG-3' 5'-CTCTGGACAAGACATCGGGTTCGTTTTGC-3'	
***ILV6*-N(104)H-F** ***ILV6*-N(104)H-R**	5'- GCCAGAGGCTTTCACATCGATTCGTTG-3' 5'-CAACGAATCGATGTGAAAGCCTCTGGC-3'	
***ILV6*-V(132)I-F** ***ILV6*-V(132)I-R**	5'- AAGATGGCGTAATCGAACAAGCACGCAGA-3' 5'-TCTGCGTGCTTGTTCGATTACGCCATCTT-3'	
***ILV6*-I(255)A-F** ***ILV6*-I(255)A-R**	5'-GCAAAACCCACACGTGCCTCTGCCTTCTTG AAG-3' 5'-CTTCAAGAAGGCAGAGGCACGTGTGGGTTT TGC-3'	
***ILV6*-I(255)R-F** ***ILV6*-I(255)R-R**	5'- GCAAAACCCACACGTCGTTCTGCCTTCTTG AAG-3' 5'- CTTCAAGAAGGCAGAACGACGTGTGGGTTT TGC-3'	
***ILV6*-M(276)A-F** ***ILV6*-M(276)A-R**	5'- GCAAGAAGCGGTATGGCCGCATTGCCAAGA ACT-3' 5'- AGTTCTTGGCAATGCGGCCATACCGCTTCTT GC-3'	
***ILV6*-M(276)D-F** ***ILV6*-M(276)D-R**	5'- GCAAGAAGCGGTATGGACGCATTGCCAAGA ACT-3' 5'-ATTCTTGGCAATGCGTCCATACCGCTTCTT GC-3'	
***BAT1-kanMX6*-F** ***-hphNT1*-F** ***BAT1-kanMX6*-R** ***-hphNT1*-F**	5'TATAAACGCAAAATCAGCTAGAACCTTAGCAT ACTAAAACCGTACGCTGCAGGTCGAC-3' 5'TTTTTTTTGGGGGGGGAGGGGATGTTTACCTTC ATTATCAATCGATGAATTCGAGCTCG-3'	
***BAT2-kanMX6*-F** ***BAT2-kanMX6*-R**	5'AAATTTAAGGGAAAGCATCTCCACGAGTTTTA AGAACGATCGTACGCTGCAGGTCGAC-3' 5'AAAATTGAAAATTAATGAAATGCATCGTTATC GCTATGAGAATTCGAGCTCGTTTAAAC-3'	
***ARO10-hphNT1*-F** ***ARO10-hphNT1*-R**	5'-TAAAGTTTATTTACAAGATAACAAAGAAACTCCC TTAAGCCGTACGCTGCAGGTCGAC-3' 5'TGTTAACCATCGTCACAAAATATTAACGCGGGTGT TCAAAGAATTCGAGCTCGTTTAAAC-3'	
F-*BAT1*-500bp-SmaI ***BAT1*-500bpUP-RV**	5'-TTTCCCGGGTATCAATAGTAAGGCTCGCA-3' 5'- GTTTTAGTATGCTAAGGTTC-3'	*Sma*I

Table 2-2 Primers used in this study. Restriction sites are underlined (continued)

Primers	Sequences (5′– 3′)	Restriction sites
***BAT1*ΔN18-FW**	5'-GAACCTTAGCATACTAAAACATGACTGGTGCCCC ATTAGATGCATCCAA-3'	
***BAT1*ΔN24-FW**	5'-GAACCTTAGCATACTAAAACATGGCATCCAAACT AAAAATTAC-3'	
***BAT1*ΔN30-FW**	5'-GAACCTTAGCATACTAAAACATGACTAGAAACCC AAATCCATC-3'	
***BAT1*-GFP-RW**	5'-CACCAGCACCTGCTCCGGATCCGTCGACCTGCAG CGTACGGTTCAAGTCGGCAACAGTTT-3'	
***BAT1*-500bpDW-FW**	5'- TAATGATAATGAAGGTAAAC-3'	
R-*BAT1*-500bp-NotI	5'-TTTGCGGCCGCGTTTAAATCAGGATTATGGAC-3'	*Not*I
GFP-FW (S3)	5'-CGTACGCTGCAGGTCGAC-3'	*Sma*I
GFP-*BAT1*-RV	5'-TTTTTGGGGGGGGAGGGGATGTTTACCTTCATT ATCATTATTATTTGTACAATTCATCCA-3'	
F-*BAT2*-500bp-SmaI	5'-TTTCCCGGGCGCTCCTTTCCAAACATCTT-3'	*Sma*I
***BAT2*-500bpUP-RV**	5'- ATCGTTCTTAAAACTCGTG-3'	
***BAT2*-MTS-FW**	5'-AGTTTTAAGAACGATATGTTGCAGAGACATT CCTTGAAGTTGGGGAAATTCTCCATCAGAACAC TCGCTACTGGTGCCCCATTAGATACCTTGGCACC CC-3'	
***BAT2*-GFP-RW**	5'-CACCAGCACCTGCTCCGGATCCGTCGACCTGC AGCGTACGGTTCAAATCAGTAACAACCC-3'	
GFP-FW (S3)	5'-CGTACGCTGCAGGTCGAC-3'	
GFP-*BAT2*-RV	5'-TTAACTTTTAATTACTTTACGTAGCAATAGCGAT ACTTCATTATTTGTACAATTCATCCA-3'	
***BAT2*-500bpDW-FW**	5'- AGTATCGCTATTGCTACGTA-3'	
R-*BAT2*-500bp-NotI	5'-TTTGCGGCCGCTCTAAGTGGGATAGGGGTAGTG-3'	*Not*I
***BAT1*(K219A)-FW**	5'-TTGGCGACAAAGCATTGGGTGCTA-3'	
***BAT1*(K219A)-RV**	5'-TAGCACCCAATGCTTTGTCGCCAA-3'	
***BAT2*(K202A)-FW**	5'-TGGTGACAAGGCACTAGGTGCAA-3'	
***BAT2*(K202A)-RV**	5'-TTGCACCTAGTGCCTTGTCACCA-3'	
***BAT1*-Si1-F**	5'-GATCCATATTGCCTTCTTATGA-3'	
***BAT1*-Si1-R**	5'-TCTTATAATAAATAAACTCAACAGG-3'	
***BAT1*-Si2-F**	5'-ATACTATCACCATGTTCCGTC-3'	
***BAT1*-Si2-R**	5'-ATTCCTTCTTGCCAGTGACT-3'	
***BAT2*-Si1-F**	5'-GATATTCGACTATTTCCTGGG-3'	
***BAT2*-Si1-R**	5'-CAGTAACTTCGCCTATAGTGAAGTA-3'	
***BAT2*-Si4-F**	5'-ATTACAAAACTGGATTTAAGGCGGTC-3'	
***BAT2*-Si2-R**	5'-GAACTAAGCACTTATCTTGCTGG-3'	
***BAT1+2*-GFP-R**	5'-TAATTCAACCAAAATTGGGA-3'	

2.1.3 Plasmids

Plasmids used in this study are shown in Table 2-3.

Table 2-3 Plasmids used in this study

Plasmids	Description	Sources
pRS415	yeast centromere vector pRS415-*LEU2*	
pRS415-Cg*HIS3MET15*	yeast centromere vector pRS415-*LEU2HIS3MET15*	
pRS416	yeast centromere vector pRS416-*URA3*	
pRS415-*BAT2-GFP*	pRS415 harboring *BAT2* with GFP tagged	This work
pRS415-*BAT2+MTS-GFP*	pRS415 harboring *BAT2+MTS* with GFP tagged	This work
pRS415-*BAT2*^{K202A}	pRS415 harboring *BAT2*^{K202A}	This work
pRS416-*BAT1-GFP*	pRS416 harboring *BAT1* with GFP tagged	This work
pRS416-*BAT1*Δ*N18-GFP*	pRS416 harboring *BAT1-MTS* with GFP tagged	This work
pRS416-*BAT1*Δ*N24-GFP*	pRS416 harboring *BAT1-MTS* with GFP tagged	This work
pRS416-*BAT1*Δ*N30-GFP*	pRS416 harboring *BAT1-MTS* with GFP tagged	This work
pRS416-*ILV2*	pRS416 harboring *ILV2*	This work
pRS416-*ILV6*	pRS416 harboring *ILV6*	This work
pRS416-*ILV6* (N86A)	pRS416 harboring Ilv6 point mutation (Asn86Ala)	This work
pRS416-*ILV6* (G89D)	pRS416 harboring Ilv6 point mutation (Gly89Asp)	This work
pRS416-*ILV6* (N104H)	pRS416 harboring Ilv6 point mutation (Asn104His)	This work
pRS416-*ILV6* (V132I)	pRS416 harboring Ilv6 point mutation (Val132Ile)	This work
pRS416-*ILV6* (I255A)	pRS416 harboring Ilv6 point mutation (Ile255Ala)	This work
pRS416-*ILV6* (I255R)	pRS416 harboring Ilv6 point mutation (Ile255Arg)	This work

Table 2-3 Plasmids used in this study (continued)

Plasmids	Description	Sources
pRS416-*ILV6* (M276A)	pRS416 harboring Ilv6 point mutation (Met276Ala)	This work
pRS416-*ILV6* (M276D)	pRS416 harboring Ilv6 point mutation (Met276Asp)	This work
pDONR221	Gateway® donor vector with attP1 and attP2 sites, KAN^R	Gateway®
pET-53-DEST	Gateway® bacterial destination vector for expressing proteins with 6X-His affinity tagged	Gateway®
pDONR221-*ILV2*	pDONR221 harboring *ILV2* without stop codon	This work
pDONR221-*ILV6*	pDONR221 harboring *ILV6* without stop codon	This work
pDONR221-*ILV2*Δ*N54*	pDONR221 harboring *ILV2* without stop codon and transit peptides	This work
pDONR221-*ILV6*Δ*N40*	pDONR221 harboring *ILV6* without stop codon and transit peptides	This work
pDONR221-*ILV6*Δ*N40* (N86A)	pDONR221 harboring mutated *ILV6* (Asn86Ala) without stop codon and transit peptides	This work
pDONR221-*ILV6*Δ*N40* (G89D)	pDONR221 harboring mutated *ILV6* (Gly89Asp) without stop codon and transit peptides	This work
pDONR221-*ILV6*Δ*N40* (N104H)	pDONR221 harboring mutated *ILV6* (Asn104His) without stop codon and transit peptides	This work
pET-53-DEST-*ILV2*	pET-53-DEST harboring *ILV2* without stop codon	This work
pET-53-DEST-*ILV6*	pET-53-DEST harboring *ILV6* without stop codon	This work
pET-53-DEST-*ILV2*Δ*N54*	pET-53-DEST harboring *ILV2* without stop codon and transit peptides	This work
pET-53-DEST-*ILV6*Δ*N40*	pET-53-DEST harboring *ILV6* without stop codon and transit peptides	This work
pET-53-DEST-*ILV6*Δ*N40* (N86A)	pET-53-DEST harboring mutated *ILV6* (Asn86Ala) without stop codon and transit peptides	This work

Table 2-3 Plasmids used in this study (continued)

Plasmids	Description	Sources
pET-53-DEST-*ILV6*Δ*N40* (G89D)	pET-53-DEST harboring mutated *ILV6* (Gly89Asp) without stop codon and transit peptides	This work
pET-53-DEST-*ILV6*Δ*N40* (N104H)	pET-53-DEST harboring mutated *ILV6* (Asn104His) without stop codon and transit peptides	This work

2.2 Methods

2.2.1 Strains and culture conditions

S. cerevisiae BY4741 (derived from S288c) was used as a host in this study. The wild-type strain was grown in YPD medium (10 g/L yeast extract, 20 g/L peptone and 20 g/L glucose) at 30 °C. *S. cerevisiae* Δ*bat1*, Δ*bat2*, Δ*aro10* and double disruption strains were cultured in YPD containing 150 μg/mL geneticin or 50 μg/mL hygromycin B (Table 2-1). Synthetic dextrose minimal (SD) medium (1.7 g/L yeast nitrogen base without amino acid and ammonium sulfate, 5 g/L ammonium sulfate and 20 g/L glucose, pH 6.0) was used for *S. cerevisiae* BY4741 cells harboring pRS416 and pRS415-Cg*HIS3MET15*, and SD medium supplemented with histidine and methionine (20 mg/L) was used for cells harboring pRS416 and pRS415 to maintain the transformant status. In addition, ammonium sulfate was omitted for preparation of SD medium without nitrogen source.

S. cerevisiae Δ*bat1*, Δ*bat2*, Δ*bat1* Δ*bat2*, Δ*aro10* and Δ*bat2* Δ*aro10* were constructed by PCR-mediated gene disruption. PCR toolbox (Janke *et. al*., 2004) was employed in this study using pFA6a-*kanMX6* and pFA6a-*hphNT1* as a template for amplification of the *kanMX6* and *hphNT1* cassettes. The primers used in this section were shown in Table 2-2. Target gene was replaced by the *kanMX6* or *hphNT1* cassette using high-efficiency transformation method (Burke *et. al*., 2000) based on homologous recombination. Transformants were selected on YPD medium containing 150 μg/mL geneticin or 50 μg/mL hygromycin B.

E. coli DH5α was grown at 37 °C in LB medium, which contains 5 g/L yeast extract, 10 g/L tryptone and 10 g/L NaCl. SOB (20 g/L tryptone, 5 g/L yeast extract, 10 mM NaCl, 2.5 mM KCl, 10 mM $MgSO_4$, 10 mM $MgCl_2$) and SOC media (SOB supplemented with 20 mM glucose) were used for competent cells preparation and transformation (Inoue *et. al*., 1990). 100 µg/mL of ampicillin was added to the LB medium to maintain the transformant status. The strains and plasmids used in this study are described in Table 2-3.

Rosetta™ (DE3) pLysS was used as a host for protein expression. Competent cells were prepared in the same manner as in *E. coli* DH5α (Inoue *et. al*., 1990). Seed culture preparation was carried out by growing the cells harboring pET-53-DEST expression vector (Table 2-3) in LB medium containing 100 µg/mL ampicillin and 30 µg/mL chloramphenicol at 30 ºC and 37 ºC for main culture. Cells were cultured at 18 ºC after 100 µM final concentration of isopropyl β-D-1-thiogalactopyranoside (IPTG) was added to induce the protein expression under the high aeration rate by shaking at 250 rpm.

2.2.2 Plasmids and DNA preparation

2.2.2.1. DNA preparation

The *S. cerevisiae* genomic DNA was prepared as follows; yeast cells were grown in YPD medium, harvested and resuspended in 300 µL of lysis buffer (100 mM Tris-HCl pH 8.0, 100 mM NaCl and 10 mM EDTA), and then, 250 µL of phenol/chloroform was added. An equal volume of 0.5 mm diameter glass beads were added to the mixture, and cells were disrupted by the multi-beads shocker (Multi-Beads Shocker, Yasui Kikai, Japan) under a following condition: 1,500 rpm, 30-sec on and 30-sec off, 2 cycles. For plasmid preparation, cells were grown in LB medium containing appropriated antibiotic, harvested and resuspended in 250 µL of P1 buffer (50 mM Tris-HCl pH 8.0, 10 mM EDTA and 100 µg/mL RNase A). 250 µL of P2 buffer (200 mM NaOH and 1% sodium dodecyl sulfate (SDS)) was added to the cell suspension and slightly mixed. Subsequently, 350 µL of N3 buffer (4.2 M guanidinium chloride and 0.9 M potassium acetate, pH 4.0) was added and centrifuged at a maximum speed for 10

min. Supernatant was transferred to a clean 1.5 ml tube where an equal volume of isopropanol was added, vortexed thoroughly and centrifuged at a maximum speed for 5 min. Plasmid pellet was washed by 500 μL of 70% ethanol, centrifuged in the same manner and dried up. Appropriate volume of milli-Q was used for resuspension. Finally, yeast genomic DNA and plasmid was quantified by Nanodrop (BioSpec-nano, Shimadzu Biotech, Japan).

2.2.2.2. Construction of yeast shuttle vectors

Yeast centromere plasmids (YCp) were employed for the construction of shuttle vectors in this study: pRS415 and pRS416 containing *S. cerevisiae LEU2* and *URA3* as selection markers, respectively. The *ILV2*, *ILV6*, *BAT1* and *BAT2* genes were amplified from *S. cerevisiae* BY4741 genomic DNA by KOD FX DNA polymerase (Toyobo, Osaka, Japan), and subsequently cut and inserted to pRS416 at the *Sma*I and *Not*I sites (see Table 2-2 for primers used in this study). To introduce the amino acid substitutions on Ilv6, Bat1 and Bat2, site-directed mutagenesis was employed using mutagenic primer pairs (Table 2-2), and then PCR products were digested with *Dpn*I before introduction to *E. coli* DH5α. Transformants were screened on LB medium containing 100 μg/mL ampicillin and confirmed by DNA sequencing. Furthermore, pRS415-Cg*HIS3MET15* (kindly provided by Dr. Susumu Morigasaki) was co-transformed with the constructed pRS416-based plasmids to complement the auxotrophic phenotype of *S. cerevisiae* BY4741.

Plasmids harboring native Bat1, Bat1-MTS, native Bat2 and Bat2+MTS tagged with GFP were constructed by PCR (see Table 2-2 for primers used for these constructions) as shown in Figure 2-1. PCR products were cut and inserted to pRS416 for Bat1 series or to pRS415 for Bat2 series at the *Sma*I and *Not*I sites. Transformants of DH5α were selected on LB medium containing 100 μg/mL ampicillin based on blue-white colony screening (40 μL of 100 mM IPTG and 120 μL of 20 mg/mL 5-bromo-4-chloro-3-indolyl-β-D-galactopyranoside (x-gal) were spread on the media). Plasmids were subsequently transformed to the wild-type strain for protein localization observation or to the Δ*bat1* Δ*bat2* strain for phenotypic study.

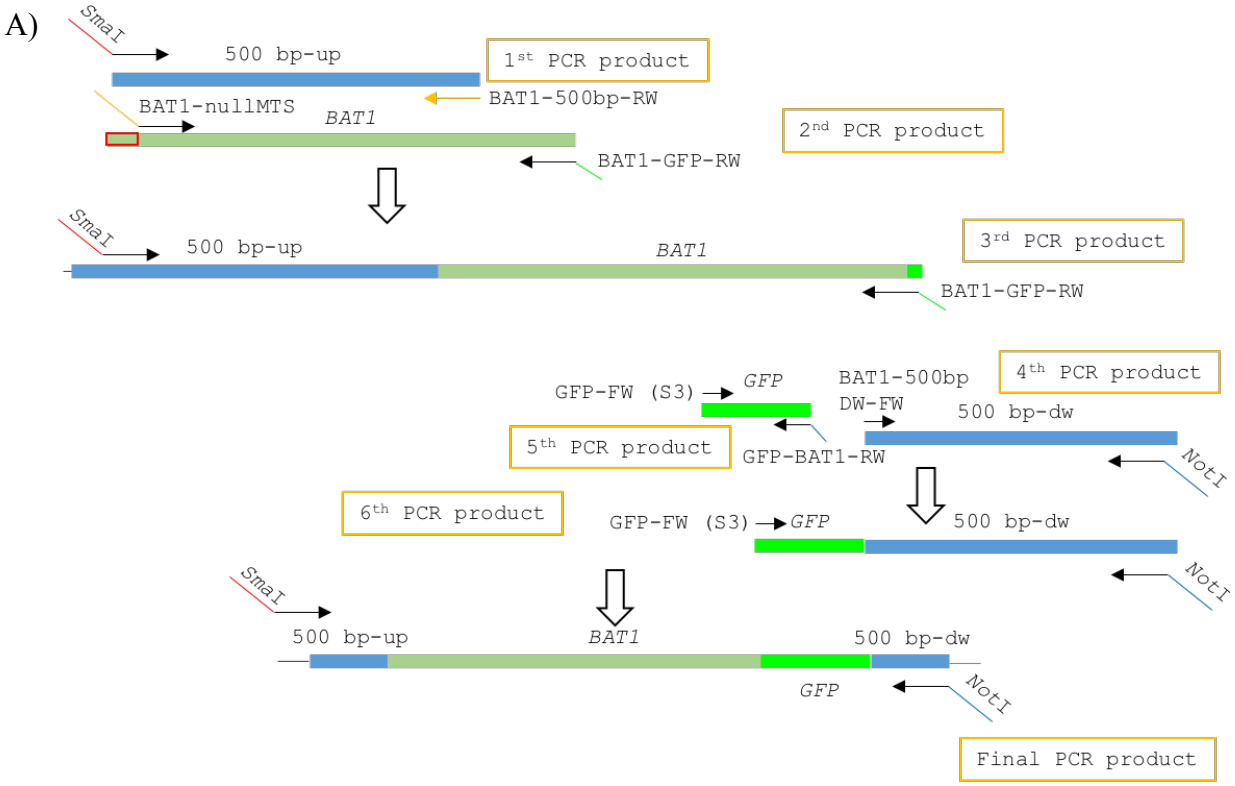
A)
SmaI
500 bp-up
1st PCR product
BAT1-500bp-RW
BAT1-nullMTS
BAT1
2nd PCR product
BAT1-GFP-RW
SmaI
500 bp-up
BAT1
3rd PCR product
BAT1-GFP-RW
GFP-FW (S3)
GFP
BAT1-500bp
DW-FW
4th PCR product
500 bp-dw
5th PCR product
GFP-BAT1-RW
NotI
6th PCR product
GFP-FW (S3)
GFP
500 bp-dw
NotI
SmaI
500 bp-up
BAT1
500 bp-dw
GFP
NotI
Final PCR product

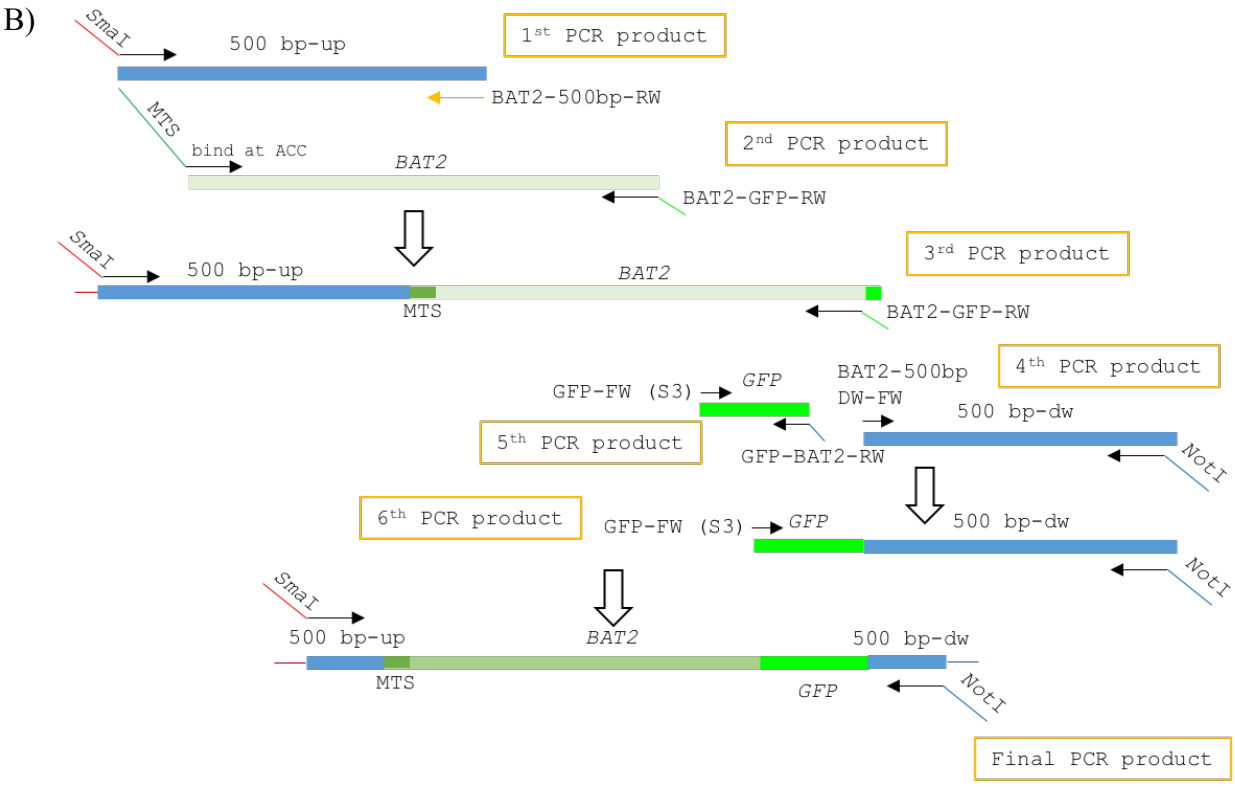
B)
SmaI
500 bp-up
1st PCR product
BAT2-500bp-RW
MTS
bind at ACC
BAT2
2nd PCR product
BAT2-GFP-RW
SmaI
500 bp-up
BAT2
3rd PCR product
MTS
BAT2-GFP-RW
GFP-FW (S3)
GFP
BAT2-500bp
DW-FW
4th PCR product
500 bp-dw
5th PCR product
GFP-BAT2-RW
NotI
6th PCR product
GFP-FW (S3)
GFP
500 bp-dw
NotI
SmaI
500 bp-up
BAT2
500 bp-dw
MTS
GFP
NotI
Final PCR product

C)

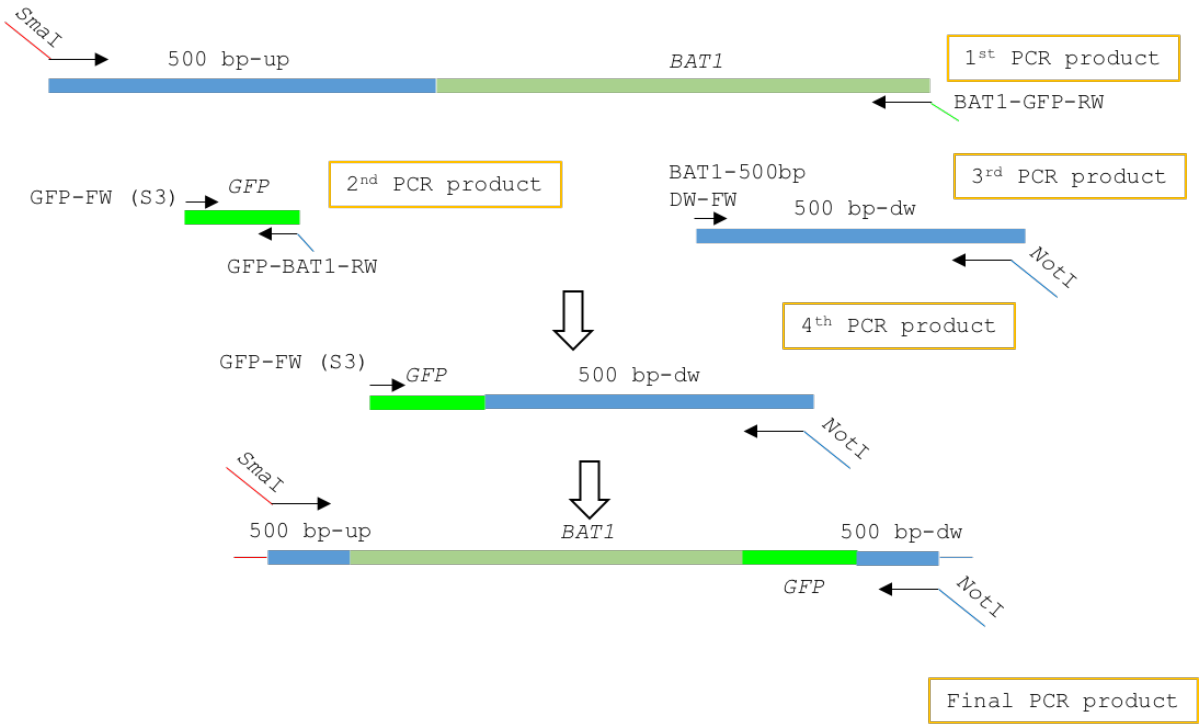

D)

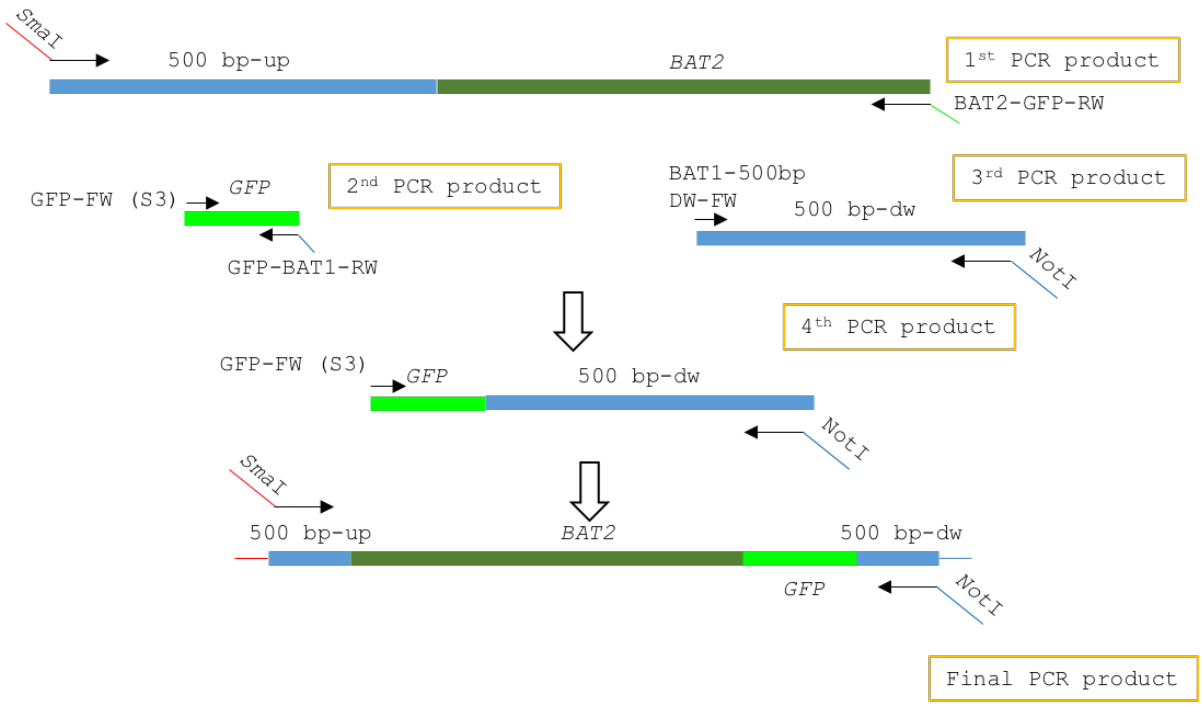

Figure 2-1. Schematic representation of construction of GFP-tagged Bat1 and Bat2 series.

(A) Bat1-GFP, (B) Bat1-MTS-GFP, (C) Bat2-GFP and (D) Bat2-MTS+GFP.

2.2.2.3. Construction of protein expression vectors

Gateway® cloning technology is employed to construct the protein expression plasmids, based on the site-specific recombination system. pDONR221 containing *att*P1 *and att*P2 was used as a donor vector in this system. pRS416 harboring wild-type *ILV2*, *ILV6* or mutant *ILV6* was used as a template for amplification with indicated primers (Table 2-3) in order to obtain the PCR products of wild-type *ILV2*, *ILV6* or mutant *ILV6* with or without the transit peptides tagged with *att*B1 and *att*B2, which react with *att*P1 *and att*P2 on pDONR221, respectively. PCR products were purified by mixing with 5 volumes of PB buffer (5 M guanidinium chloride and 30% isopropanol) and 10 µL of 3 M sodium acetate, pH 5.0. PCR mixture was applied to an FADF column and centrifuged at 13000g for 1 min, and the flow through was discarded. The column was treated with 750 µL of PE buffer (10 mM Tris-HCl, pH 7.5 and 80% ethanol) and centrifuged for 1 min to wash the purified PCR products. The flow through was discarded, and the column was centrifuged again. 50 µL of milli-Q water was applied to the column to elute purified PCR product by centrifugation. The DNA concentration was measured using Nanodrop.

Construction of pDONR221 harboring *ILV2* and *ILV6* series was carried out by mixing 75 ng/µL of pDONR221 and 75 ng/µL *att*B-PCR product within the total volume of 4 µL. Then, 1 µL of BP clonase™ II (Invitrogen, USA) was added, and incubated at 25 ºC for 1 h overnight. 0.5 µL of proteinase K solution was added to the mixture and incubated at 37 ºC for 10 min. BP clonase mixture was subsequently introduced to *E. coli* DH5α cells, which were selected on LB medium containing 50 µg/mL of kanamycin. Desired transformants were subjected to plasmid DNA extraction as described above (see 2.2.2.1). To construct the protein expression vectors, 75 ng/µL of pDONR221 harboring the *ILV2* and *ILV6* series were incubated with 75 ng/µL of pET-53-DEST and performed in the same manner as the BP clonase reaction but LR clonase™ II was used instead. Transformants were screened on LB containing 100 µg/mL of ampicillin. pET-53-DEST harboring *ILV2* and *ILV6* series were introduced to the Rosetta™ (DE3) pLysS strain.

2.2.3 DNA sequencing reaction

BigDye® Terminator v3.1 Cycle Sequencing Kit (Applied Biosystems, USA) was used for sequencing reaction. Sequencing primers of each gene were shown in Table 2-2. *ILV2*-si1-F/R and *ILV2*-si3-F/R were used for *ILV2* sequencing, and *ILV6*-Si1-FW/RV were used for *ILV6*. Native Bat1 and Bat2 without GFP were sequenced using the *BAT1*-Si1-F/*BAT1*-Si2-R and *BAT1*-Si2-F/*BAT1*-Si1-R pairs and the *BAT2*-Si1-F/*BAT2*-Si2-R and *BAT2*-Si2-F/*BAT2*-Si4-R pairs, respectively. To carry out the DNA sequencing reaction of Bat1 and Bat2 tagged with GFP, the *BAT1*-Si1-F/*BAT1*-Si2-R, *BAT1*-Si2-F/BAT1+2-GFP-R and GFP-FW (S3)/*BAT1*-Si1-R pairs were used for Bat1, and the *BAT2*-Si1-F/*BAT2*-Si1-R, *BAT2*-Si4-F/BAT1+2-GFP-R and GFP-FW (S3)/*BAT2*-Si2-R pairs were used for Bat2. 20 µL of DNA sequencing reaction consisted of 100 ng/µL of purified DNA, 3.5 µL of BigDye® Terminator v3.1 Cycle 5x sequencing buffer, 1 µL of BigDye® Terminator v3.1 Cycle sequencing reagent and 1.6 µL of 2 µM primer. PCR products were subjected to ethanol/EDTA precipitation and analyzed by a DNA sequencer (Applied Biosystem 3130xl/Genetic Analyzer, USA).

2.2.4 Screening for valine-accumulating strains

S. cerevisiae wild-type cells harboring pRS416-*ILV6* series were cultured in 5 mL of SD medium at 30 ºC for 16 h. Cells were harvested and washed with sterile distilled water, and subsequently, a 10-fold serial dilutions of each strain were prepared. 2.5 µL of each dilution was dropped on the SD medium without nitrogen source which contained 1 mg/mL or 10 mg/mL of DL-norvaline. Plates were incubated at 30 ºC for 3 days.

2.2.5 Intracellular amino acid analysis

S. cerevisiae strains were pre-cultured in 5 ml of SD medium for 16 h at 30 °C and transferred to 25 mL of SD medium for cultivation at 30 °C with shaking at 200 rpm. Yeast cells were collected at mid-log phase with OD_{600} = 10/mL. Cells were washed 3 times with sterile distilled water and resuspended

with 500 µL of sterile distilled water. Intracellular amino acids were extracted by boiling the cell suspension at 100 °C for 15 min. Cell debris was centrifuged at 13000g for 1 min and subsequently omitted by filtration using 0.2 µm syringe filter (mdi™, India). Samples were subjected to analysis by an amino acid analyzer (AminoTac™ JL500/V, USA). Intracellular amino acid concentrations were represented as percent of dry cell weight (% of DCW).

2.2.6 Effect of stress conditions on *S. cerevisiae* variants

S. cerevisiae strains were prepared in the same manner as described in section 2.2.4. Yeast cells were spotted on SD media containing sodium chloride (1 M, 1.5 M or 2 M) for salinity stress tolerance, glucose (15%, 20% or 25%) for osmotic stress tolerance and ethanol (8%, 10% or 12%) for ethanol stress tolerance. To assay freezing stress tolerance, cells were frozen at -30 ºC for 2, 4 and 7 days before dropped on SD medium. High-temperature stress tolerance was tested by incubating the medium plates at 39 ºC. All the plates were incubated for 3 days at 30 ºC except for the high-temperature stress tolerance test.

2.2.7 Protein expression and purification

Rosetta™ (DE3) pLysS cells with pET-53-DEST harboring *ILV2* and *ILV6* series were pre-cultured at 30 ºC for overnight in LB medium containing 100 µg/mL ampicillin and 30 µg/mL chloramphenicol. Cells were harvested and resuspended in the same medium. Main culture was performed by inoculating the cells into a 300 mL flask at the initial OD_{600} of 0.008 and incubating at 37 ºC. 100 µM IPTG as the final concentration was added to the main culture when OD_{600} of 0.3 - 0.4 was reached. It is noted that cells were placed on ice for 20 min before the addition of IPTG and cultured at 18 ºC for 18 h with high aeration rate by shaking at 250 rpm.

Cells were kept on ice for 5 min and then centrifuged at 4 ºC for 10 min at 5000g. Cells pellet was resuspended with ice-cold lysis buffer (20 mM Tris-HCl, pH 7.9, 500 mM NaCl containing protease inhibitor and incubated on ice for 30 min. Lysozyme (10 mg/g cells) was added to the mixture. Cell lysate

mixture was subjected to sonication (duty cycle 50%, output = 2, 30 sec/on ice 1 min for 5 cycles). Cell lysate was centrifuged at 10000g for 20 min at 4 ºC and filtrated by 0.45 µM diameter filter. 400 µL of His-accept (Nacalai, Japan) was applied to 6 ml column, washed and equilibrated with binding buffer (20mM Tris-HCl, pH 7.9, 500 mM NaCl and 5 mM imidazole). The protein solution was applied to the washed column and incubated for 1 h. It was optional to re-apply the flow through to increase protein yields. 3-fold volume of binding buffer was applied to the column to remove the unbound proteins, followed by 4-fold volume of wash buffer (20 mM Tris-HCl, pH 7.9, 500 mM NaCl and 30 mM imidazole). This step was repeated twice. Targeted-protein was eluted from the column by elution buffer (20 mM Tris-HCl, pH 7.9, 500 mM NaCl and 200 mM imidazole). Purified proteins were collected in 1.5 ml tubes containing 100 mM of dithiothreitol (DTT). In case of the purified Ilv2, potassium phosphate, pH 6.0 with the final concentration of 0.2 M was immediately added to maintain the catalytic activity.

Purified proteins can be stored according to following procedures: the purified Ilv2 was stored in the elution buffer contains 10 µM FAD and 20% glycerol. For the purified Ilv6, 0.1 M final concentration of potassium phosphate pH 7.0 and 20% glycerol were added to the buffer. Small aliquots were kept at -80 ºC. It is noted that the catalytic activity was reduced by 80% when the protein was stored overnight at 4 ºC.

2.2.8 Protein quantitative analysis and SDS-PAGE

In general, recombinant proteins are accumulated as an inclusion body in the insoluble fraction. Supernatant obtained from cell lysate and remaining pellet are referred to as soluble and insoluble fractions, respectively. To determine the expression of recombinant protein produced in Rosetta™ (DE3) pLysS, SDS-PAGE was employed. Cell lysate was resuspended in a buffer containing 100 mM Tris-HCl, pH 7.0, 5 mM EDTA, 5 mM DTT, 2 M urea and 2% (w/v) Triton X-100. Protein concentrations in both soluble and insoluble fractions were determined by Bradford protein assay using Bio-Rad Protein Assay (Bio-Rad, USA). Two-hundred µL of dye reagent was mixed with 800 µL of 100-times

diluted proteins and subjected to absorbance measurement at 595 nm. Protein concentrations were determined using a standard curve of 125 to 1,000 µg/mL of BSA. Five µg of each sample was subjected to SDS-PAGE in order to verify the expression of recombinant protein by mixing sample with 5x SDS loading buffer (250 mM Tris-HCl, pH 6.8, 10% SDS, 30% (w/v) glycerol, 10 mM DTT, 0.05% (w/v) bromophenol blue). Sample mixture was heated at 95 ºC for 10 min. 10 % SDS-polyacrylamide gel was prepared as shown in Table 2-4. Protein samples were loaded to the gel, and electrophoresis was performed at 80V, 40 mA for 10 min for stacking gel and at 110V, 40 mA for 110 min for running gel. Gel was stained with Quick-CBB (Wako, USA).

Table 2-4 Preparation of SDS-polyacrylamide gel for SDS-PAGE

Stacking gel	Running gel
942 µL of distilled water	3.83 mL of distilled water
150 µL of 40% Acrylamide (2.6%)	1.17 mL of 40% Acrylamide (2.6%)
375 µL of 0.5 M Tris-HCl, pH 6.8	1.31 mL of 2 M Tris-HCl, pH 8.8
15 µL of 10% SDS	70 µL of 10% SDS
15 µL of 10% APS	63 µL of 10% APS
3 µL of TEMED	6.3 µL of TEMED

2.2.9 Reconstitution of purified AHAS subunits and AHAS enzymatic assay

Since the product of the AHAS enzymatic reaction, α-acetolactate, is unstable and rapidly decarboxylated into acetoin, acetoin was quantified instead. The reaction mixture contained 200 mM pyruvate, 1 mM thiamine pyrophosphate (ThDP), 10 mM magnesium chloride and 10 µM FAD in 1 M potassium phosphate buffer, pH 7.0 (Pang and Duggleby, 2001). The ratio of the concentrations (nM) of AHAS catalytic subunit (Ilv2) and regulatory subunit (Ilv6) in the reaction mixture were 1:100 since large amount of Ilv6 is required for the reconstitution of AHAS. The catalytic subunit (710 nM) was used in this study. The enzyme was pre-incubated at 30 ºC for 15 min in 225 µL of reaction mixture

without pyruvate. Twenty-five μL of 2 M pyruvate was later added to the mixture, and further incubated for 20 min at 30 ºC. In case of the valine inhibitory experiment, 0.25 mM to 1 mM valine was added before the incubation. Thirty-five μL of 50% (v/v) sulphuric acid was added to stop the reaction, and further incubated at 60 ºC for 15 min to facilitate the conversion of α-acetolactate to acetoin. AHAS activity was measured by single-point colorimetry, as described by Singh *et. al*., (1988). To develop a color, 400 μL of 0.5 % (w/v) creatine and 5% (w/v) α-napthol (in 4 M sodium hydroxide) were added. This mixture was incubated at 60 ºC for 15 min and cool down to room temperature. The color mixture was subsequently measured by a spectrophotometer (U-1100 Spectrophotometer, Hitachi, Japan) at 525 nm, using the data in a reaction without enzyme as a blank. Standard acetoin was varied from 0.2 μM to 20 μM. One unit of enzymatic activity is defined as that producing 1 μmol of α-acetolactate per min under the above conditions. Specific activity is expressed as enzyme units per mg of catalytic subunit as determined by the Bradford protein assay.

2.2.10 Fluorescent microscopic observation

Wild-type yeast strains individually harboring pRS416-*BAT1-GFP*, pRS416-*BAT1*Δ*N18-GFP*, pRS415-*BAT2-GFP* and pRS415-*BAT2+MTS-GFP* were cultured in minimal media, and log-phase cells and late log-phase cells were collected. Cell pellet was washed by sterile distilled water and resuspended with sterile distilled water contains 40 nM of MitroTracker® (Invitrogen, USA). Cell suspension were incubated at 30 ºC for 30 min. Five μL of poly-L-lysine was coated on slides and dried up to promote the attachment of cells. Ten μL of cell suspension was applied on the slide, covered with coverslip and sealed with enamel coating. The localization of each protein was observed under a fluorescent microscope (Zeiss Axiovert 200M, Germany).

CHAPTER III
RESULTS

3.1 Effects of amino acid substitutions of AHAS regulatory subunit (Ilv6) on the DL-norvaline-resistance

A previous study in *E. coli* demonstrated that several amino acid substitutions in the AHAS regulatory subunit, IlvH, confer the resistance to feedback inhibition by valine (Mendel *et. al.*, 2001; Kaplun *et. al*., 2006). Since *E. coli* and *S. cerevisiae* have a similar regulatory mechanism of BCAAs biosynthesis in which the AHAS regulatory subunit is subjected to feedback inhibition by valine, the *E. coli* AHAS IlvH was used as a model in this study. The protein sequence alignment of the *E. coli* IlvH and the *S. cerevisiae* Ilv6 revealed a comparable structure at the ACT domain and the acetohydroxyacid synthase, small subunit, C-terminal (ALS ss C) domain (Figure 3-1A). Based on this, it was speculated that amino acid residues required for the resistance to feedback inhibition by valine are Asn86, Gly89, Asn104, Ile255 and Met276 of Ilv6 in *S. cerevisiae*, which are corresponding to Asn11, Gly14, Asn29, Leu131 and Val153 of IlvH in *E. coli*, respectively (Figure 3-1B). It was noticeable that Asn11, Gly14 and Asn29 are conserved among the organisms. The Asn11Ala, Gly14Asp and Asn29His substitutions were identified from the spontaneous mutants, while the Leu131Ala/Arg and Val153Ala/Asp substitutions were identified by PCR-based random mutagenesis at the C-terminal of IlvH. (Mendel *et. al.*, 2001; Kaplun *et. al*, 2006). Thus, amino acid substitutions of Ilv6 that correspond to the previously reported mutations of IlvH were introduced as follows: Asn86Ala, Gly89Asp, Asn104His, Ile255Ala/Arg and Met276Ala/Asp. Furthermore, the substitution of Val132Ile was found in a previously isolated DL-norvaline-tolerant mutant of *S. cerevisiae* S288c (unpublished results).

A

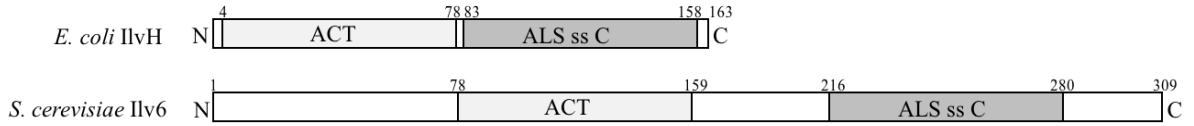

B

```
                                                                    *
E. coli  IlvH          2  RRILSVLLENESGALSRVIGLFSQRGYNIESLTVAPTDDPTLSRMTIQTVGDEKVLEQIE  61
                          + +L+ L++NE G LSRV G  + RG+NI+SL V  T+   LSRMTI   G + V+EQ
S. cerevisiae Ilv6    77  QHVLNCLVQNEPGVLSRVSGTLAARGFNIDSLVVCNTEVKDLSRMTIVLQGQDGVVEQAR  136

E. coli  IlvH         62  KQLHKLVDVLRVSELGQGAHVEREIMLVKIQASG--YGRD--------------------  99
                          +Q+  LV V  V +      ++RE+++ +I   G  Y  D
S. cerevisiae Ilv6   137  RQIEDLVPVYAVLDYTNSEIIKRELVMARISLLGTEYFEDLLLHHHTSTNAGAADSQELV  196
                                                                    ↓
E. coli  IlvH        100  ---------------------------EVKRNTEIFRGQIIDVTPSLYTVQLAGTSDKLD  132
                                                     ++   T  F G+++D++ +   V+L+    ++
S. cerevisiae Ilv6   197  AEIREKQFHPANLPASEVLRLKHEHLNDITNLTNNFGGRVVDISETSCIVELSAKPTRIS  256
                                      ↓
E. coli  IlvH        133  AFLASIRDVAKIVEVARSGVVGLSR  157
                          AFL  +     ++E ARSG++ L R
S. cerevisiae Ilv6   257  AFLKLVEPFG-VLECARSGMMALPR  280
```

Figure 3-1 The amino acid sequence alignment of AHAS regulatory subunits, the *E. coli* IlvH and the *S. cerevisiae* Ilv6.

(A) The domain structures of the *E. coli* IlvH and the *S. cerevisiae* Ilv6. The ACT domain and the ALS ss C domain were indicated by light grey and dark grey boxes, respectively. (B) Amino acid sequence alignment of *E. coli* IlvH and *S. cerevisiae* Ilv6. Open boxes, an asterisk and arrows indicate the conserved residues in the ACT domain (Asn86, Gly89 and Asn104 in Ilv6) (Mendel *et. al*, 2001), a mutation site found in a DL-norvaline-resistant mutant, which were previously identified in our lab (Val132 in Ilv6; unpublished) and two residues in the ALS ss C domain responsible for the resistance to feedback inhibition by valine in IlvH (Ile255 and Met276 in Ilv6) (Kaplun *et. al.*, 2006), respectively.

To screen Ilv6 mutations that abrogate feedback inhibition by valine, I first tested the effects of the (candidate) mutations on cell growth in the presence of DL-norvaline, which is a toxic analog of valine. It was expected that valine-accumulating mutants alleviate the toxicity of DL-norvaline. The growth test on a minimal medium that was supplemented with 0.1% allantoin as a sole nitrogen source and contained 1 mg/mL or 10 mg/mL DL-norvaline showed that among the Ilv6 variants, only Asn86Ala, Gly89Asp and Asn104His mutations showed the DL-norvaline-resistant phenotype as compared to the wild-type and the other variants (Figure 3-2A). This result suggests accumulation of intracellular valine by these mutations, which was consistent with the previous studies in *E. coli* (Mendel *et. al.*, 2001;

Kaplun *et. al.*, 2006). However, the amino acid substitution at Val132, as well as at Ile255 and Met276 in the ALS ss C domain, did not clearly contributed to the DL-norvaline resistance. Although the Val132Ile mutation was found in a DL-norvaline-resistant isolate, it was unlikely the responsible mutation. The amino acid substitutions in the ALS ss C domain of *S. cerevisiae* exhibited a different effect from the corresponding mutations in *E. coli*. Based on these results, I identified the Asn86Ala, Gly89Asp and Asn104His mutations on Ilv6 responsible for the DL-norvaline-resistant phenotype in *S. cerevisiae*. The structure of the yeast Ilv6 (based on PSI-blast and PyMOL) obviously showed that Asn86, Gly89 and Asn104 are located in the vicinity of the valine-binding site in the ACT domain (Figure 3-3). It was noticed that Asn104 binds to valine upon the dimer assembly. Since the binding of valine to these residues have not been studied well, I further tested the effects of different amino acid substitutions on Asn86, Gly89 and Asn104 on the DL-norvaline resistance. I selected several amino acids to be substituted, based on the side-chain polarity, charge and the hydropathy index (Table 3-1). Consequently, any substitution at these positions increased the DL-norvaline tolerance to the same degree (Figure 3-2B). In addition, I also found that the combination of Asn86Ala or Gly89Asp with Asn104His did not show any clear additive effects.

Table 3-1 List of amino acid substitutions at the positions 86, 89 and 104 in Ilv6

Amino acid	Side chain polarity	Side chain charge (pH 7.4)	Hydropathy index
Asn (wild-type)	polar	neutral	-3.5
Asn86Ala	nonpolar	neutral	1.8
Asn86Cys	nonpolar	neutral	2.5
Asn86Lys	polar	positive	-3.9
Asn86Thr	polar	neutral	-0.7
Gly (wild-type)	nonpolar	neutral	-0.4
Gly89Asp	polar	negative	-3.5
Gly89Val	nonpolar	neutral	4.2
Gly89Arg	polar	neutral	-4.5

Table 3-1 List of amino acid substitutions at the positions 86, 89 and 104 in Ilv6 (continued)

Amino acid	Side chain polarity	Side chain charge (pH 7.4)	Hydropathy index
Gly89Thr	polar	neutral	-0.7
Asn (wild-type)	polar	neutral	-3.5
Asn104His	polar	positive (10%), neutral (90%)	-3.2
Asn104Ala	nonpolar	neutral	1.8
Asn104Asp	polar	negative	-3.5
Asn104Cys	nonpolar	neutral	2.5

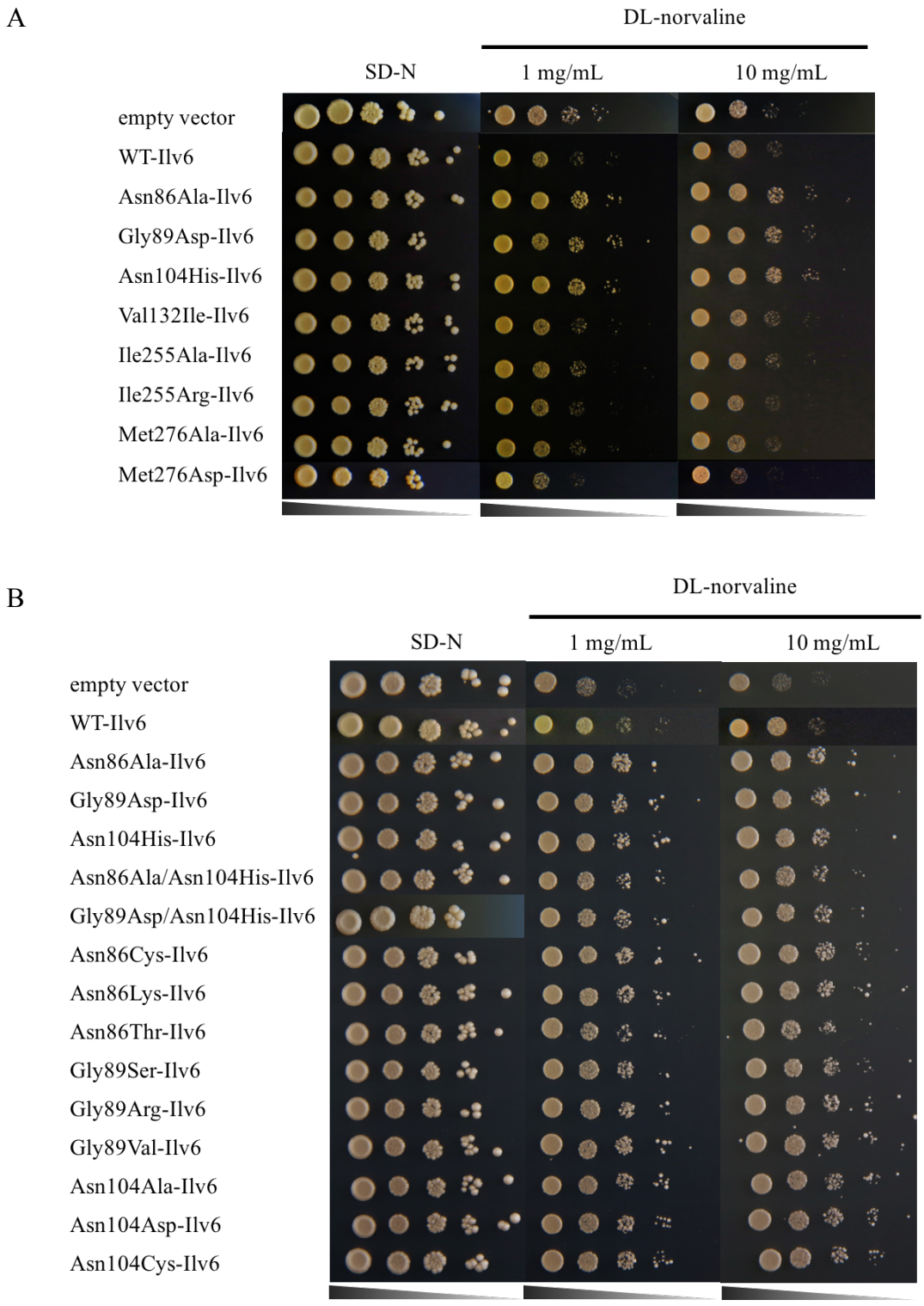

Figure 3-2 Screening of high valine-accumulating candidates.

Cell suspensions with 10-fold serial dilutions were dropped (2.5 µL each) on minimal medium (SD) that was supplemented with allantoin as a sole nitrogen source and contained 1 or 10 mg/mL DL-norvaline, and incubated at 30 °C for 3 days. (A) Effects of the amino acid substitutions, based on a previous the *E. coli* IlvH study. (B) Effects of various and combined amino acid substitutions at Asn86, Gly89, and Asn104. Wild-type (BY4741) harboring an empty vector and a plasmid pRS416-Ilv6 were used as a control.

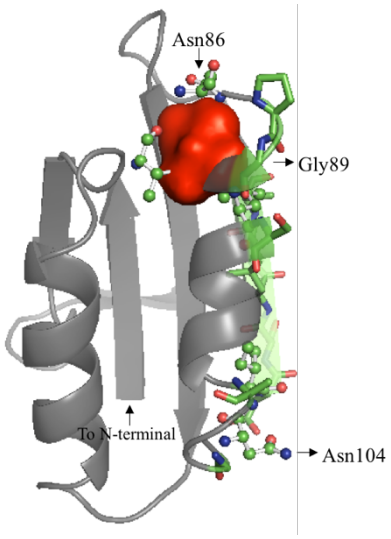

Figure 3-3 Homology modeling of valine-binding site on the Ilv6 monomer.

Based on the known *E. coli* IlvH molecular structure, the yeast Ilv6 molecular structure was remodeled using PyMOL (The PyMOL Molecular Graphics System, Version 1.8 Schrödinger, LLC.). The positions of amino acid substitutions are indicated. The red molecule represents valine.

3.2 Effects of amino acid substitutions of AHAS regulatory subunit (Ilv6) on the intracellular valine contents

To examine whether the DL-norvaline resistant phenotype is associated with valine accumulation, the intracellular valine contents were determined by an amino acid analyzer. Cells were cultured in a minimal medium to eliminate the uptake of exogenous amino acids and collected at the log phase. The result showed that intracellular valine increased approximately 4-fold, as well as by the combined mutations Asn86Ala/Asn104His, and Gly89Asp/Asn104His, as compared to the wild-type and the other Ilv6-varaints (Figure 3-4). This result was consistent with the growth phenotype on a minimal medium containing DL-norvaline. It was observed that the Ilv6 variants did not have any significant effect on the intracellular level of leucine and isoleucine ($p < 0.05$). Thus, it was concluded that by the Asn86Ala, Gly89Asp and Asn104His mutations in Ilv6 specifically increases the intracellular valine contents.

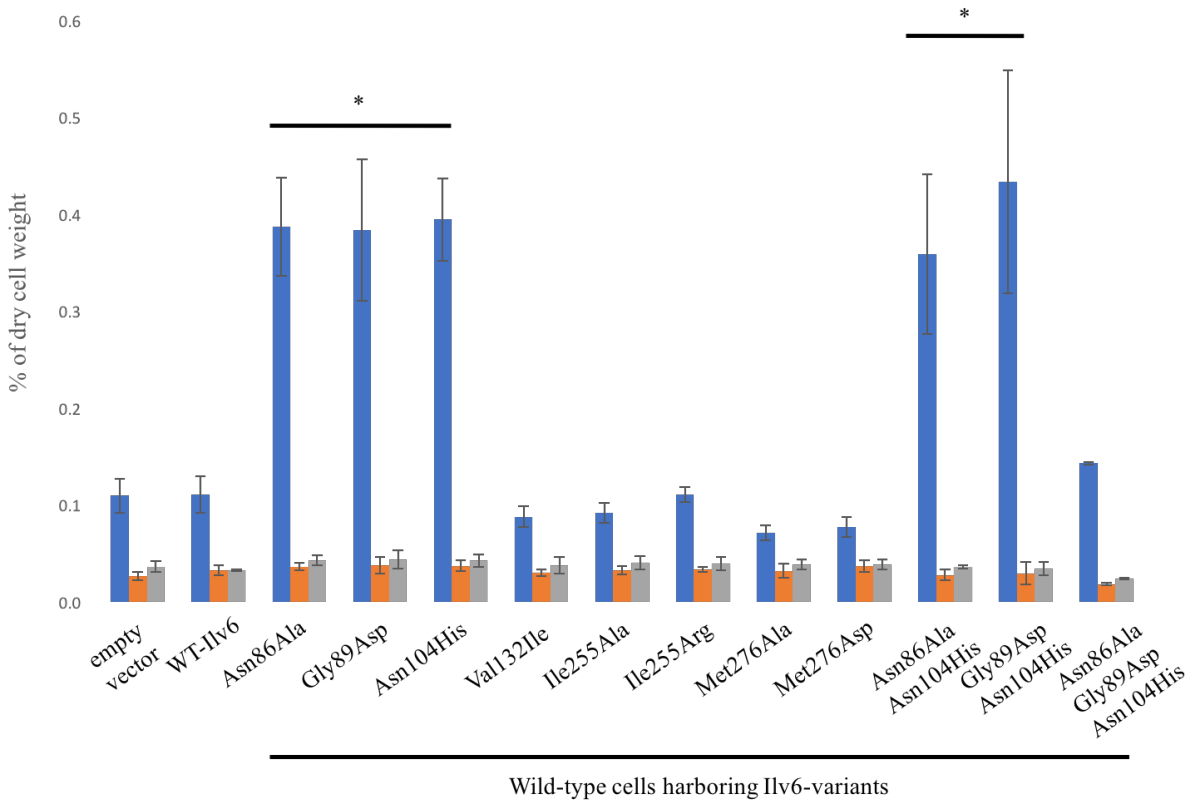

Figure 3.4 Intracellular branched-chain amino acid contents

Cells were grown in minimal medium (pH 6.0) at 30ºC and collected at log-phase (15 h after inoculation). Blue, orange and gray bars represent intracellular valine, leucine and isoleucine contents, respectively. Data represent the averages of three independent experiments and standard deviations. Asterisks indicate statistically significant differences in comparison to the control (wild-type cells (BY4741) with the empty vector) (Tukey's test, $p < 0.05$).

3.3 Effects of amino acid substitutions of AHAS regulatory subunit (Ilv6) on the AHAS activity and feedback inhibition by valine

Since the Ilv6 variants, Asn86Ala, Gly89Asp and Asn104Ala, exhibited the DL-norvaline resistant phenotype and higher intracellular valine contents, I hypothesized that these amino acid substitutions affect the conformation of the valine-binding site, leading to the reduced valine-binding affinity. In order to endorse this hypothesis, the AHAS enzymatic activity was determined using *in vitro* reconstituted AHAS. To prepare the recombinant proteins, Ilv2 (catalytic subunit) and Ilv6 (regulatory subunit) were tagged with 6x His at the amino termini were expressed in the Rosetta™ (DE3) pLysS strain as the first trial. Consequently, bacterial-expressed Ilv2 and Ilv6 were not detected in the soluble fraction, but were accumulated as inclusion bodies (Figure 3-5A). Rare codon analysis using GenScript

Rare Codon Analysis Tool (http://www.genscript.com/tools/rare-codon-analysis) revealed a low codon adaptation index (CAI) ratio, 0.62 for Ilv2 and 0.57 for Ilv6, suggesting that a poor expression of these eukaryotic proteins in *E. coli* is due to a difference in codon usage. To improve the protein solubility, the transit peptides at the amino termini of Ilv2 (54 amino acids) and Ilv6 (40 amino acids), which are not required for bacterial protein expression, were removed since the previous studies suggested an association between the formation of inclusion bodies and the targeting signal peptides (Pang and Duggleby, 1999). As a result, the solubility of Ilv2 and Ilv6 without transit peptides was increased as shown in Figure 3-5B.

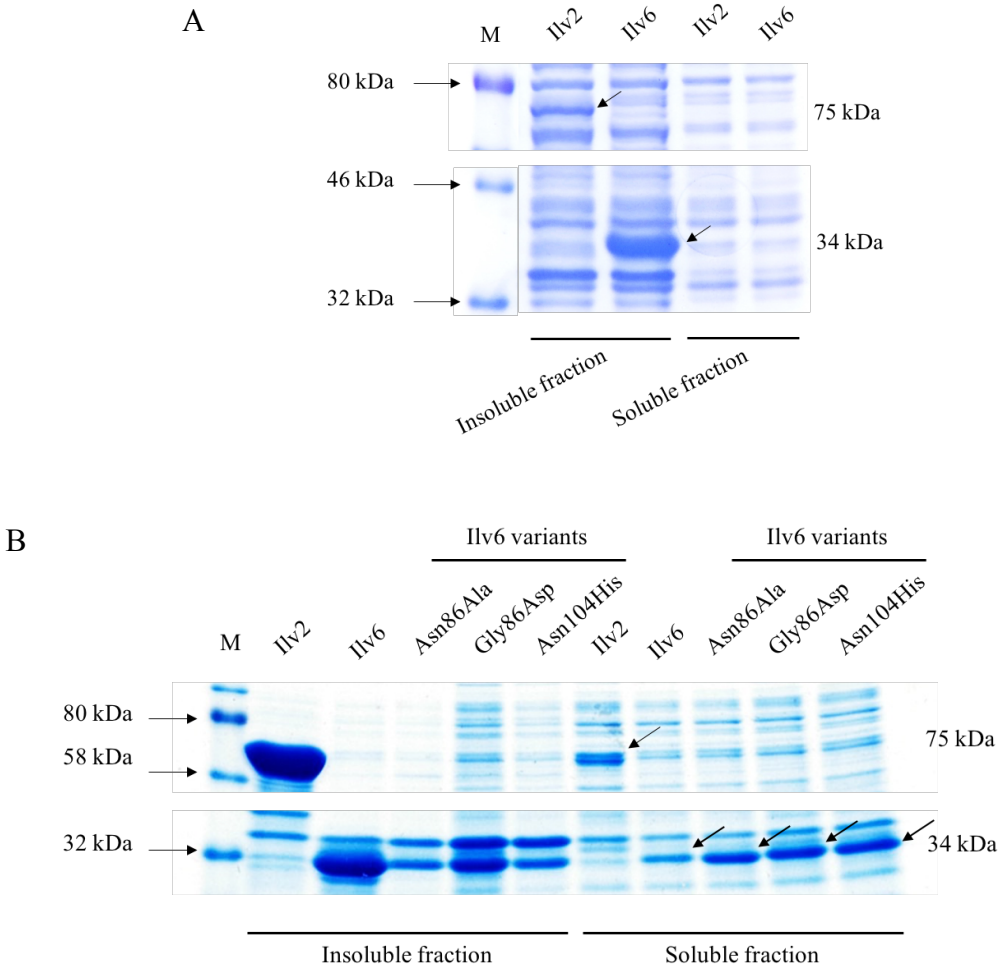

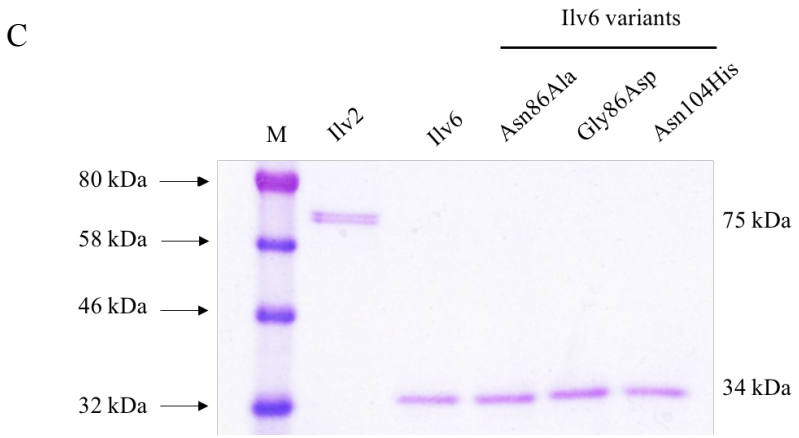

Figure 3-5 Ilv2 and Ilv6 expression using the Rosseta™ (DE3) pLysS strain.

(A) Bacterial expression of Ilv2 and Ilv6 in native forms. (B) Bacterial expression of Ilv2 and Ilv6 without transit peptides and (C) purified-Ilv2 and purified-Ilv6. 5 µg of proteins were mixed with the SDS sample buffer and heated at 95 ºC for 10 minutes and loaded onto a 10 % SDS-PAGE gel. The SDS-PAGE gel was stained with Coomassie Brilliant Blue. M, molecular markers. The bacterial-expressed Ilv2 and Ilv6 were marked with an arrow, 75 kDa for Ilv2 and 34 kDa for Ilv6, respectively.

The AHAS activity of purified-recombinant Ilv2 and Ilv6 was determined based on the level of acetoin (Figure 3-5C), which is converted from acetolactate, the product from the AHAS reaction. The acetoin standard curve, ranged from 2 to 20 µM, was shown in Figure 3-6. The AHAS activity in purified Ilv2 was 34.06 U/mg protein, while no AHAS activity was detected in the reaction containing purified Ilv6 alone. In *S. cerevisiae*, the catalytic subunit, Ilv2, has been firstly identified and cloned to complement of the AHAS activity in ilv$^-$ mutant (Poliana, 1984;). However, there was no regulatory subunit gene has been cloned as compared the *E. coli* AHAS sequences. The regulatory subunit of AHAS has been later identified based on the similarity of bacterial AHAS (Oliver *et. al.*, 1992). The function of Ilv6 is not involved in the catalytic activity, however, it responsible to valine inhibition since the AHAS activity in Δ*ilv6* was no longer inhibited by valine (Cullin *et. al*., 1996). In addition, with the increasing of Ilv6, the AHAS activity was significantly increased until reach the saturation point where the concentration of Ilv6 was around 100-folds of Ilv2 (Pang and Duggleby, 1999). This result suggested that Ilv6 is required to achieve the full AHAS activity. In this study, high AHAS activity was observed in the reaction contained Ilv2 and Ilv6 with the ratio 1:100 (124.62 U/mg protein for wild-type), whereas, only 34.06 U/mg protein of AHAS was detected in the reaction contained only Ilv2. Based on these results, it

was suggested that reconstitution of purified Ilv2 and Ilv6 was successfully carried out in this experiment (Table 3-2).

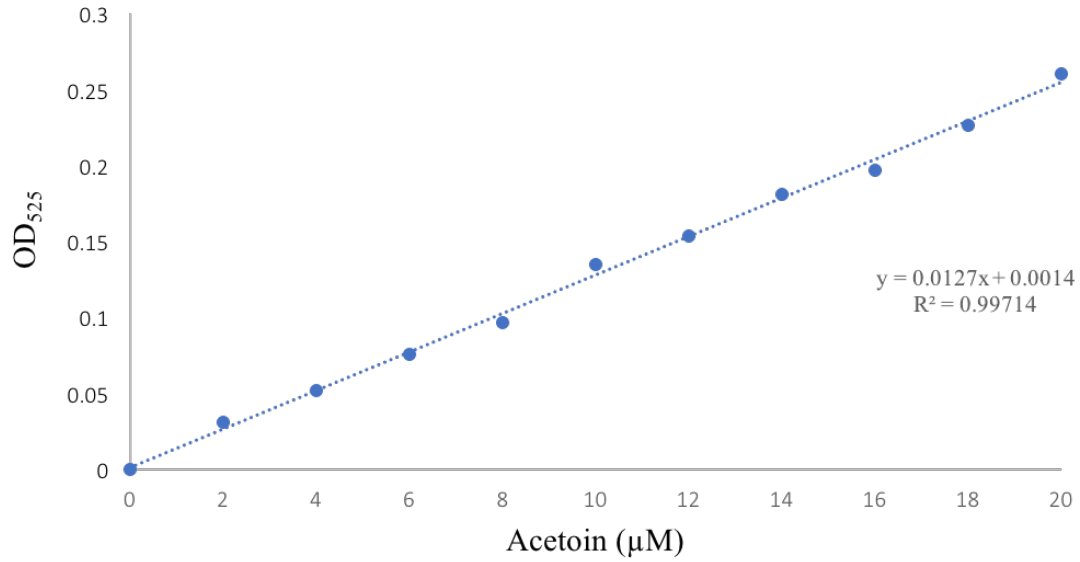

Figure 3-6 Acetoin standard curve for determination of the AHAS activity.

Table 3-2 Specific activity of reconstituted AHAS

AHAS activity was measured from single subunit and reconstituted AHAS which were wild-type Ilv2 reconstituted with wild-type Ilv6 and Ilv6 variants, respectively. Activity was expressed as the percentage of the reconstituted activity without valine added.

	Single subunit		**Reconstituted AHAS (Ilv2+Ilv6)**			
Valine (mM)	Ilv2	Ilv6	Wild-type	Asn86Ala	Gly89Ala	Asn104His
0	25.9	n.d.	100	100	100	100
0.2	-	-	44.8	93.4	81.4	96.9
0.4	-	-	27.9	88.2	79.5	89.3
0.6	-	-	25.6	88.7	76.1	83.6
0.8	-	-	27.3	86.7	77.1	82.1
1.0	-	-	26.7	87.2	66.6	70.8

* n.d. = not detectable

Moreover, the feedback inhibition of the AHAS activity by valine was analyzed (Figure 3-7). The AHAS activity of each Ilv2-Ilv6 mixture was almost the same in the absence of valine. When wild-type Ilv6 was used, addition of 0.2 M or higher concentrations of valine severely inhibited the AHAS specific activity, whereas the Ilv6 variants (Asn86Ala, Gly89Asp and Asn104His) reconstituted with Ilv2 remained the high AHAS activity even under higher concentrations of valine (~1.0 M). This result indicates that the feedback control of the AHAS activity by valine is almost fully abrogated by the Asn86Ala, Gly89Asp and Asn104His mutations. As in the introduction states that AHAS consists of two subunits, Ilv2 which responsible for catalytic activity, and Ilv6 modulates the catalytic subunit by increasing the AHAS activity and responsible for the valine feedback inhibition. From the result, it is noted that the AHAS activity of wild-type AHAS in the presence of valine was decreased to the similar level as observed in single Ilv2 (34.06 U/mg protein), indicating that AHAS activity is inhibited by valine concentration via the regulatory subunit, Ilv6.

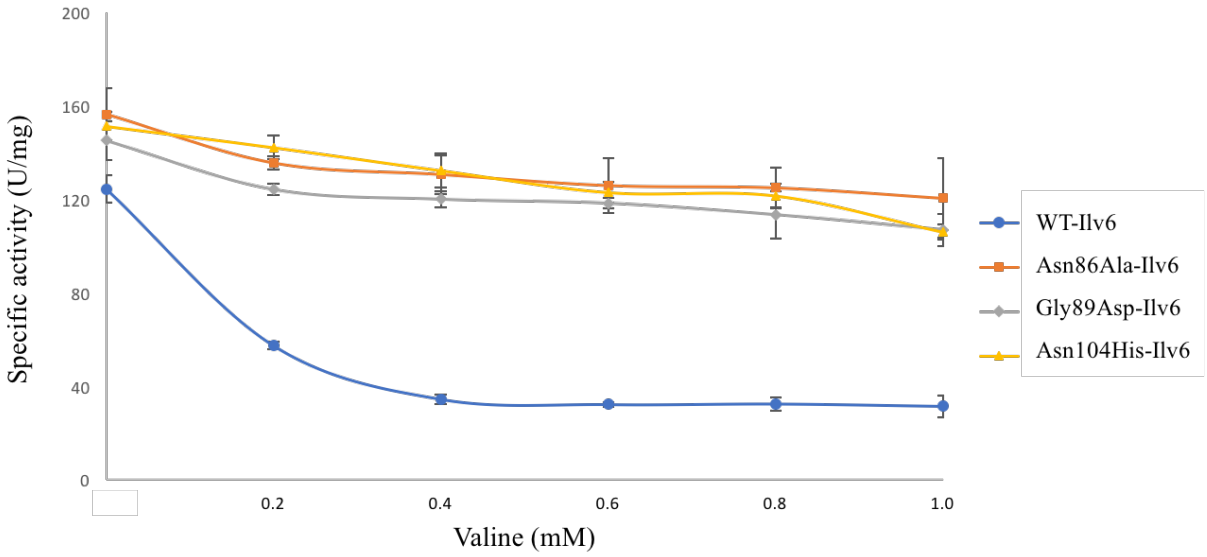

Figure 3-7 Effects of valine on the AHAS specific activity

In vitro reconstituted complex of Ilv2 with wild-type (blue), Asn86Ala (orange), Gly89Asp (gray) or Asn104His-Ilv6 (yellow) was used for the AHAS activity assay. Specific activity is expressed as enzyme units per mg of the catalytic subunit. Data represent the averages of three independent experiments and standard deviations.

3.4 Effects of BCATs (Bat1 and Bat2) on the intracellular valine contents

In *S. cerevisiae*, Bat1 and Bat2 are paralogous proteins that catalyze transamination of BCAAs in mitochondria and cytosol, respectively. I found that, however, Δ*bat1* cells exhibited the slow-growth phenotype in comparison to the wild-type and Δ*bat2* cells under amino acid-starved conditions (Figure 3-8). This result suggested that Bat1, not Bat2, plays a predominant role in BCAAs synthesis. In fact, the intracellular valine was markedly decreased in Δ*bat1* cells, compared to the wild-type and Δ*bat2* cells (Figure 3-9). Intriguingly, the levels of leucine and isoleucine were affected by neither Δ*bat1* nor Δ*bat2*. Thus, the mitochondrial BCAT Bat1 is specifically important for valine biosynthesis.

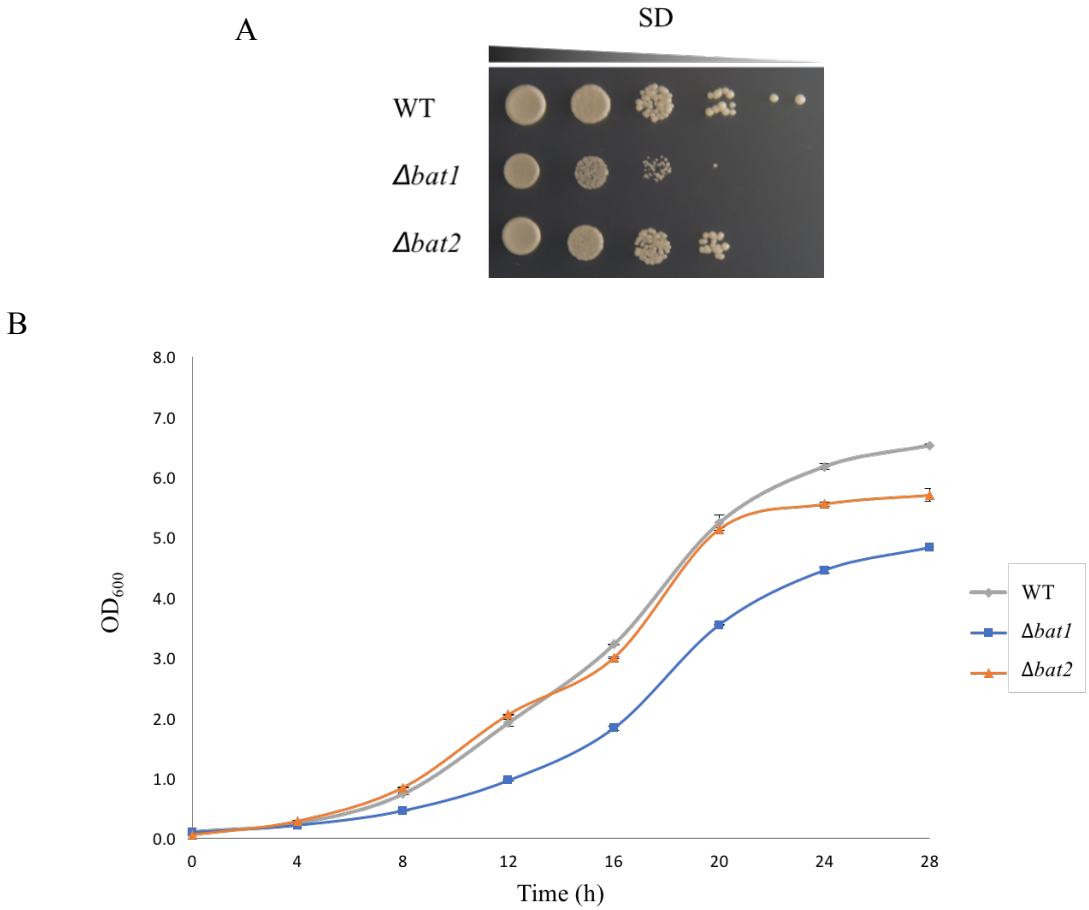

Figure 3-8 Growth of *S. cerevisiae* BY4741 (WT), Δ*bat1* and Δ*bat2* cells in SD medium.

(A) Cell suspensions with 10-fold serial dilutions were dropped (2.5 µL each) on minimal medium (SD) that was supplemented with 0.5 % ammonium sulfate as a sole nitrogen source and incubated at 30 °C for 3 days. (B) Cells were grown in liquid minimal medium supplemented with 0.5 % ammonium sulfate and collected every 4 hours interval for growth measurement at OD_{600}. Wild-type cells were represented as gray line, whereas, blue and orange lines were Δ*bat1* and Δ*bat2*, respectively.

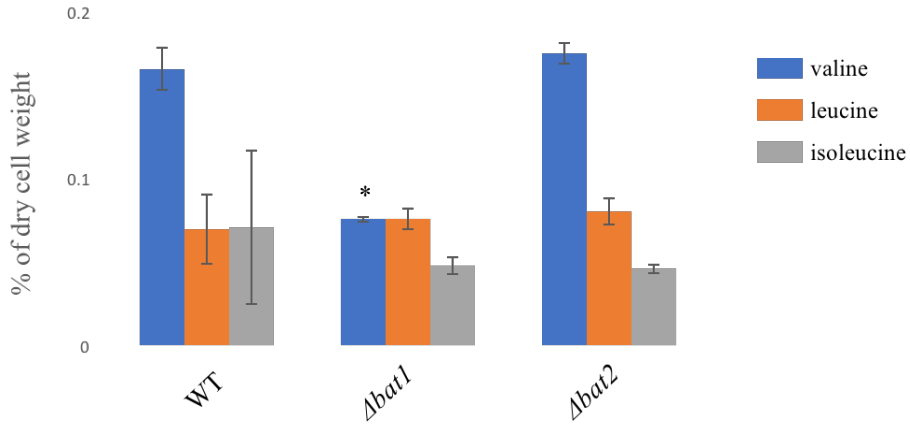

Figure 3-9 Intracellular branched-chain amino acid contents.

Wild-type (BY4741), Δ*bat1* and Δ*bat2* cells were grown in minimal medium (SD) at 30ºC and collected at the log-phase (15 h). Blue, orange, gray bars represent intracellular valine, leucine, and isoleucine, respectively. *statistical difference with $p < 0.05$.

3.5 Effects of subcellular localization of BCATs (Bat1 and Bat2) on the intracellular valine contents

Based on the results described above, it was presumed that mitochondrial valine synthesis by Bat1 is more important than cytosolic valine synthesis by Bat2. In order to address this, cytosolic Bat1 (without MTS) and mitochondrial Bat2 (with MTS) were constructed. A putative MTS is resided in the amino terminus of Bat1 only (Figure 3-10). 18 amino-terminal residues were removed from Bat1 (referred to as Bat1-MTS), while 24 amino-terminal residues of Bat1 were attached to the amino-terminus of Bat2 (referred to as Bat2+MTS). When tagged with GFP at the carboxyl termini, clear mitochondrial localization of Bat1 was lost in Bat-MTS, whereas Bat2+MTS was relocalized into mitochondria (Figure 3-11). Based on this result, the amino terminus of Bat1 was found a functional MTS, and the switching subcellular localization of Bat1 and Bat2 was succeeded.

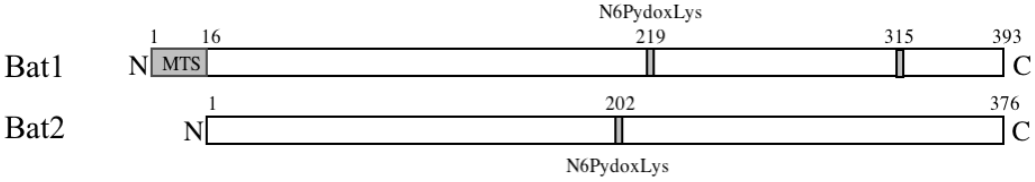

Figure 3-10 Schematic structure of Bat1 and Bat2.

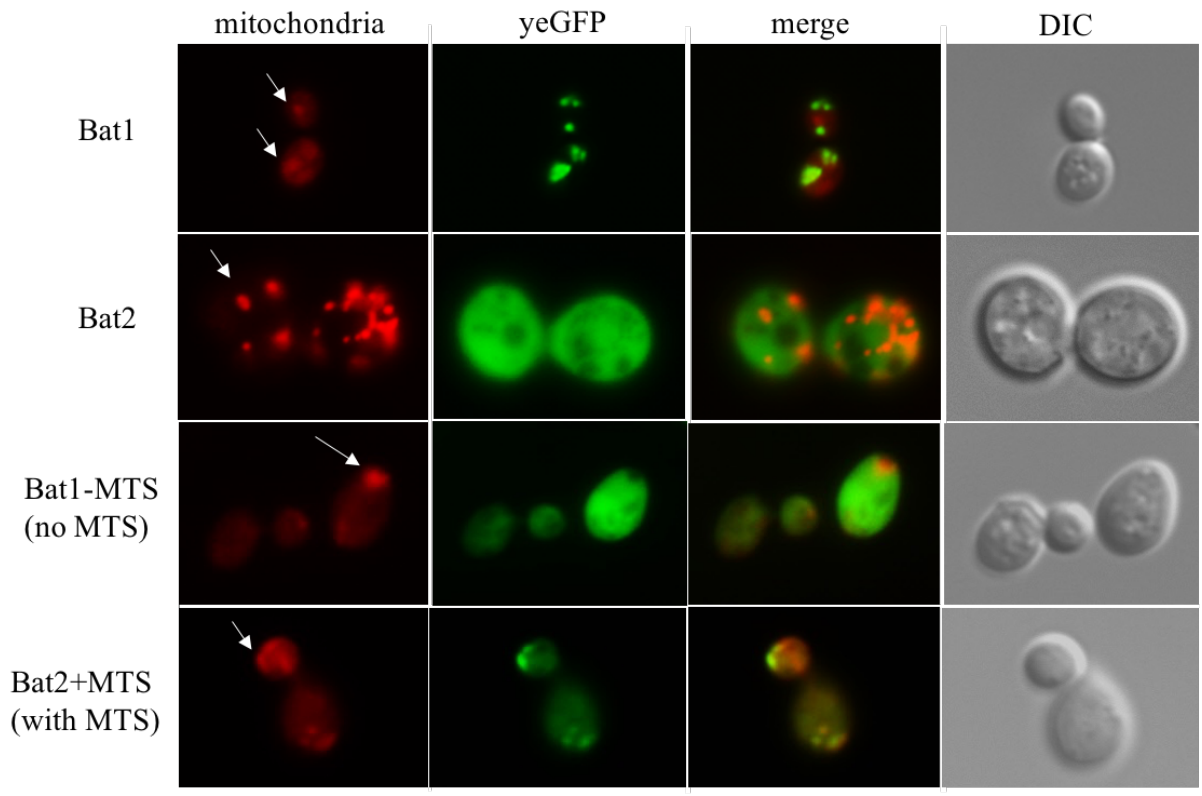

Figure 3-11 Localization of Bat1 and Bat2.

Wild-type cells (BY4741) harboring wild-type Bat1 or Bat2 and Bat1-MTS or Bat2+MTS were grown in minimal medium (SD) supplemented 0.5 % ammonium sulfate and 20 mg/L histidine and methionine at 30ºC for 15 h (log-phase). Mitochondria was stained with MitoTracker®, indicated as a red spot and marked with an arrow. Target protein was fused with GFP at the C-terminal was represented as green.

Proper functions of Bat1-MTS and Bat2+MTS were confirmed by introducing them into Δ*bat1* Δ*bat2* cells. While the expression of inactive BCATs, K219A-Bat1 and K202A-Bat2 (Kingsbury *et. al*., 2015), did not recover the growth of the Δ*bat1* Δ*bat2* cells in BCAAs-depleted or leucine-depleted medium, Δ*bat1* Δ*bat2* cells harboring Bat1-MTS grew similarly to the single Δ*bat1* cells (Figure 3-12A; formed small colonies on the BCAAs-depleted medium). The expression of Bat2+MTS fully restored the growth of Δ*bat1* Δ*bat2* cells to the same extent as wild-type and Δ*bat2* cells. Similar tendency was observed also in the liquid culture (Figure 3-12B). This result suggests that both Bat1-MTS and Bat2+MTS are functional, and Bat1 and Bat2+MTS have a predominant role in valine synthesis as mitochondrial BCATs, while Bat2 and Bat1-MTS have a minor role as cytosolic BCATs.

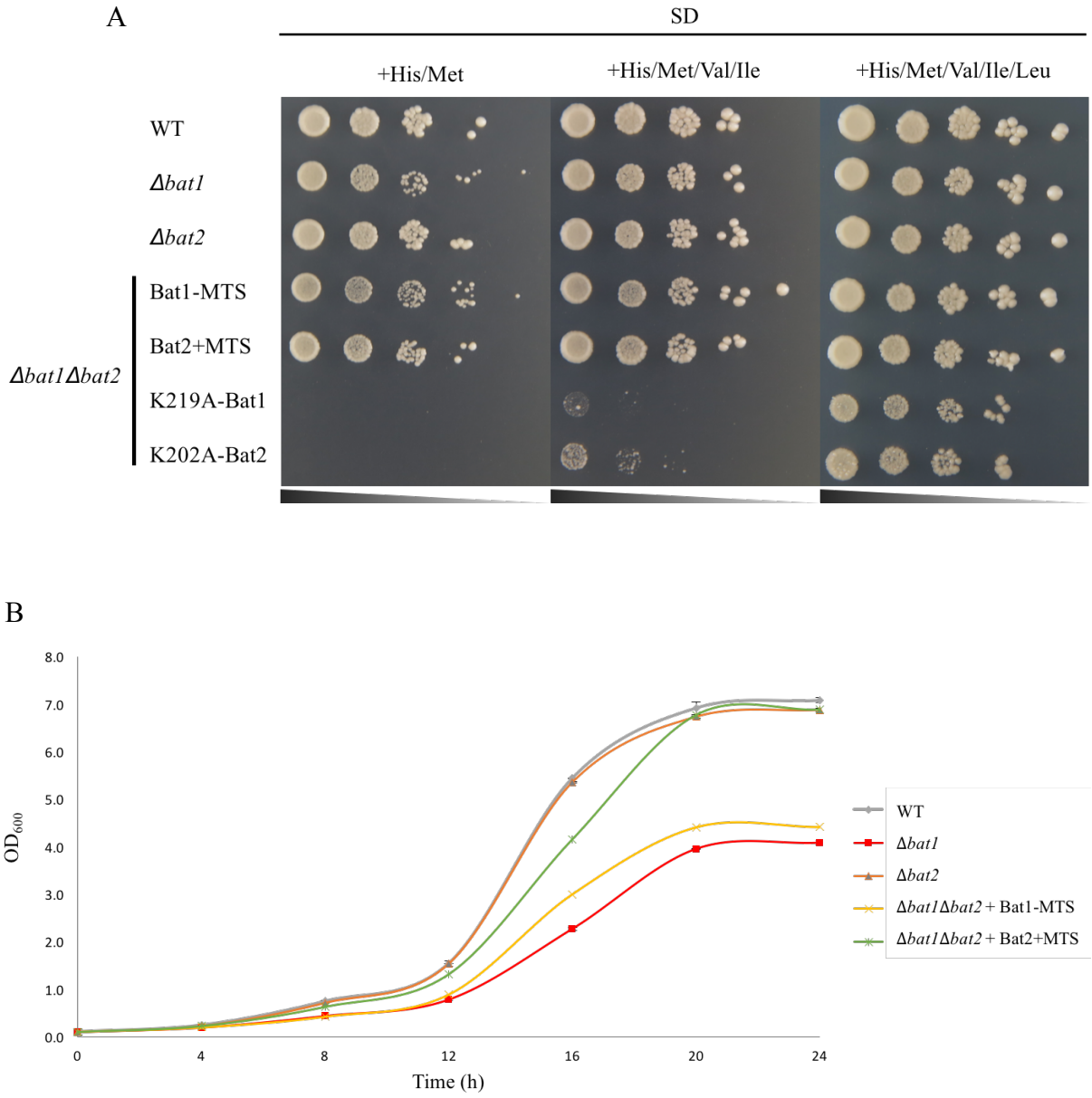

Figure 3-12 Growth of *S. cerevisiae* BY4741 (WT), Δ*bat1*, Δ*bat2*, Δ*bat1*Δ*bat2* cells harboring Bat1-MTS and Bat2+MTS

(A) Cell suspensions with 10-fold serial dilutions were dropped (2.5 µL each) on minimal medium (SD) that was supplemented with 0.5 % ammonium sulfate and 20 mg/L histidine and methionine or with valine and isoleucine as 150 and 100 mg/L, respectively. (B) Cells were grown in liquid minimal medium supplemented with 0.5 % ammonium sulfate, 20 mg/L histidine, and methionine. Cells were collected every 4 hours interval for growth measurement at OD_{600}.

It was noticeable that the combination of exogenous valine and isoleucine did not support the cell growth in the absence of BCATs activity ($Bat1^{K219A}$ and $Bat2^{K202A}$). In this experiment, leucine was not added to the tested media in order to maintains the plasmid

stability, therefore, this phenomenon may affect the cell growth. To confirm this hypothesis, Δ*bat1*Δ*bat2* cells harboring both inactive Bat1 and Bat2 were grown on minimal media which contains all valine, leucine and isoleucine (Figure 3-12A). The result showed that addition of leucine could recover the cell growth in these mutant cells, suggesting that leucine may has others specific role in the cell. However, the growth of these mutants could not be fully recovered as compared to wild-type and Δ*bat2* cells on minimal media without BCAAs, suggesting that intracellular BCAAs are required to maintain the cell growth.

To verify that the growth restoration by Bat1-MTS or Bat2+MTS was related to the intracellular valine contents, the intracellular BCAAs was determined (Figure 3-13). The data indicated that the intracellular valine content in Δ*bat1*Δ*bat2* cells harboring Bat1-MTS was similar to Δ*bat1* cells. On the other hand, the intracellular valine content in Δ*bat1* Δ*bat2* cells harboring Bat2+MTS was almost the same level as those of wild-type and Δ*bat2* cells. Altogether, it was suggested that mitochondrial BCATs is required for effective valine synthesis since the BCAT activity of Bat2+MTS can fulfill the valine biosynthesis by increase the intracellular valine content to the comparable level as wild-type and Δ*bat2*, resulting the growth restoration.

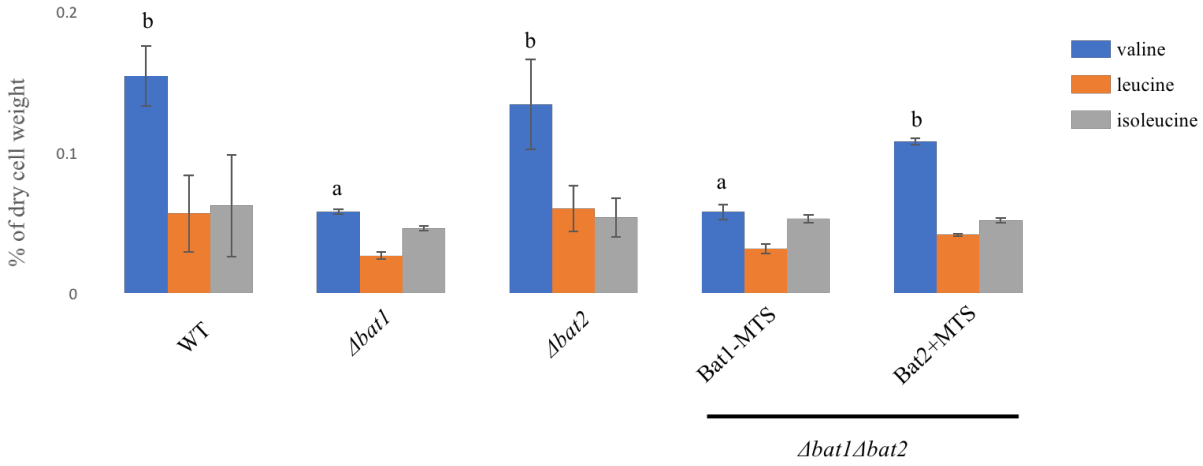

Figure 3-13 Intracellular branched-chain amino acid in *S. cerevisiae* BY4741 (WT), Δ*bat1*, Δ*bat2*, Δ*bat1*Δ*bat2* expressing Bat1-MTS and Bat2+MTS

Cells were grown in minimal medium (SD) at 30ºC and collected at log-phase (15 h). Blue, orange, gray bars represent intracellular valine, leucine, and isoleucine, respectively. [a,b] statistical difference with $p < 0.05$.

3.6 Effects of intracellular and exogenous valine on stress tolerance

Previously, our lab discovered that accumulation of intracellular proline or exogenous addition of proline confers stress tolerance on *S. cerevisiae* cells, indicating an alternative role of proline as a stress protectant (Takagi, 2008). Here we addressed effects of intracellular and exogenous valine on the growth under various stress conditions. The Asn86Ala, Gly89Asp and Asn104His mutations on Ilv6, which abrogates the feedback inhibition of AHAS, and the deletion of the BCAT genes *BAT1* and *BAT2* did not show the growth effect under salinity, osmotic, freezing, ethanol, or high-temperature stress conditions in minimal medium (Figures 3-14A, 3-15). These results indicate that intracellular valine accumulation did not confer stress tolerance on yeast cells. When the nitrogen source in the minimal medium was shifted from ammonium sulfate to valine, leucine or isoleucine, basically similar results were obtained under salinity, osmotic, freezing, or high-temperature stress conditions (Figure 3-14B). It was noticeable that under ethanol stress condition, exogenous valine could slightly recover the growth in comparable to leucine and isoleucine. To investigate the actual role of exogenous valine under ethanol stress, the growth of wild-type and Ilv6-varaints were again examined on minimal medium in the presence or absence of ammonium sulfate. The result showed that under ethanol stress, ammonium sulfate can support the cell growth similar to exogenous valine (Figure 3-16). These results suggested that under insufficient nitrogen sources, exogenous valine can be utilized as a sole nitrogen source for support the cell growth under ethanol stress.

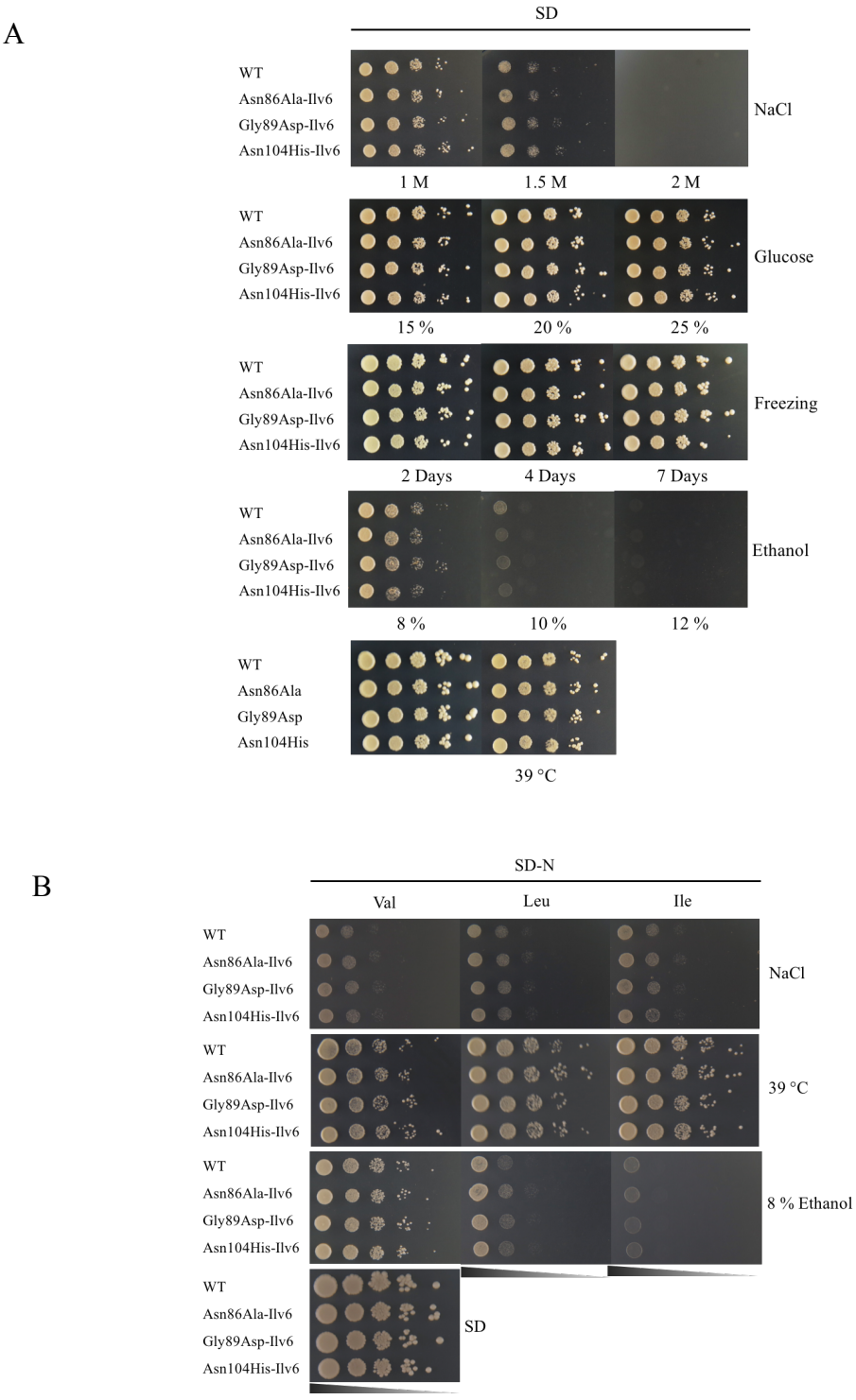

Figure 3-14 Effect of intracellular and exogenous BCAAs on stress tolerance on SD medium.

Cell suspensions with 10-fold serial dilutions were dropped (2.5 µL each) on (A) minimal medium (SD) that was supplemented with 0.5 % ammonium sulfate as a sole nitrogen in the presence of NaCl (salinity stress), glucose (osmotic stress), freezing stress (-30 ºC), ethanol stress and high temperature stress at 39 ºC. (B) Minimal medium was supplemented with valine, leucine, and isoleucine (150 mg/L, 100 mg/L, and 30 mg/L, respectively). Plates were incubated for 3 days at 30 ºC except for high temperature stress.

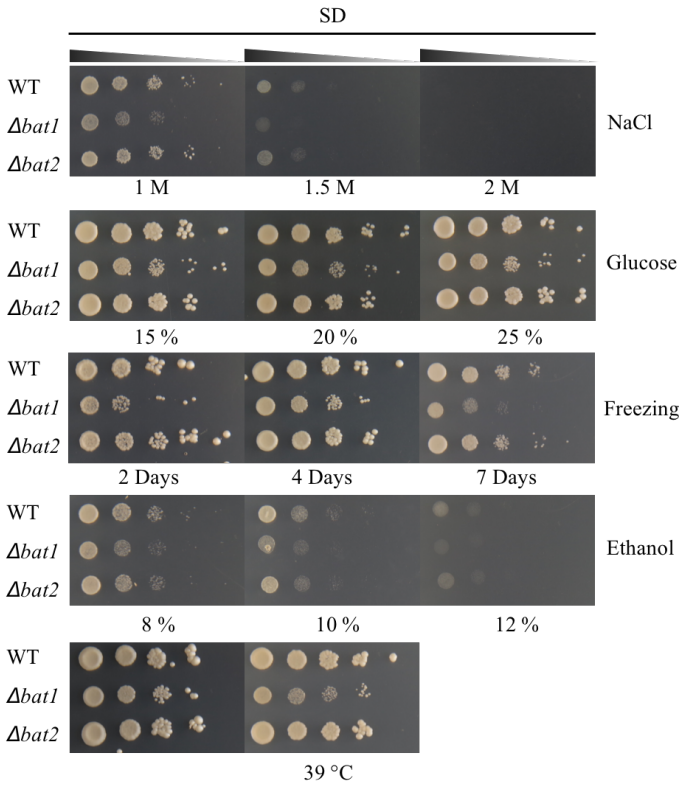

Figure 3-15 Growth of *S. cerevisiae* BY4741 (WT), Δ*bat1* and Δ*bat2* cells under various stress conditions.

Cell suspensions with 10-fold serial dilutions were dropped (2.5 µL each) on minimal medium (SD) that was supplemented with 0.5 % ammonium sulfate as a sole nitrogen source in the presence of NaCl (salinity stress), glucose (osmotic stress), freezing stress (-30 ºC), ethanol stress and high temperature stress at 39 ºC. Plates were incubated for 3 days at 30 ºC except for high temperature stress. Plates were incubated at 30 °C for 3 days.

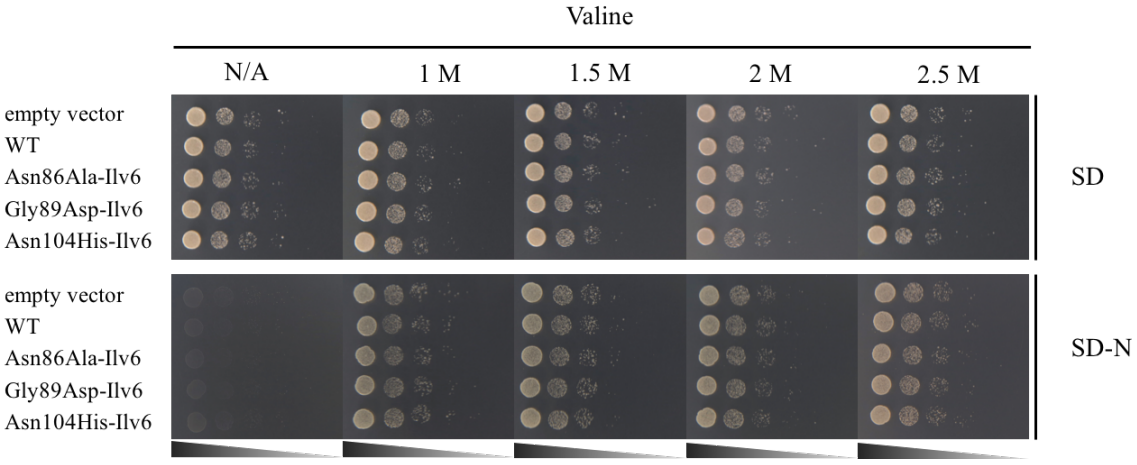

Figure 3-16 Effect of exogenous valine on ethanol tolerance on SD medium.

Cell suspensions with 10-fold serial dilutions were dropped (2.5 µL each) on minimal medium (SD) that was supplemented with 0.5 % ammonium sulfate or valine as a sole nitrogen source in the presence of 8 % ethanol. Plates were incubated at 30 °C for 3 days.

CHAPTER IV
DISCUSSIONS

4.1. Amino acid substitutions on the valine-binding sites of Ilv6 affect valine feedback inhibition and increase intracellular valine in *S. cerevisiae*

Improvement of valine productivity not only contributes to the amino acid and pharmaceutical industries, but also is applicable for isobutanol production since valine is the key intermediate for the Ehrlich pathway, the pathway for isobutanol production. For many years, researchers have attempted to improve the isobutanol production using the metabolic engineering approach, such as overexpression of the genes in the valine biosynthetic pathway (Brat *et. al.,* 2012). In this study, an alternative strategy was studied since the major issue that limited the valine biosynthesis is caused by valine feedback inhibition. Here, valine feedback inhibition was successfully removed by introduction of the amino acid substitutions on the yeast AHAS regulatory subunit, Ilv6, using the *E. coli* IlvH as a model. The protein sequence alignment between the *E. coli* IlvH and the *S. cerevisiae* Ilv6 showed similar conserved regions at the ACT domain and the carboxyl-terminal domain (Figure 3-1). From my results, the intercellular valine increased approximately 4-folds in the Ilv6-variants (Figure 3-3), Asn86Ala, Gly89Asp and Asn104His, which are located at the ACT domain in the amino terminus of the AHAS regulatory subunit. On the other hand, amino acid substitutions at the ALS ss C domain, Ile255Ala, Ile255Arg, Met276Ala, and Met276Asp, did not have any effects on the valine feedback inhibition.

In general, the ACT domain is responsible for the binding to ligands or small molecules for the regulation of BCAAs biosynthesis, whereas the ALS ss C domain was reported to be involved in herbicide inhibition (Duggleby, 1997). In *E. coli*, Asn11, Gly14 and Asn29 in AHAS III SSUs (IlvH) are highly conserved residues among several microorganisms including *S. cerevisiae*, isuggesting that the mutations at these three positions lead to the reduction of valine feedback inhibition. In *S. cerevisiae*, Asn86 and Asn104 are predicted to be at the putative valine-binding site (Figure 3-2), hence, the mutations at the valine-binding sites probably affect the conformation of this pocket. The valine inhibitory experiments also showed that the reconstituted-AHAS with the wild-type Ilv6 was subjected to feedback inhibition by 0.2 mM of valine, and the AHAS specific activity was decreased to

the basal level (a similar level to Ilv2 alone) upon an increase in the valine concentration. On the other hand, the specific activities of AHAS reconstituted with the Ilv6 variants were slightly decreased even if the valine concentration was increased up to 1.0 mM. This result supported the hypothesis that amino acid substitutions within the valine-binding site remove the valine feedback inhibition and finally increase the intracellular valine content (Figure 3-3 and 3-4).

It is noteworthy that Asn104 binds to valine upon dimer assembly, whereas Gly89 functions as a dimer interface between Ilv6 monomers. When the binding site structure is mutated, the interaction between the ligand and proteins may be perturbed. A good example is 3-phosphoglycerate dehydrogenase (3-PGDH). This enzyme also contains the ACT domain that is regulated through feedback inhibition by serine. In the serine-binding site, His404 acts as the major residue that binds to serine via the side-chains interaction between Asn406 and Asn424 (Grant *et. al*., 1996; Chipman and Shaanan, 2001). This binding is supposedly based on the polar-polar interaction since histidine, serine and asparagine contain a polar side-chains. This assumption is complementary to a previous study in *E. coli* in which the mutated AHAS IlvH at Gly14 and Asn29 was unable to bind with valine, based on the conserved residues of a 3-PGDH model (Grant *et. Al.*, 1996; Mendel *et. al.*, 2001). However, the interaction between valine and its binding site in the AHAS regulatory subunit, Ilv6, is still unclear due to amino acid side-chains of the valine-binding site associating with polar and non-polar. Meanwhile, Asn86Ala, Gly89Asp, and Asn104His variants displayed the DL-norvaline-resistant phenotype; the Val132Ile mutant which is also located at ACT domain was opposed. This mutant was constructed from DL-norvaline resistant mutant *S. cerevisiae* S288C in which the mutation at Val132 on Ilv6 has been observed (data not shown). This result suggests that not only the genes in BCAAs biosynthesis pathway can affect a DL-norvaline resistance by increasing of valine productivity but also that there are some upstream pathways which play a role in DL-norvaline resistance in a valine-independent manner.

Amino acid substitutions at the carboxyl terminus of Ilv6, Ile255Ala/Arg and Met276Ala/Asp, in *S. cerevisiae* did not cause any effects on DL-norvaline resistance and the intracellular valine; in contrast to Leu131 and Val153 in *E. coli* IlvH, respectively. Both Leu131 and Val153 are located in the hydrophobic core of the ALS ss C domain. Leu131 links between the α-4 helix and the β-sheet, and a mutation can affect the α-4 helix folding. Val153 is located between two monomers and is involved in the inter-monomer interaction

(Figure 4-1A) (Kaplun *et. al*., 2006). Homology modeling of the *S. cerevisiae* Ilv6 (Figure 4-1B), based on the *E. coli* IlvH, suggests that there are hydrogen bonds between Ile255, Lys251 and Leu259 that is not directly involved in α-helix packing compared to the corresponding position on the *E. coli* IlvH, Leu131, which bound to Thr127, Ser128, Phe134, and Leu153 (Figure 4-1A). This evidence supports my hypothesis that amino substitution at position 255 in Ilv6 is not involved in valine feedback inhibition in *S. cerevisiae*. Met275Ala/Asp is apparently not involved in valine feedback inhibition in comparison to Val153 of the *E. coli* IlvH. However, there is no distinct elucidation to support this conjecture due to Met276 in the *S. cerevisiae* Ilv6 is also located between two β-sheets and form two hydrogen bonds among them, similar to Val153 in *E. coli* (Figure 4-1A). The ALS ss C domain of AHAS in *S. cerevisiae* might be responsible for another ligand-binding. Taken together, this evidence is consistent with my results in which the amino acid substitutions at Asn86, Gly89 and Asn104 removed the valine-feedback inhibition and increased the intracellular valine content approximately 4-folds due to the conformational change in the valine-binding site, suggesting by increase in intracellular valine content (Figure 3-4) and reduction of valine-feedback inhibition (Figure 3-7) of these three Ilv6 variants.

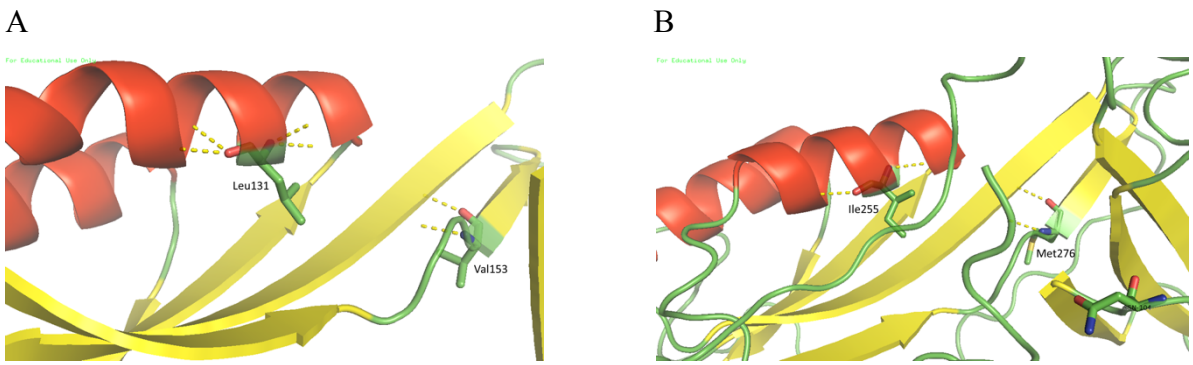

Figure 4-1 Amino acid substitution at ALS ss C domain of yeast Ilv6

(A) The ALS ss C domain of *E. coli* the IlvH and (B) the ALS ss C domain the of *S. cerevisiae* Ilv6. Homology modeling was illustrated by Phyre2 and Pymol (Kelley *et. al.,* 2015). All colors were given according to the secondary structure; red, yellow, green indicates a helix structure, a sheet structure and a loop structure, respectively. The mutation position was labeled as stick with yellow dashes which indicating hydrogen bonds.

In contrast to intracellular valine, these Ilv6-variants did not confer leucine and isoleucine accumulation (Figure 3-4). It has been known that leucine and isoleucine biosynthesis originally initiates from the same pathway as valine biosynthesis, although

threonine is a substrate for isoleucine instead of pyruvate. KIV or α-ketoisovalerate is the main precursor for both leucine and valine biosynthesis, and thus, an increase in the AHAS specific activity may certainly lead to intracellular accumulation of KIV. However, the accumulation of KIV or higher AHAS specific activity did not increase the intracellular leucine and isoleucine. The *LEU4* and *LEU9* genes encode α-isopropylmalate synthases I and II, respectively. Leu4 is a rate-limiting step of leucine biosynthesis which proceeds the first step of leucine biosynthesis and subjected to leucine feedback inhibition (Kohlhaw, 2003). In the case of isoleucine, threonine deaminase (Ilv1) catalyzes the conversion of threonine to α-ketobutyrate which is a starting point of isoleucine biosynthesis. There has been reported that this enzyme activity is inhibited by the presence of isoleucine (Berg JM *et. al.*, 2002) (Figure 4-2). Therefore, neither more KIV availability nor higher AHAS specific activity can remove the feedback inhibition caused by leucine and isoleucine, suggesting that leucine or isoleucine feedback inhibition are regulated by the AHAS-independent manner in *S. cerevisiae*. Unfortunately, the intracellular leucine and isoleucine has not been reported in the bacterial valine feedback inhibition-resistant AHAS strain, thus, the relationship between each BCAA feedback inhibition is still unknown. However, leucine level in *Arabidopsis thaliana* with valine feedback inhibition-resistant AHAS increased by approximately 4-folds, while, only 3-folds was observed for valine (Chen *et. al.,* 2010). In comparison, two repeated of the AHAS regulatory domain in *A. thaliana* (VAT1) was observed, whereas, only single domain is presented in the yeast Ilv6. Moreover, *A. thaliana* AHAS enzymatic activity is rather inhibited by all BCAAs, especially leucine (Lee and Duggleby, 2001), suggesting the regulation of BCAA biosynthesis via AHAS in each organism may be difference.

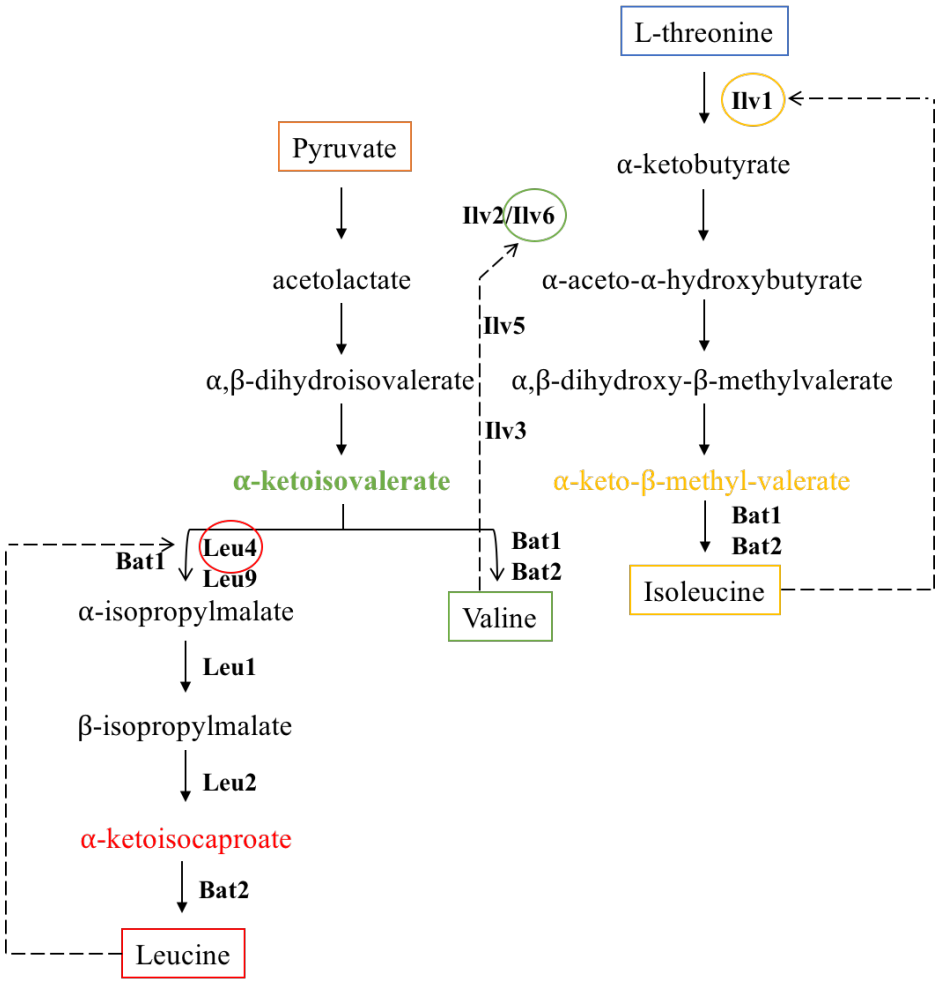

Figure 4-2 Overall BCAAs biosynthesis pathway

The rate-limiting step of each BCAA was circled in red for leucine, green for valine and yellow for isoleucine. Enzymes in the biosynthetic pathway were written as bold letters. Ilv1 = threonine deaminase, Ilv2 = catalytic subunit of acetohydroxyacid synthase, Ilv6 = regulatory subunit of acetohydroxyacid synthase, Ilv5 = acetohydroxyacid reductoismerase, Ilv3 = dihydroxyacid dehydratase, Leu4 = α-isopropylmalate synthase I, Leu9 = α-isopropylmalate synthase II, Leu1 = isopropylmalate isomerase, Leu2 = β-isopropylmalate dehydrogenase, Bat1 = mitochondrial BCAA aminotransferase and Bat2 = cytosolic BCAA aminotransferase

4.2 Intracellular valine does not confer stress tolerance on *S. cerevisiae*, whereas exogenous valine acts as a nitrogen source and supports mitochondrial function in the presence of ethanol

It is known that accumulation of some amino acids, such as proline and arginine, contribute to stress tolerance in many organisms. Our lab previously found the association between intracellular proline accumulation and freezing tolerant phenotype in yeast in which proline acts as a cryoprotectant by forming strong hydrogen bonds with free water in the cell, preventing the macromolecules from damages (Takagi, 2008). Moreover, it also serves as an osmoprotectant and protects the cells from a variety of stresses, including salinity, ethanol and high temperature. In the case of intracellular valine accumulation, high intracellular valine content did not tolerate to stresses tested in my experiment, such as, salinity, osmotic, ethanol, freezing, and high-temperature. However, addition of exogenous valine could restore cell growth in the presence of ethanol under nitrogen starvation conditions. This result suggests that valine does not have specific physiological functions as discovered in a proline-accumulating cells, although valine is better utilized as a sole nitrogen source to support growth in the presence of ethanol in comparison to other BCAAs. These results were consistence with the previous study that valine is a good nitrogen source that supports the rapid cell growth, whereas, using leucine and isoleucine as nitrogen source only supports the slow growth phenotype, indicating the difference role of valine in the metabolic processes (Godard *et. al*., 2007).

Exogenous valine probably plays a metabolic role in resisting toward ethanol stress. In general, ethanol stress primarily affects membrane fluidity which subsequently leads to proteins denaturation and activates the other cellular stress responsive processes caused by the increase of membrane permeability (Mishra and Prasad, 1989). As a result, a large amount of reactive oxygen species (ROS) is gradually generated in mitochondria, however, the exact cause of ROS generation under ethanol stress is still unknown. Mitochondrial damaged is one of the tentative possibility, therefore, activation of mitochondrial ROS defense system is essential for cells survival. The previous study revealed that BCAAs supplementation activates the ROS defense system by increasing the transcription of enzymes involved in ROS neutralization, such as Sod1 and Sod2, resulting in decreased formation of intracellular H_2O_2 (D'Antona *et. al.*, 2010). Moreover, chronical exposure to ethanol stress can affect mitochondrial structures and functions, including the respiration capacity and ATP levels.

There has been reported that exogenous valine and its catabolites, α-ketoisovalerate, act as the best respiratory substrate in which support mitochondrial activity as compared to leucine, isoleucine and their α-ketoacids (Taylor *et. al.*, 2004). Therefore, exogenous valine, not intracellular valine, may contribute to ethanol tolerance on yeast cells. It is noticed that intracellular valine is a product from the biosynthetic pathway, whereas exogenous valine directly goes to the catabolic pathway; both pathways are distinct and response to the cellular metabolism in a different manner.

4.3 Absence of Bat1 does not have any effect on Intracellular leucine and isoleucine content

My results obviously indicate that absence of Bat1 has a huge impacts on intracellular valine, however, there has no effect on intracellular leucine and isoleucine content (Figure 3-9). Leucine biosynthesis is branched from the valine biosynthetic pathway by conversion of KIV to α-isopropylmate via Leu4/Leu9 (Figure 4-2). Thereafter, α-isopropylmate is transported to cytosol and converted to KIC, which is the key intermediate of leucine biosynthesis, at this step KIC is changed to leucine by the activation of Bat2 (KEGG PATHWAY database: Kanehisa and Goto, 2000). Therefore, intracellular leucine is likely not affected by lacking of Bat1. On the other hand, Bat1 is required for the conversion of KMV, which is the key intermediate of isoleucine biosynthesis, to isoleucine in the same manner as valine biosynthesis. However, the intracellular isoleucine did not significantly decrease by the absence of Bat1. Among BCAAs intermediates, KMV has the lowest substrate specificity since transaminase activity was slightly detected when it was used as a substrate. On the contrary, the highest transaminase activity was observed in the reaction contained KIV. In addition, previous study showed that the BCAAs aminotransferase activity still remains in Δ*bat1* and Δ*bat1*Δ*bat2* cells when KMV was used as substrate, suggesting that there is unknown BCAAs aminotransferase exist in mitochondria which catalyst the transaminase reaction of KMV to isoleucine (Kispal *et. al.*, 1996). These data propose that transamination of KMV to isoleucine is probably driven by Bat1 and other unknown BCATs, and thus, the BCAT activity of Bat1 is not essential for isoleucine biosynthesis (Colón *et. al.*, 2011).

There has been stated that *S. cerevisiae* proceeds both BCAAs biosynthesis and degradation by Bat1 and Bat2. As mentioned above, KIV is preferentially recognized by BCAT and promotes the biosynthetic activity, at the same time, valine is the best substrate for BCAAs degradation via BCAT with the higher BCAT specific activity compared to leucine and isoleucine. Therefore, it is theoretically suggested that intracellular valine is effectively degraded to higher alcohol via the Ehrlich pathway (Yu *et. al.*, 2014; Bezsudnova *et. al.*, 2016). This information suggest that valine biosynthesis is influenced by disruption of *BAT1*, whereas, valine degradation is, instead, rapidly carried out by Bat2 in comparison to leucine and isoleucine; thus, only intracellular valine is affected by the Bat1 deficiency.

4.4 Mitochondrial BCAAs aminotransferase (mBCAT) is important for valine biosynthesis and maintenace of normal cell growth

BCAAs aminotransferase (BCAT) in *S. cerevisiae* consists of two isoforms, Bat1 and Bat2. These two proteins are homologous to ECA39 and ECA40 in mammals, which are located in mitochondria and cytosol, respectively (Eden *et. al.,* 1996). Bat1 proceeds the transaminase activity of BCAAs in mitochondria, whereas, the reaction in the cytosol is carried out by Bat2. My results revealed that lacking of Bat1, not Bat2, led to slow-growth phenotype including increased sensitivity to many stresses, such as, salinity, osmotic, freezing and high-temperature in *S. cerevisiae.* This phenomenon probably caused by a dramatic decrease in intracellular valine content (Figure 3-9). The previous study reported the distinct function of Bat1 and Bat2 in which that Bat1 activity is mainly required for the BCAAs biosynthesis, although Bat2 is likely involved in the catabolic pathway (Colón *et. al.*, 2011). Moreover, in total cell extracts revealed that the transaminase activity of Bat1 seems to be higher than that of Bat2 total cell extract (Prohl *et. al*., 2000), supporting the result that lack of Bat1 activity has more impact on the cellular valine pool.

Since Bat1 and Bat2 share 77 % identity and catalyze the same reaction, it is suspicious that Bat1 itself or the location of BCAT activity is required for valine biosynthesis. The putative Bat1 without mitochondrial targeting signal: MTS (Bat1ΔN18, Bat1ΔN24 and Bat1ΔN30) and Bat2 attached with MTS (Bat2+MTS) were constructed based on the protein database (UniProt). However, the removal of 24 and 30 amino acids from the amino terminus of Bat1 impaired the BCAT activity (data not shown), while the removal of 18 amino acids

can relocalize Bat1 from mitochondria to cytosol without perturbing the BCAT activity. These results suggest that only 18 amino acid residues are responsible for the mitochondrial targeting. Bat1-MTS and Bat2+MTS were then transformed into Δ*bat1*Δ*bat2* cells to observe the phenotype of these putative proteins. As a result, Bat1-MTS can exert the function of Bat2, whereas the Bat1 function was complemented by Bat2+MTS (Figure 3-12), suggesting that if either Bat1 or Bat2 is localized into mitochondria, it can fulfill the valine biosynthesis and restore the cell growth. Moreover, the intracellular valine can be restored in Δ*bat1*Δ*bat2* cells harboring Bat2+MTS, suggesting that the mitochondrial BCAT activity is required for valine biosynthesis (Figure 3-13). It simply states that mitochondrial BCAT is important for valine biosynthesis and regulates cell growth through the valine homeostasis. Meanwhile, neither Δ*bat1*Δ*bat2* cells harboring inactive Bat1 ($Bat1^{K219A}$) nor Bat2 ($Bat2^{K202A}$) can grow on minimal media in the absent BCAAs. This result strongly supports the importance of BCATs activity in the cell growth (Figure 3-12A). On the other hand, addition of valine and isoleucine to the minimal media did not restore growth to the comparable level as compared to wild-type or Δ*bat1* and Δ*bat2* cells (Figure 3-12A), suggesting that BCATs may associated with other cellular metabolic pathways, for an example, TORC1 signaling pathway. TORC1 plays role in the regulation of yeast cell growth through the phosphorylation of three major effectors branches such as activation of ribosome biogenesis via Sch9 protein kinase (Urban *et. al.,* 2007). There has been reported that leucine was involved in the regulation of TORC1 in which leucine starvation led to Sch9 phosphorylation deficiency in Δ*bat1*Δ*bat2* cells (Kingsbury, 2015). Moreover, lacking of Bat1 and Bat2 activity also affect the metabolite homeostasis in the central metabolic pathway such as glutamate and glutamine (Stracka *et. al.,* 2014). This information supports the results that addition of valine and isoleucine could not recover the growth of Δ*bat1*Δ*bat2* cells harboring inactive Bat1 and Bat2 due to leucine and BCATs activity deficiency. It is noticeable that intracellular BCAAs are the products from biosynthetic pathway which is mainly produced in mitochondria, whereas, exogenous BCAAs certainly enter to the catabolic pathway in cytosol. Therefore, the transportation of BCAAs including their α-ketoacids from mitochondria to cytosol or cytosol to mitochondrial should affect the biosynthesis or catabolism of BCAAs as well. However, the level of mitochondrial BCAAs and cytosolic BCAAs were not quantified in this study since the effective method is not available. Moreover, the evidences on the transportation of BCAAs including other amino acids, both in and out from mitochondria, are still unclear; therefore, the regulation mechanisms of BCAAs metabolism under biosynthetic and catabolic conditions need to be further studied.

According to the introduction that unusual BCAAs metabolism leads to metabolic disorder diseases, neurological, and cardiovascular diseases in human, there are several studies attempt to clarify the BCAAs metabolism in *S. cerevisiae* as a model for higher eukaryotes. A quantitative trait loci analysis has revealed that Bat1 and Bat2 are categorized into a B1B2 module (together with Rpn11, Hsp60 and Ilv2), which are functionally related to BCAAs metabolism and physiologically associated to mitochondria (Picotti *et. al*., 2013). In mammalian cells, amino acid starvation activates the YY1-dependent genes in response to amino acid degradation to serve the mitochondrial protein synthesis requirement and accelerates TCA cycle in order to upregulate the respiratory electron transport chain (Johnson *et. al.*, 2014). On the other hand, BCAAs metabolism also involves in cell aging, lifespan and amino acid homeostasis in several organisms. In the case of *S. cerevisiae*, BCAAs potentially promotes cell survival under calorie restriction condition (CR) in which BCAAs can neutralize ROS in mitochondria and reduce the expression *GCN4*, which is the suppressor of choronological lifespan (CLS) (Alvers *et. al.*, 2009; D'Antona *et. al.*, 2010). Furthermore, it has been known that an increase in the mitochondrial respiratory system, mitochondrial function, and TCA-cycle activity are the responsive mechanisms in yeast CR lifespan. There has been reported that BCATs and their metabolites, leucine and α-ketoisocaproate, act as an upstream regulation of TORC1 by sensing the leucine availability to EGOC, the exit from G_0 Complex GTPase. In addition, Bat1 plays a non-enzymatic role in cellular mechanisms by directly interacts with TCA-cycle enzymes to facilitate the TCA-cycle flux which eventually affects the ATP level (Kingsbury *et. al.*, 2015) (Figure 4-3).

In this study, Δ*bat1* cells exhibited slow-growth phenotype under amino acid starvation condition was a result from the absence of mitochondrial BCAT that has a huge impact on the intracellular valine content. It is notable that mitochondrial BCAT plays a major role in valine biosynthesis by converting mitochondrial KIV into valine, whereas cytosolic KIV is partially entered the Ehrlich pathway and forming the fusel acids and alcohol as previously mentioned (Brat *et. al.,* 2012). Moreover, loss of mitochondrial BCAT likewise perturbs mitochondrial metabolites, especially valine pool, which certainly impairs mitochondrial protein synthesis and subsequently affects the respiratory electron transport chain. In mammals, it is known that BCAAs metabolism provides important precursors for TCA cycle, succinyl-CoA and acetyl-CoA. Therefore, the absence of mitochondrial BCAT possibly leads to a TCA-cycle flux imbalance, and consequently less NADH and FADH enter the respiratory electron transport chain, resulting in lower ATP generation afterward.

However, BCAAs catabolism in budding yeast is totally different from mammals in which BCAAs can only be utilized as a sole nitrogen source (Dickinson, 2000) and BCAAs catabolism in *S. cerevisiae* is carried out by the Ehrlich pathway which produces fusel acids and alcohol as endoproducts. Moreover, it has been previously mentioned that the transaminase activity of Bat1 in cell extract was higher than that observed in Bat2, it may be explained as the mitochondrial environment is more suitable for enzymatic reaction, for examples, high pH, lower oxygen concentration and more reducing redox potential (Avalos *et. at*., 2013).

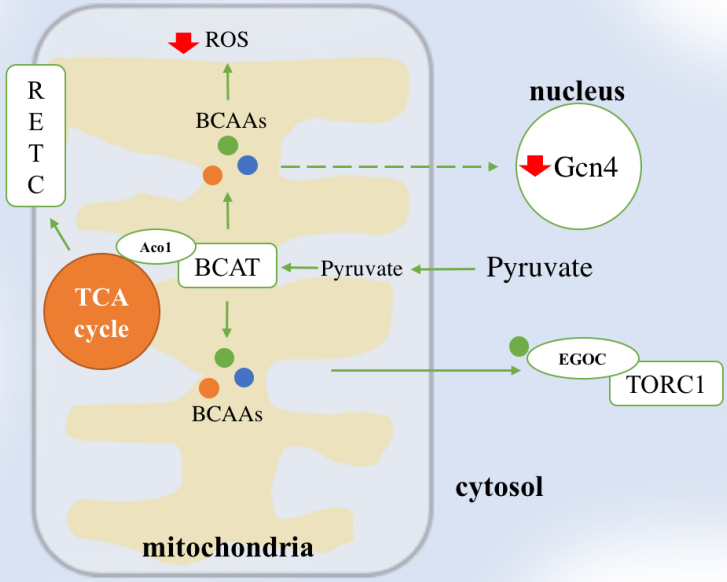

Figure 4-3 The importance of mitochondrial BCAT in *S. cerevisiae*

Proteins were labeled in green. Branched-chain amino acids were circled in orange, green and blue as valine, leucine and isoleucine, respectively. RETC = respiratory electron transport chain, Aco1 = aconitase 1, BCAT = branched-chain amino acid aminotransferase, Gcn4 = transcription factor for amino acid biosynthesis, EGOC = the exit from G_0 complex GTPase, TORC1 = target of rapamycin.

Taken all of the clues together, my results suggest that mitochondrial BCAT is important for valine biosynthesis due to: (1) cytosolic KIV is partially converted into fusel acids and alcohol via the Ehrlich pathway, and thus, the major valine source is produced in mitochondria, (2) only Bat1 acts as a mitochondrial BCAT responsible for valine biosynthesis in mitochondria, and thus, Bat2 can replace mitochondrial BCAT activity at the similar rate as Bat1 and maintain normal valine biosynthesis, (3) the confined environments of mitochondria facilitates a better BCAT enzymatic reaction which accelerates the conversion of KIV into valine, and (4) since KIV is only produced in mitochondria, therefore, it can be directly converted into valine without any transport limitation.

Finally, this study provides a better understanding in valine biosynthesis regulation, as well as the role of mitochondrial valine biosynthesis on cell growth. This applicable knowledge can be benefited for the development of superior yeast strains for industrial applications and can be employed in medical research to completely disclose the regulation of BCAA metabolism in human which lead to a better treatment of metabolic disorder diseases, neurological diseases and cardiovascular diseases.

ACKNOWLEDGEMENTS

Firstly, I would like to express my sincere appreciation to Prof. Hiroshi Takagi, my major supervisor at the Laboratory of Applied Stress Microbiology, who always works hard and had provided me his valuable time, suggestions and comments during my study in his lab. Besides being as the best supervisor who has put his helpful experiences at my research, he also handed me a good opportunity to be an intern student in Gekkeikan Sake Co., Ltd., my first impressive Japanese company. Moreover, by his great recommendation, I got a chance to work in Mitsui Chemicals Singapore R&D Centre Pte. Ltd. which is one of the most challenge in my life after graduation. I would like to give the deepest sense of gratitude to my immediate advisor, Assist. Prof. Daisuke Watanabe and Assist. Prof. Ryo Nasuno from our lab for their great interest, valuable guidance and assistance in my experiment.

I would like to give a special thanks to Prof. Hisaji Maki and Assoc. Prof. Yuki Kimata for providing me a great piece of advices. In addition, this doctoral thesis would not have been completed without the precious information from Dr. Ikuhisa Nishida - my great senpai, Sugimoto san - our super lab technician and aid of our laboratory members, and also the other persons who have not been presented in this place. I would like give a thanks to my partial research sponsor, Ajinomoto Co., Inc., as well as the Japanese Government scholarship (Monbukagakusho) for making my life in Japan goes smoothly.

Finally, I am grateful to thanks my husband, Dr. Nachai Limsettho and my family for their moral support, close attention and understanding in any situation that I encountered with.

Natthaporn Takpho

REFERENCES

Altschul, S.F., Madden, T.L., Schäffer, A.A., Zhang, J., Zhang, Z., Miller, W. and Lipman, D.J. (1997). Gapped BLAST and PSI-BLAST: a new generation of protein database search programs. Nucleic Acids Res 25,3389-3402.

Alvers, A. L., Fishwick, L. K., Wood, M. S., Hu, D., Chung, H. S., Dunn, W. A., Jr., and Aris, J. P. (2009). Autophagy and amino acid homeostasis are required for chronological longevity in *Saccharomyces cerevisiae*. Aging Cell *8*(4), 353-369.

Avalos, J. L., Fink, G. R., and Stephanopoulos, G. (2013). Compartmentalization of metabolic pathways in yeast mitochondria improves the production of branched-chain alcohols. Nat Biotechnol *31*(4), 335-341.

Avruch, J., Long, X., Ortiz-Vega, S., Rapley, J., Papageorgiou, A., and Dai, N. (2009). Amino acid regulation of TOR complex 1. Am J of Physiol - Endocrinology and Metabolism *296*(4), E592-E602.

Bai, J., Greene, E., Li, W., Kidd, M. T., and Dridi, S. (2015). Branched-chain amino acids modulate the expression of hepatic fatty acid metabolism-related genes in female broiler chickens. Mol Nutr Food Res *59*(6), 1171-1181.

Ben-Yosef, T., Yanuka, O., and Benvenisty, N. (1996). ECA39 is regulated by c-Myc in human and by a Jun/Fos homolog, Gcn4, in yeast. Oncogene *13*(9), 1859-1866.

Berman, H.M., Westbrook, J., Feng, Z., Gilliland, G., Bhat, T.N., Weissig, H., Shindyalov, I.N., and Bourne, P.E. (2000). The Protein Data Bank - Nucleic Acids Res *28*, 235-242.

Berg, J.M., Tymoczko, J.L., and Stryer, L. (2002). Amino acid Biosynthesis Is Regulated by Feedback Inhibition. Biochemistry 5th edition. (New York: W H Freeman), section 24.3.

Bezsudnova, E. Y., Stekhanova, T. N., Suplatov, D. A., Mardanov, A. V., Ravin, N. V., and Popov, V. O. (2016). Experimental and computational studies on the unusual substrate specificity of branched-chain amino acid aminotransferase from *Thermoproteus uzoniensis*. Arch Biochem Biophys *607*, 27-36.

Brat, D., Weber, C., Lorenzen, W., Bode, H. B., and Boles, E. (2012). Cytosolic re-localization and optimization of valine synthesis and catabolism enables increased isobutanol production with the yeast *Saccharomyces cerevisiae*. Biotechnol Biofuels *5*(1), 65.

Burke, D., Dawson, D., and Stearlns, T. (2000). Methods in Yeast Genetics. A Cold Spring Harbor Laboratory Course Manual 2000 edition. (New York: Cold Spring Harbor Laboratory Press), 103-105

Calder, P. C. (2006). Branched-chain amino acids and immunity. J Nutr *136*(1 Suppl), 288S-293S.

Chen, H., Saksa, K., Zhao, F., Qiu, J., and Xiong, L. (2010). Genetic analysis of pathway regulation for enhancing branched-chain amino acid biosynthesis in plants. Plant J *63*(4), 573-583.

Cherry, J. M., Hong, E. L., Amundsen, C., Balakrishnan, R., Binkley, G., Chan, E. T., and Wong, E. D. (2012). *Saccharomyces* Genome Database: the genomics resource of budding yeast. Nucleic Acids Res *40*(Database issue), D700-705.

Chipman, D. M., and Shaanan, B. (2001). The ACT domain family. Curr Opin Struct Biol *11*(6), 694-700.

Cole, J. T. (2015). Metabolism of BCAAs. In R. Rajendram, V. R. Preedy and V. B. Patel Eds. Branched Chain Amino Acids in Clinical Nutrition: Volume 1. (New York, NY: Springer New York), pp. 13-24.

Colón, M., Hernández, F., López, K., Quezada, H., González, J., López, G., and González, A. (2011). *Saccharomyces cerevisiae* Bat1 and Bat2 Aminotransferases Have Functionally Diverged from the Ancestral-Like *Kluyveromyces lactis* Orthologous Enzyme. PLOS ONE *6*(1), e16099.

Cullin, C., Baudin-Baillieu, A., Guillemet, E., and Ozier-Kalogeropoulos, O. (1996). Functional analysis of YCL09C: Evidence for a role as the regulatory subunit of acetolactate synthase. Yeast *12*(15), 1511-1518.

Dahnum, D., Tasum, S. O., Triwahyuni, E., Nurdin, M., and Abimanyu, H. (2015). Comparison of SHF and SSF Processes Using Enzyme and Dry Yeast for Optimization of Bioethanol Production from Empty Fruit Bunch. Energy Procedia *68*, 107-116.

D'Antona, G., Ragni, M., Cardile, A., Tedesco, L., Dossena, M., Bruttini, F., and Nisoli, E. (2010). Branched-chain amino acid supplementation promotes survival and supports cardiac and skeletal muscle mitochondrial biogenesis in middle-aged mice. Cell Metab *12*(4), 362-372.

De Bandt, J. P., and Cynober, L. (2006). Therapeutic use of branched-chain amino acids in burn, trauma, and sepsis. J Nutr *136*(1 Suppl), 308S-313S.

Dickinson, J. R. (2000). Pathways of leucine and valine catabolism in yeast. Methods Enzymol *324*, 80-92.

Doi, M., Yamaoka, I., Fukunaga, T., and Nakayama, M. (2003). Isoleucine, a potent plasma glucose-lowering amino acid, stimulates glucose uptake in C2C12 myotubes. Biochem Biophys Res Commun *312*(4), 1111-1117.

Duggleby, R. G. (1997). Identification of an acetolactate synthase small subunit gene in two eukaryotes. Gene *190*(2), 245-249.

Eden, A., Simchen, G., and Benvenisty, N. (1996). Two yeast homologs of ECA39, a target for c-Myc regulation, code for cytosolic and mitochondrial branched-chain amino acid aminotransferases. J Biol Chem *271*(34), 20242-20245.

Eggeling L., Pfefferle W., and Sahm H. (2001). Amino acids. In: Ratledge C, Bjoern K eds. Basic biotechnology. (Cambridge: Cambridge University Press), pp. 281–303.

Elišáková, V., Pátek, M., Holátko, J., Nešvera, J., Leyval, D., Goergen, J.-L., and Delaunay, S. (2005). Feedback-Resistant Acetohydroxy Acid Synthase Increases Valine Production in *Corynebacterium glutamicum*. Appl Environ Microbiol *71*(1), 207-213.

Engel, S., Vyazmensky, M., Berkovich, D., Barak, Z., and Chipman, D. M. (2004). Substrate range of acetohydroxy acid synthase I from *Escherichia coli* in the stereoselective synthesis of alpha-hydroxy ketones. Biotechnol Bioeng *88*(7), 825-831.

Engel, S., Vyazmensky, M., Geresh, S., Barak, Z. e., and Chipman, D. M. (2003). Acetohydroxyacid synthase: a new enzyme for chiral synthesis of R-phenylacetylcarbinol. Biotechnol Bioeng *83*(7), 833-840.

Godard, P., Urrestarazu, A., Vissers, S., Kontos, K., Bontempi, G., van Helden, J., and André, B. (2007). Effect of 21 Different Nitrogen Sources on Global Gene Expression in the Yeast *Saccharomyces cerevisiae*. Mol Cell Biol *27*(8), 3065-3086.

Goichon, A., Chan, P., Lecleire, S., Coquard, A., Cailleux, A.-F., Walrand, S., and Coëffier, M. (2013). An enteral leucine supply modulates human duodenal mucosal proteome and decreases the expression of enzymes involved in fatty acid beta-oxidation. J Proteomics *78*, 535-544.

Gollop, N., Damri, B., Chipman, D., and Barak, Z. (1990). Physiological implications of the substrate specificities of acetohydroxy acid synthases from varied organisms. J Bacteriol *172*(6), 3444-3449.

Grant, G. A., Schuller, D. J., and Banaszak, L. J. (1996). A model for the regulation of D-3-phosphoglycerate dehydrogenase, a Vmax-type allosteric enzyme. Protein Sci *5*(1), 34-41.

Hazelwood, L. A., Daran, J.-M., van Maris, A. J. A., Pronk, J. T., and Dickinson, J. R. (2008). The Ehrlich Pathway for Fusel Alcohol Production: a Century of Research on *Saccharomyces cerevisiae* Metabolism. Appl Environ Microbiol *74*(8), 2259-2266.

Hill, C. M., Pang, S. S., and Duggleby, R. G. (1997). Purification of *Escherichia coli* acetohydroxyacid synthase isoenzyme II and reconstitution of active enzyme from its individual pure subunits. Biochem J *327*(Pt 3), 891-898.

Holzer, H., Goedde, H., Göggel, K.-H., and Ulrich, B. (1960). Identification of α-hydroxyethyl thiamine pyrophosphate (active acetaldehyde) as an intermediate in the oxidation of pyruvate by pyruvic oxidase from yeast mitochondria. Biochem Biophys Res Communn *3*(6), 599-z

Inoue, H., Nojima, H., and Okayama, H. (1990). High efficiency transformation of *Escherichia coli* with plasmids. Gene *96*(1), 23-28.

Janke, C., Magiera, M. M., Rathfelder, N., Taxis, C., Reber, S., Maekawa, H., and Knop, M. (2004). A versatile toolbox for PCR-based tagging of yeast genes: new fluorescent proteins, more markers and promoter substitution cassettes. Yeast *21*(11), 947-962.

Jiang, W.-D., Deng, Y.-P., Liu, Y., Qu, B., Jiang, J., Kuang, S.-Y., and Feng, L. (2015). Dietary leucine regulates the intestinal immune status, immune-related signalling molecules and tight junction transcript abundance in grass carp (*Ctenopharyngodon idella*). Aquaculture *444*, 134-142.

Johnson, M. A., Vidoni, S., Durigon, R., Pearce, S. F., Rorbach, J., He, J., and Spinazzola, A. (2014). Amino Acid Starvation Has Opposite Effects on Mitochondrial and Cytosolic Protein Synthesis. PLOS ONE *9*(4), e93597.

Kanehisa, M., and Goto, S. (2000). KEGG: kyoto encyclopedia of genes and genomes. Nucleic Acids Res *28*(1), 27-30.

Kaplun, A., Vyazmensky, M., Zherdev, Y., Belenky, I., Slutzker, A., Mendel, S., Barak, Z., Chipman, D. M., and Shaanan, B. (2006). Structure of the regulatory subunit of acetohydroxyacid synthase isozyme III from *Escherichia coli*. J Mol Biol *357*(3), 951-963.

Kelley, L. A., Mezulis, S., Yates, C. M., Wass, M. N., and Sternberg, M. J. E. (2015). The Phyre2 web portal for protein modeling, prediction and analysis. [Protocol]. Nat. Protocols, *10*(6), 845-858.

Kephart, W. C., Wachs, T. D., Mac Thompson, R., Brooks Mobley, C., Fox, C. D., McDonald, J. R., and Roberts, M. D. (2016). Ten weeks of branched-chain amino acid supplementation improves select performance and immunological variables in trained cyclists. Amino Acids *48*(3), 779-789.

Kingsbury, J. M., Sen, N. D., and Cardenas, M. E. (2015). Branched-Chain Aminotransferases Control TORC1 Signaling in *Saccharomyces cerevisiae*. PLoS Genetics *11*(12), e1005714.

Kispal, G., Steiner, H., Court, D. A., Rolinski, B., and Lill, R. (1996). Mitochondrial and cytosolic branched-chain amino acid transaminases from yeast, homologs of the myc oncogene-regulated Eca39 protein. J Biol Chem *271*(40), 24458-24464.

Knoshaug, E. P., and Zhang, M. (2009). Butanol tolerance in a selection of microorganisms. Appl Biochem Biotechnol *153*(1-3), 13-20.

Kohlhaw, G. B. (2003). Leucine biosynthesis in fungi: entering metabolism through the back door. Microbiol Mol Biol Rev *67*(1), 1-15, table of contents.

Lee, Y. T., and Duggleby, R. G. (2001). Identification of the regulatory subunit of *Arabidopsis thaliana* acetohydroxyacid synthase and reconstitution with its catalytic subunit. Biochemistry *40*(23), 6836-6844.

Lonhienne, T., Garcia, M. D., Fraser, J. A., Williams, C. M., and Guddat, L. W. (2017). The 2.0 A X-ray structure for yeast acetohydroxyacid synthase provides new insights into its cofactor and quaternary structure requirements. PLOS ONE *12*(2), e0171443.

Luo, J. B., Feng, L., Jiang, W. D., Liu, Y., Wu, P., Jiang, J., and Zhou, X. Q. (2014). The impaired intestinal mucosal immune system by valine deficiency for young grass carp (*Ctenopharyngodon idella*) is associated with decreasing immune status and regulating tight junction proteins transcript abundance in the intestine. Fish Shellfish Immunol *40*(1), 197-207.

Magee, P., and Robichon-Szulmajster, H. D. (1968). The Regulation of Isoleucine-Valine Biosynthesis in *Saccharomyces cerevisiae*. Eur J Biochem *3*(4), 507-511.

Manelli, J. C., Garabedian, M., Ounis, N., Houvenaeghel, M., Ottomani, A., and Bimar, J. (1984). Effects on muscular and general proteolysis in burn patients of a solution enriched with branched amino acids. Ann Fr Anesth Reanim *3*(4), 256-260.

Mao, X., Qi, S., Yu, B., He, J., Yu, J., and Chen, D. (2013). Zn2+ and l-isoleucine induce the expressions of porcine β-defensins in IPEC-J2 cells. Mol Biol Rep *40*(2), 1547-1552.

McCourt, J. A., and Duggleby, R. G. (2005). How an enzyme answers multiple-choice questions. Trends Biochem Sci *30*(5), 222-225.

Mishra, P., and Prasad, R. (1989). Relationship between ethanol tolerance and fatty acyl composition of *Saccharomyces cerevisiae*. Appl Microbiol Biotechnol *30*(3), 294-298.

Mendel, S., Elkayam, T., Sella, C., Vinogradov, V., Vyazmensky, M., Chipman, D. M., and Barak, Z. e. (2001). Acetohydroxyacid synthase: A proposed structure for regulatory subunits supported by evidence from mutagenesis1. J Mol Biol *307*(1), 465-477.

Monirujjaman, M., and Ferdouse, A. (2014). Metabolic and Physiological Roles of Branched-Chain Amino Acids. Adv MolBiol *2014*, 6.

Nakamura, I. (2014). Impairment of innate immune responses in cirrhotic patients and treatment by branched-chain amino acids. World J Gastroentero *20*(23), 7298-7305.

Nishitani, S., Matsumura, T., Fujitani, S., Sonaka, I., Miura, Y., and Yagasaki, K. (2002). Leucine promotes glucose uptake in skeletal muscles of rats. Biochem Biophys Res Commun *299*(5), 693-696.

Nishitani, S., Takehana, K., Fujitani, S., and Sonaka, I. (2005). Branched-chain amino acids improve glucose metabolism in rats with liver cirrhosis. Am J Physiol Gastrointest Liver Physiol *288*(6), G1292-1300.

Oldiges, M., Eikmanns, B. J., and Blombach, B. (2014). Application of metabolic engineering for the biotechnological production of L-valine. Appl Microbiol Biotechnol *98*(13), 5859-5870.

Oliver, S. G., van der Aart, Q. J., Agostoni-Carbone, M. L., Aigle, M., Alberghina, L., Alexandraki, D., *et al*. (1992). The complete DNA sequence of yeast chromosome III. Nature *357*(6373), 38-46.

Pang, S. S., and Duggleby, R. G. (1999). Expression, Purification, Characterization, and Reconstitution of the Large and Small Subunits of Yeast Acetohydroxyacid Synthase. Biochemistry *38*(16), 5222-5231.

Pang, S. S., and Duggleby, R. G. (2001). Regulation of yeast acetohydroxyacid synthase by valine and ATP. Biochem J *357*(Pt 3), 749-757.

Pang, S. S., Duggleby, R. G., and Guddat, L. W. (2002). Crystal structure of yeast acetohydroxyacid synthase: a target for herbicidal inhibitors. J Mol Biol *317*(2), 249-262.

Pang, S. S., Guddat, L. W. and Duggleby, R.G. (2002). Yeast acetohydroxyacid synthase. Crystal structure of an enzyme containing non-catalytic FAD. In: 14th International Symposium on Flavins and Flavoproteins. 14th Int Symposium on Flavins and Flavoproteins, Cambridge, UK. 14-18 July, 2002.

Pang, S. S., Guddat, L. W., and Duggleby, R. G. (2003). Molecular basis of sulfonylurea herbicide inhibition of acetohydroxyacid synthase. J Biol Chem *278*(9), 7639-7644.

Park, J. H., Lee, K. H., Kim, T. Y., and Lee, S. Y. (2007). Metabolic engineering of *Escherichia coli* for the production of L-valine based on transcriptome analysis and in silico gene knockout simulation. Proc Natl Acad Sci U S A*, 104*(19), 7797-7802.

Park, J. H., and Lee, S. Y. (2010). Fermentative production of branched chain amino acids: a focus on metabolic engineering. Appl Microbiol Biotechnol *85*(3), 491-506.

Pátek, M. (2007). Branched-Chain Amino Acids. In V. F. Wendisch Ed. Amino Acid Biosynthesis ~ Pathways, Regulation and Metabolic Engineering. (Berlin, Heidelberg: Springer Berlin Heidelberg), pp. 129-162

Peralta-Yahya, P. P., Zhang, F., del Cardayre, S. B., and Keasling, J. D. (2012). Microbial engineering for the production of advanced biofuels. Nature *488*(7411), 320-328.

Petersen, J. G., and Holmberg, S. (1986). The *ILV5* gene of *Saccharomyces cerevisiae* is highly expressed. Nucleic Acids Res *14*(24), 9631-9651.

Petro, T. M., and Bhattacharjee, J. K. (1981). Effect of Dietary Essential Amino Acid Limitations upon the Susceptibility to Salmonella typhimurium and the Effect Upon Humoral and Cellular Immune Responses in Mice. Infect Immun *32*(1), 251-259.

Picotti, P., Clement-Ziza, M., Lam, H., Campbell, D. S., Schmidt, A., Deutsch, E. W., and Aebersold, R. (2013). A complete mass-spectrometric map of the yeast proteome applied to quantitative trait analysis. Nature *494*(7436), 266-270.

Polaina, J. (1984). Cloning of *ILV2*, *ILV3* and *ILV5* genes of *Saccharomyces cerevisiae.* Carlsberg Res Commun *49*. 577-584

Prohl, C., Kispal, G., and Lill, R. (2000). Branched-Chain-Amino-Acid Transaminases of Yeast *Saccharomyces cerevisiae*. Methods Enzymol *324*, 365-375.

Ren, M., Zhang, S. H., Zeng, X. F., Liu, H., and Qiao, S. Y. (2015). Branched-chain Amino Acids are Beneficial to Maintain Growth Performance and Intestinal Immune-related Function in Weaned Piglets Fed Protein Restricted Diet. Asian-Australas J Anim Sci *28*(12), 1742-1750.

Rivas-Santiago, C. E., Rivas-Santiago, B., León, D. A., Castañeda-Delgado, J., and Hernández Pando, R. (2011). Induction of β-defensins by L-isoleucine as novel immunotherapy in experimental murine tuberculosis. Clin Exp Immunol *164*(1), 80-89.

Singh, B. K., Stidham, M. A., and Shaner, D. L. (1988). Assay of acetohydroxyacid synthase. Anal Biochem *171*(1), 173-179.

Skeie, B., Kvetan, V., Gil, K. M., Rothkopf, M. M., Newsholme, E. A., and Askanazi, J. (1990). Branch-chain amino acids: Their metabolism and clinical utility. Crit Care Med *18*(5), 549-571.

Stracka, D., Jozefczuk, S., Rudroff, F., Sauer, U., and Hall, M. N. (2014). Nitrogen Source Activates TOR (Target of Rapamycin) Complex 1 via Glutamine and Independently of Gtr/Rag Proteins. J Biol Chem *289*(36), 25010-25020.

Takagi, H. (2008). Proline as a stress protectant in yeast: physiological functions, metabolic regulations, and biotechnological applications. Appl Microbiol Biotechnol *81*(2), 211-223.

Taylor, N. L., Heazlewood, J. L., Day, D. A., and Millar, A. H. (2004). Lipoic Acid-Dependent Oxidative Catabolism of α-Keto Acids in Mitochondria Provides Evidence for Branched-Chain Amino Acid Catabolism in *Arabidopsis*. Plant Physiol *134*(2), 838-848.

The UniProt Consortium (2017) UniProt: the universal protein knowledgebase. Nucleic Acids Res *45*(D1), D158-D169.

Tittmann, K., Golbik, R., Uhlemann, K., Khailova, L., Schneider, G., Patel, M., and Hübner, G. (2003). NMR analysis of covalent intermediates in thiamin diphosphate enzymes. Biochemistry *42*(26), 7885-7891.

Umbarger, H. E., and Brown, B. (1958). Isoleucine and valine metabolism in *Escherichia coli* VIII. The formation of acetolactate. J Biol Chem *233*(5), 1156-1160.

Umbarger, H. E. (1996). Biosynthesis of the branched-chain amino acids. In F. C. Neidhardt, R. Curtiss III, J. L. Ingraham, E. C. C. Lin, K. B. Low, B. Magasanik, W. S. Reznikoff, M. Riley, M. Schaechter, and H. E Umbarger ed. *Escherichia coli* and *Salmonella*: cellular and molecular biology, 2nd ed. (Washington D.C.: ASM Press), pp. 442-457

Urban, J., Soulard, A., Huber, A., Lippman, S., Mukhopadhyay, D., Deloche, O., and Loewith, R. (2007). Sch9 Is a Major Target of TORC1 in *Saccharomyces cerevisiae*. Mol Cell *26*(5), 663-674.

Wishart D.S., Jewison T., Guo A.C., Wilson M., Knox C., *et al*. (2013) HMDB 3.0 — The Human Metabolome Database in 2013. Nucleic Acids Res *41*(D1), D801-7. 23161693

Woontner, M., and Jaehning, J. A. (1990). Accurate initiation by RNA polymerase II in a whole cell extract from *Saccharomyces cerevisiae*. J Biol Chem *265*(16), 8979-8982.

Xiao, W., and Rank, G. H. (1988). The yeast *ILV2* gene is under general amino acid control. Genome *30*(6), 984-986.

Yu, X., Wang, X., and Engel, P. C. (2014). The specificity and kinetic mechanism of branched-chain amino acid aminotransferase from *Escherichia coli* studied with a new improved coupled assay procedure and the enzyme's potential for biocatalysis. FEBS J *281*(1), 391-400.

Zhang, S., Zeng, X., Ren, M., Mao, X., and Qiao, S. (2017). Novel metabolic and physiological functions of branched chain amino acids: a review. J Anim Sci Biotechnol *8*, 10.

CheilJedang (2013). Report. Retrieved from http://english.cj.net/company/news/press/press_view.asp?ps_idx=5883andNO=41